

Recommended Practice for Soft Ground Site Characterization: Arthur Casagrande Lecture

Práctica Recomendada para la Caracterización de Sitios en Terreno Blando: Conferencia Arthur Casagrande

by

Charles C. Ladd, Hon. M., ASCE

Edmund K. Turner Professor Emeritus

Department of Civil and Environmental Engineering,

Massachusetts Institute of Technology, Cambridge, MA, USA

ccladd@mit.edu

and

Don J. DeGroot, M., ASCE

Associate Professor

Department of Civil and Environmental Engineering,

University of Massachusetts Amherst, Amherst, MA, USA

degroot@ecs.umass.edu

prepared for

12th Panamerican Conference on Soil Mechanics and Geotechnical Engineering
Massachusetts Institute of Technology
Cambridge, MA USA
June 22 – 25, 2003

April 10, 2003

Revised: May 9, 2004

Table of Contents

List of Tables	iii
List of Figures.....	iv
ABSTRACT	1
1. INTRODUCTION.....	2
2. GENERAL METHODOLOGY	4
3. SOIL STRATIGRAPHY, SOIL CLASSIFICATION AND GROUND WATER CONDITIONS	5
4. UNDISTURBED SAMPLING & SAMPLE DISTURBANCE.....	6
4.1 Sources of Disturbance and Procedures to Minimize	6
4.2 Radiography	10
4.3 Assessing Sample Quality.....	10
5. IN SITU TESTING	14
5.1 Field Vane Test	14
5.2 Piezocone Test	16
5.3 Principal Recommendations	22
6. LABORATORY CONSOLIDATION TESTING.....	23
6.1 Fundamentals	23
6.2 Compression Curves	24
6.3 Flow Characteristics.....	27
6.4 Principal Recommendations	27
7. UNDRAINED SHEAR BEHAVIOR AND STABILITY ANALYSES.....	29
7.1 Review of Behavioral Fundamentals	29
7.2 Problems with Conventional UUC and CIUC Tests.....	34
7.3 Strength Testing for Undrained Stability Analyses	35
7.4 Three Dimensional End Effects	39
7.5 Principal Recommendations	39
8. LABORATORY CONSOLIDATED-UNDRAINED SHEAR TESTING	40
8.1 Experimental Capabilities and Testing Procedures.....	40
8.2 Reconsolidation Procedure	42
8.3 Interpretation of Strength Data.....	46
8.4 Principal Recommendations	50
9. SUMMARY AND CONCLUSIONS	51
10. ACKNOWLEDGMENTS	52
REFERENCES.....	53

List of Tables

Table 1.1	Clay Properties for Soft Ground Construction	3
Table 2.2	Pros and Cons of In Situ vs. Laboratory Testing for Soil Profiling and Engineering Properties.....	4
Table 3.1	Atterberg Limits for Soft Bangkok Clay	6
Table 7.1	Levels of Sophistication for Evaluating Undrained Stability	35
Table 7.2	Level C Values of S and m for Estimating $s_u(\text{ave})$ via SHANSEP Equation (slightly modified from Section 5.3 of Ladd 1991)	36
Table 8.1	Effect of Consolidation Time on NC s_u/σ'_{vc} from CK_0 UDSS Tests.....	43
Table 8.2	SHANSEP Design Parameters for Sergipe Clay (Ladd and Lee 1993)	49

List of Figures

Figure 3.1	Soil Behavior Type Classification Chart Based on Normalized CPT/CPTU Data (after Robertson 1990, Lunne et al. 1997b)	5
Figure 4.1	Hypothetical Stress Path During Tube Sampling and Specimen Preparation of Centerline Element of Low OCR Clay (after Ladd and Lambe 1963, Baligh et al. 1987).....	7
Figure 4.2	Effect of Drilling Mud Weight and Depth to Water Table on Borehole Stability for $OCR = 1$ Clays	8
Figure 4.3	MIT Procedure for Obtaining Test Specimen from Tube Sample (Germaine 2003)	9
Figure 4.4	Results of Radiography and s_u Index Tests on Deep Tube Sample of Offshore Orinoco Clay (from Ladd et al. 1980)	11
Figure 4.5	Results of Oedometer Tests on Deep Tube Sample of Offshore Orinoco Clay (from Ladd et al. 1980)	12
Figure 4.6	(a) Specimen Quality Designation and (b) Stress History for Boston Blue Clay At CA/T South Boston (after Ladd et al. 1999 and Haley and Aldrich 1993)	13
Figure 4.7	Effects of Sample Disturbance on CR_{\max} from Oedometer Tests (LIR = 1) on Highly Plastic Organic Clay (numbers are negative elevation (m) for $OCR \geq 1$; GS El. = + 2m).....	13
Figure 5.1	Field Vane Correction Factor vs. Plasticity Index Derived from Embankment Failures (after Ladd et al. 1977)	15
Figure 5.2	Field Vane Undrained Strength Ratio at $OCR = 1$ vs. Plasticity Index for Homogeneous Clays (no shells or sand) [data points from Lacasse et al. 1978 and Jamiolkowski et al. 1985]	15
Figure 5.3	Location Plan of Bridge Abutments with Preload Fill and Preconstruction Borings and In Situ Tests.....	16
Figure 5.4	Depth vs. Atterberg Limits, Measured $s_u(FV)$ and Stress History for Highway Project in Northern Ontario	17
Figure 5.5	Revised Stress History with $\sigma'_p(FV)$ and MIT Lab Tests.....	17
Figure 5.6	Illustration of Piezocone (CPTU) with Area = 10 cm^2 (adapted from ASTM D5778 and Lunne et al. 1997b)	17
Figure 5.7	Example of Very Low Penetration Pore Pressure from CPTU Sounding for I-15 Reconstruction, Salt Lake City (record provide by Steven Saye)	18

Figure 5.8 Comparison of Stress History and CPTU Cone Factor for Boston Blue Clay at CA/T South Boston and MIT Bldg 68: Reference s_u (DSS) from SHANSEP CK ₀ UDSS Tests (after Ladd et al. 1999 and Berman et al. 1993).....	19
Figure 5.9 Comparison of CPTU Normalized Net Cone Resistance vs. OCR for BBC at South Boston and MIT Bldg 68.....	20
Figure 5.10 Cross-Section of TPS Breakwater Showing Initial Failure, Redesign, and Instrumentation at QM2.....	20
Figure 5.11 TPS Location Plan (Adapted from Geoprojetos, Ltda.)	21
Figure 5.12 Atterberg Limits and Stress History of Sergipe Clay (Ladd and Lee 1993)	22
Figure 5.13 Selected Stress History of Sergipe Clay Using CPTU Data from B2 – B5 Soundings (Ladd and Lee 1993).....	22
Figure 6.1 Fundamentals of 1-D Consolidation Behavior: Compression Curve, Hydraulic Conductivity, Coefficient of Consolidation and Secondary Compression vs. Normalized Vertical Effective Stress	24
Figure 6.2 Comparison of Compression Curves from CRS and IL Tests on Sherbrooke Block Samples (CRS tests run with $\Delta\varepsilon/\Delta t = 1\%/\text{hr}$): (a) Gloucester Clay, Ottawa, Canada; (b) Boston Blue Clay, Newbury, MA	26
Figure 6.3 Vertical Strain – Time Curves for Increments Spanning σ'_p from the IL Test on BBC Plotted in Fig. 6.2b.....	26
Figure 6.4 Estimation of Preconsolidation Stress Using the Strain Energy Method (after Becker et al. 1987)	27
Figure 6.5 Results of CRS Test on Structured CH Lacustrine Clay, Northern Ontario, Canada ($z = 15.7 \text{ m}$, $w_n = 72\%$, Est. LL = $75 \pm 10\%$, PI = $47 \pm 7\%$).....	28
Figure 7.1 OCR versus Undrained Strength Ratio and Shear Strain at Failure from CK ₀ U Tests: (a) AGS Plastic Marine Clay (PI = 43%, LI = 0.6) via SHANSEP (Koutsoftas and Ladd 1985); and (b) James Bay Sensitive Marine Clay (PI = 13%, LI = 1.9) via Recompression (B-6 data from Lefebvre et al. 1983) [after Ladd 1991].....	30
Figure 7.2 Stress Systems Achievable by Shear Devices for CK ₀ U Testing (modified from Germaine 1982) [Ladd 1991].....	31
Figure 7.3 Undrained Strength Anisotropy from CK ₀ U Tests on Normally Consolidated Clays and Silts (data from Lefebvre et al. 1983; Vaid and Campanella 1974; and various MIT and NGI Reports) [Ladd 1991]	31
Figure 7.4 Normalized Stress-Strain Data for AGS Marine Clay Illustrating Progressive Failure and the Strain Compatibility Technique (after Koutsoftas and Ladd 1985) [Ladd 1991]	32
Figure 7.5 Normalized Undrained Shear Strength versus Strain Rate, CK ₀ UC Tests, Resedimented BBC (Sheahan et al. 1996).....	32
Figure 7.6 Schematic Illustration of Effect of Rate of Shearing on Measured s_u from In Situ and Lab Tests on Low OCR Clay	33
Figure 7.7 Effects of Sample Disturbance on Stress-Strain-Effective Stress Paths from UUC Tests on NC Resedimented BBC (Santagata and Germaine 2002)	34
Figure 7.8 Hypothetical Cross-Section for Example 2: CU Case with Circular Arc Analysis and Isotropic s_u	37
Figure 7.9 Elevation vs. Stress History From IL Oedometer Tests, Measured and Normalized s_u (FV) and s_u (Torvane) and CPTU Data for Bridge Project Located North of Boston, MA	38
Figure 7.10 Interpreted Stress History and Predicted Undrained Shear Strength Profiles Using a Level C Prediction of SHANSEP Parameters	38

Figure 8.1 Example of 1-D Consolidation Data from MIT's Automated Stress Path Triaxial Cell	42
Figure 8.2 Recompression and SHANSEP Consolidation Procedure for Laboratory CK ₀ U Testing (after Ladd 1991)	42
Figure 8.3 Comparison of SHANSEP and Recompression CK ₀ U Triaxial Strength Data on Natural BBC (after Ladd et al. 1999)	44
Figure 8.4 Comparison of SHANSEP and Recompression CK ₀ U Triaxial Modulus Data on Natural BBC (after Ladd et al. 1999)	44
Figure 8.5 Comparison of SHANSEP and Recompression CK ₀ UDSS Strength Data on CVVC (after DeGroot 2003)	45
Figure 8.6 CVVC UMass Site: (a) Stress History Profile; (b) SHANSEP and Recompression DSS Strength Profiles (after DeGroot 2003)	45
Figure 8.7 Plane Strain Anisotropic Undrained Strength Ratios vs. Plasticity Index for Truly Normally Consolidated Non-Layered CL and CH Clays (mostly adjusted data from Ladd 1991)	48
Figure 8.8 TPS Stability Analyses for Redesign Stages 2 and 3 Using SHANSEP $s_u(\alpha)$ at $t_c = 5/15/92$ (Lee 1995)	49
Figure 8.9 SHANSEP DSS Strength Profiles for TPS Stability Analysis for Virgin and Normally Consolidated Sergipe Clay: (a) Zone 2; (b) Zone 4 (Lee 1995)	50
Figure 8.10 Normalized Undrained Strength Anisotropy vs. Shear Surface Inclination for OC and NC Sergipe Clay (Ladd and Lee 1993)	50

Recommended Practice for Soft Ground Site Characterization: Arthur Casagrande Lecture

Práctica Recomendada para la Caracterización de Sitios en Terreno Blando: Conferencia Arthur Casagrande

Charles C. Ladd, Hon. M., ASCE

*Edmund K. Turner Professor Emeritus, Dept. of Civil and Environmental Engineering,
Massachusetts Institute of Technology, Cambridge, MA, USA*

Don J. DeGroot, M., ASCE

*Associate Professor, Dept. of Civil and Environmental Engineering,
University of Massachusetts Amherst, Amherst, MA, USA*

Abstract

A soft ground condition exists whenever construction loads a cohesive foundation soil beyond its preconsolidation stress, as often occurs with saturated clays and silts having SPT blow counts that are near zero. The paper recommends testing programs, testing methods and data interpretation techniques for developing design parameters for settlement and stability analyses. It hopes to move the state-of-practice closer to the state-of-the-art and thus is intended for geotechnical practitioners and teachers rather than researchers. Components of site characterization covered include site stratigraphy, undisturbed sampling and in situ testing, and laboratory consolidation and strength testing. The importance of developing a reliable stress history for the site is emphasized. Specific recommendations for improving practice that are relatively easy to implement include: using fixed piston samples with drilling mud and debonded sample extrusion to reduce sample disturbance; either running oedometer tests with smaller increments or preferably using CRS consolidation tests to better define the compression curve; and deleting UU and CIU triaxial tests, which do not provide useful information. Radiography provides a cost effective means of assessing sample quality and selecting representative soil for engineering tests and automated stress path triaxial cells enable higher quality CK₀U shear tests in less time than manually operated equipment. Utilization of regional facilities having these specialized capabilities would enhance geotechnical practice.

Resumen

Existe una condición de terreno blando cuando la construcción carga un suelo cohesivo de cimentación más allá de su esfuerzo de preconsolidación, como ocurre a menudo con arcillas saturadas y limos con valores cercanos a cero en el conteo de golpes del ensayo SPT. El artículo recomienda programas de prueba, métodos de ensayos y técnicas de interpretación de datos para desarrollar los parámetros de diseño a utilizarse en el análisis de asentamiento y estabilidad. Espera acercar el estado de la práctica hacia el estado del arte y por lo tanto está dirigido a personas que practican la geotecnia y a los profesores, más que a los investigadores. Los componentes de la caracterización del terreno tratados en este artículo incluyen la estratigrafía del sitio, muestreo inalterado y pruebas in situ y ensayos de consolidación y resistencia en laboratorio. Se acentúa la importancia de desarrollar una historia de carga confiable para el sitio. Las recomendaciones específicas para mejorar la práctica, las cuales son relativamente fáciles de implementar, incluyen: usar el pistón fijo para la extracción de muestras desde sondeos estabilizados con lodo y la extrusión de muestras previamente despegadas del tubo de muestreo para reducir la alteración de la misma; ya sea el correr ensayos de odómetro con incrementos de carga menores o preferiblemente usar ensayos de consolidación tipo CRS para la mejor definición de la curva de compresión; y suprimir los ensayos triaxiales tipo UU y CIU, los cuales no proporcionan información útil. El uso de radiografía es una opción de bajo costo que permite el determinar la calidad de la muestra y la selección de suelo representativo para los ensayos. Las celdas triaxiales de trayectoria de esfuerzos automatizadas permiten ensayos de corte CK₀U de más alta calidad y en menos tiempo que el que toma el equipo manual. La utilización instalaciones regionales que tengan estas capacidades especializadas mejoraría la práctica geotécnica.

1 INTRODUCTION

Soft ground construction is defined in this paper as projects wherein the applied surface load produces stresses that significantly exceed the preconsolidation stress of the underlying predominately cohesive foundation soil. Cohesive soils encompass clays (CL and CH), silts (ML and MH), and organic soils (OL and OH) of low to high plasticity, although the text will usually use "clay" to denote all cohesive soils. Those clays of prime interest usually have been deposited in an alluvial, lacustrine or marine environment and are essentially saturated (i.e., either under water or have a shallow water table). Standard Penetration Test (SPT) blow counts are often weight-of-rod or hammer and seldom exceed $N = 2 - 4$, except within surface drying crusts.

Soft ground construction requires estimates of the amount and rate of expected settlement and assessment of undrained foundation stability. Part A of Table 1.1 lists and defines clays properties (design parameters) that are needed to perform various types of settlement analysis and Part B does likewise for undrained stability analyses during periods of loading.

For settlement analyses, the magnitude of the final consolidation settlement is always important and can be estimated using

$$\rho_{cf} = \Sigma [H_0 (RR \log \sigma'_p / \sigma'_{v0} + CR \log \sigma'_{vf} / \sigma'_{p0})] \quad (1.1)$$

where H_0 is the initial thickness of each layer (Note: σ'_{vf} replaces σ'_{p0} if only recompression and σ'_{v0} replaces σ'_{p0} if only virgin compression within a given layer). The most important in situ soil parameters in Eq. 1.1 are the stress history (SH = values of σ'_{v0} , σ'_{p0} and OCR = $\sigma'_{p0}/\sigma'_{v0}$) and the value of CR. Typical practice assumes that the total settlement at the end of consolidation equals ρ_{cf} , i.e., initial settlements due to undrained shear deformations (ρ_i) are ignored. This is reasonable except for highly plastic (CH) and organic (OH) foundation soils with low factors of safety and slow rates of consolidation (large t_p). As discussed in Foott and Ladd (1981), such conditions can lead to large settlements both during loading (low E_u/s_u) and after loading (excessive undrained creep).

For projects involving preloading (with or without surcharging) and staged construction, predictions of the rate of consolidation are required for design. These involve estimates of c_v for vertical drainage and also c_h for horizontal drainage if vertical drains are installed to increase

the rate of consolidation. In both cases the selected values should focus on normally consolidated (NC) clay, even when using a computer program that can vary c_v and c_h as a function of σ'_{vc} .

Settlements due to secondary compression become important only with rapid rates of primary consolidation, as occurs within zones having vertical drains. For such situations, designs often use surcharging to produce overconsolidated soil under the final stresses, which reduces the rate of secondary compression.

Part B of Table 1.1 describes undrained stability analyses for two conditions: the UU Case, which assumes no drainage during (rapid) initial loading; and the CU Case, which accounts for increases in strength due to drainage that occurs during staged construction. Both cases require knowledge of the variation in s_u with depth for virgin soil. However, the CU Case also needs to estimate values of s_u for NC clay because the first stage of loading should produce $\sigma'_{vc} > \sigma'_{p0}$ within a significant portion of the foundation (there is minimal change in s_u during recompression). Most stability analyses use "isotropic" strengths, that is $s_u = s_u(\text{ave})$, while anisotropic analyses explicitly model the variation in s_u with inclination of the failure surface (as covered in Sections 7 and 8). Knowledge of the initial stress history is highly desirable for the UU Case, in order to check the reasonableness of the s_u/σ'_{v0} ratios selected for design, and is essential for the CU Case.

The authors believe that the quality of soft ground site investigation programs and selection of soil properties has regressed during the past 10 to 20 years (at least in the U.S.) in spite of significant advances in both the knowledge of clay behavior and field-laboratory testing capabilities. Part of this problem can be attributed to the client's increasing reluctance to spend money on the "underground" (i.e., more jobs go to the low bidder independent of qualifications). However, geotechnical "ignorance" is also thought to be a major factor. Too many engineers either do not know (or have forgotten) how to achieve better quality information or do not appreciate the extent to which data from poor quality sampling and testing can adversely affect the design and performance (and hence overall cost) of geotechnical projects.

Hence the objective of this paper is to provide recommendations that can reverse the above trend by moving the state-of-the-practice closer to the state-of-the-art. The paper is aimed at practitioners and teachers, not researchers. Most of the recommendations involve relatively little extra

time and cost. The paper starts with a general methodology for site characterization and then suggests specific recommendations regarding:

- Soil stratigraphy and soil classification (Section 3)
- Undisturbed sampling and assessing sample disturbance (Section 4)
- In situ testing for soil profiling and some properties (Section 5)
- Laboratory consolidation testing (Section 6)

- Laboratory consolidated-undrained shear testing (Section 8), which is preceded by a section summarizing key aspects of undrained shear behavior (Section 7).

Several case histories are included to illustrate implementation of the recommendations.

A common theme throughout is the importance of determining the stress history of the foundation clay since it is needed to "understand" the deposit and it plays a dominant role in controlling both compressibility and strength.

Table 1.1 Clay Properties for Soft Ground Construction

A. SETTLEMENT ANALYSES

Analysis	Design Parameters	Remarks
1. Initial due to undrained shear deformations (ρ_i)	<ul style="list-style-type: none"> • Young's modulus (E_u) • Initial shear stress ratio (f) 	<ul style="list-style-type: none"> • See Foott & Ladd (1981)
2. Final consolidation settlement (ρ_{cf})	<ul style="list-style-type: none"> • Initial overburden stress (σ'_{v0}) • Preconsolidation stress (σ'_p) • Final consolidation stress (σ'_{vf}) • Recompression Ratio (RR) • Virgin Compression Ratio [CR = $C_v/(1 + e_0)$] 	<ul style="list-style-type: none"> • Check if hydrostatic u • Most important • Elastic stress distribution • $RR \approx 0.1 - 0.2 \times CR$ • Very important
3. Rate of consolidation: vertical drainage (\bar{U}_v)	<ul style="list-style-type: none"> • Coef. of consolidation ($c_v = k_v/m_v\gamma_w$) 	<ul style="list-style-type: none"> • Need NC value
4. Rate of consolidation: horiz. drainage (\bar{U}_h)	<ul style="list-style-type: none"> • Horiz. coef. of consol. ($c_h = c_v \cdot k_h/k_v$) 	<ul style="list-style-type: none"> • Effective $c_h <$ in situ c_h due to mandrel disturbance
5. Secondary compression settlement (ρ_s)	<ul style="list-style-type: none"> • Rate of secondary compression ($C_\alpha = \Delta e_v/\Delta \log t$) 	<ul style="list-style-type: none"> • ρ_s only important for low t_p • $C_\alpha(NC)/CR = 0.045 \pm 0.015^\dagger$

B. UNDRAINED STABILITY ANALYSES

1. During initial loading: assumes no drainage (UU Case)	<ul style="list-style-type: none"> • Initial in situ undrained shear strength (s_u) 	<ul style="list-style-type: none"> • Isotropic vs. anisotropic s_u analyses • SH very desirable to evaluate s_u/σ'_{v0}
2. During subsequent (staged) loading: includes drainage (CU case)	<ul style="list-style-type: none"> • Initial s_u for virgin clay • Increased s_u for NC clay ($S = s_u/\sigma'_{vc}$ at $OCR = 1$) • Results from A.3 & A.4 	<ul style="list-style-type: none"> • Isotropic vs. anisotropic s_u • SH essential to determine when $\sigma'_{vc} > \sigma'_p$

Other Notation: NC = Normally Consolidated; OCR = Overconsolidation Ratio; SH = Stress History; t_p = time for primary consolidation; σ'_{vc} = vertical consolidation stress. [†]Note: \pm is defined as a range unless followed by SD then it defines \pm one standard deviation.

2 GENERAL METHODOLOGY

Site characterization has two components: determination of the stratigraphy (soil profile) and ground water conditions; and estimation of the relevant engineering properties. The first identifies the locations of the principal soil types and their relative state (i.e., estimates of relative density of granular soils and of consistency (strength/stiffness) of cohesive soils) and the location of the water table and possible deviations from hydrostatic pore pressures. The second quantifies the properties of the foundation soils needed for design, such as those listed in Table 1.1.

The best approach for soft ground site characterization includes a combination of both in situ testing and laboratory testing on undisturbed samples for the reasons summarized in Table 2.1. In situ tests, such as with the piezocone (CPTU) or perhaps the Marchetti (1980) flat plate dilatometer (DMT), are best suited for soil

profiling since they provide rapid means for identifying the distribution of soil types with depth (at least granular vs. cohesive) and information about their relative state. But the CPTU and DMT generally cannot yield reliable predictions of design parameters for soft clays due to excessive scatter in the highly empirical correlations used to estimate strength-deformation properties. Conversely, properly selected laboratory tests can provide reliable consolidation and strength properties for design if carefully run on undisturbed samples of good quality. However, the high cost of good quality sampling and lab testing obviously makes this approach ill-suited for soil profiling. Moreover, poor quality lab data often give erroneous spatial trends in consistency and stress history due to variable degrees of sample disturbance with depth. In fact, the prevalence of misleading lab results may have pushed in situ testing beyond reasonable limits by development of empirical correlations for properties that have no rational basis.

Table 2.1 Pros and Cons of In Situ and Laboratory Testing for Soil Profiling and Engineering Properties

		In Situ Testing (e.g., Piezocone & Dilatometer)	Laboratory Testing on Undisturbed Samples
		BEST FOR SOIL PROFILING	BEST FOR ENGINEERING PROPERTIES
PROS		1) More economical and less time consuming 2) (Semi) continuous record of data 3) Response of larger soil mass in its natural environment	1) Well defined stress-strain boundary conditions 2) Controlled drainage & stress conditions 3) Know soil type and macrofabric
CONS		REQUIRES EMPIRICAL CORRELATIONS FOR ENGR. PROPERTIES	POOR FOR SOIL PROFILING
		1) Poorly defined stress-strain boundary conditions 2) Cannot control drainage conditions 3) Unknown effects of installation disturbance and very fast rate of testing	1) Expensive and time consuming 2) Small, discontinuous test specimens 3) Unavoidable stress relief and variable degrees of sample disturbance

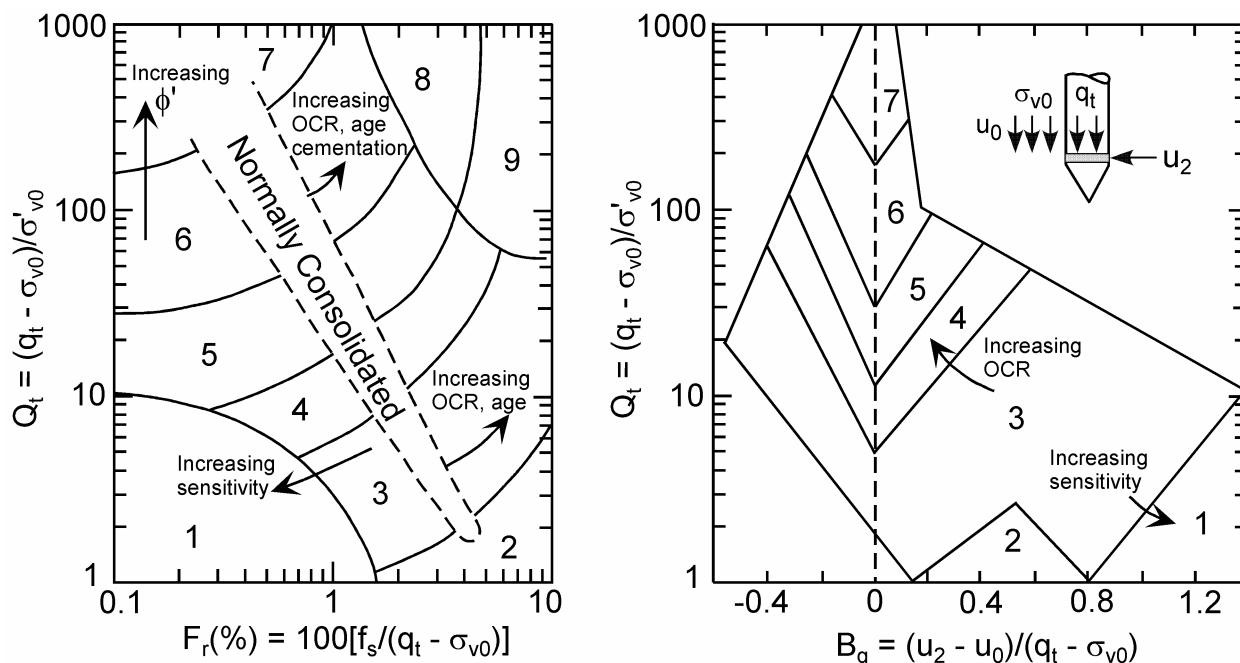
Note: See Section 3 for discussion of SPT and Section 5 for the field vane test

3 SOIL STRATIGRAPHY, SOIL CLASSIFICATION AND GROUND WATER CONDITIONS

As described above, soil stratigraphy refers to the location of soil types and their relative state. The most widely used methods for soil profiling are borings with Standard Penetration Tests (SPT) that recover split spoon samples, continuous samplers, and (semi) continuous penetration tests such as with the CPTU or perhaps the DMT. The SPT approach has the advantage of providing samples for visual classification that can be further refined by lab testing (water content, Atterberg Limits, grain size distribution, etc.). Borings advanced by a wash pipe with a chopping bit (i.e., the old fashion "wash boring" as per Section 11.2.2 in Terzaghi et al. 1996) have the advantage that a good driller can detect changes in the soil profile and take SPT samples of all representative soils, rather than at arbitrary intervals of 1.5 m or so. The equilibrium water level in a wash boring also defines the water table (but only for hydrostatic conditions). However, most SPT boreholes now use either rotary drilling with a drilling mud or hollow stem augers, both of

which may miss strata and give misleading water table elevations (Note: hollow stem augers should be filled with water or mud to prevent inflow of granular soils and bottom heave of cohesive soils). In any case, the SPT approach is too crude to give spatial changes in the s_u of soft clays, especially since N often equals zero. But do document the SPT procedures (at least drilling method and hammer type for prediction of sand properties from N data).

Piezocene soundings provide the most rapid and detailed approach for soil profiling. The chart in Fig. 3.1 is one widely used example of soil type descriptions derived from CPTU data (Section 5 discusses estimates of s_u and OCR). Note that the Zones are imprecise compared to the Unified Soil Classification (USC) system and thus the site investigation must also include sampling for final classification of soft cohesive strata. However, CPTU testing can readily differentiate between soft cohesive and free draining deposits and the presence of interbedded granular-cohesive soils. Dissipation tests should be run in high permeability soils (especially in deep layers) to check the ground water conditions (hydrostatic, artesian or pumping).



Soil Behavior Type by Zone Number

1. Sensitive, fine grained	4. Silt mixtures: clayey silt to silty clay	7. Gravelly sand to sand
2. Organic soils-peats	5. Sand mixtures: silty sand to sand silty	8. Very stiff sand to clayey sand
3. Clays: clay to silty clay	6. Sands: clean sands to silty sands	9. Very stiff fine grained

Figure 3.1 Soil Behavior Type Classification Chart Based on Normalized CPT/CPTU Data (after Robertson 1990, Lunne et al. 1997b)

The final developed soil profile should always include the USC designation for each soil type. Cohesive test specimens should be mixed at their *natural* water content for determination of Atterberg Limits and Liquidity Index. Atterberg Limits on dried soil are appropriate only to distinguish between CL-CH and OL-OH designations (as per ASTM D2487) since drying can cause very significant reductions in plasticity. Table 3.1 illustrates this fact for the soft Bangkok Clay: oven drying predicts a sensitive CL soil, whereas it actually is an insensitive CH-OH soil. Values of specific gravity are needed to check the degree of saturation of test specimens and to compute unit weights from profiles of average w_n . Hydrometer analyses are less important, although knowledge of the clay fraction (% - 2 μm) and Activity = PI/Clay Fraction may help to explain unusual properties.

The geotechnical report should contain appropriate summary plots of the results from at least the Atterberg Limits (e.g., a Plasticity Chart and depth vs. w_n relative to the Liquid and Plastic Limits), the variation in unit weights, and the ground water conditions. These data help to develop a conceptual framework of the anticipated engineering behavior. Even though of little interest to many clients, this exercise insures that someone has evaluated the data and also greatly assist peer review. The first author has spent untold hours in developing such plots from tabulated data for consulting projects worldwide.

Finally, the approach and scope selected to determine soil stratigraphy obviously should be compatible with available knowledge regarding the site geology, prior results from exploration programs, and the size and difficulty of the proposed construction.

Table 3.1 Atterberg Limits on Soft Bangkok Clay

Preparation	w_n (%)	LL (%)	PL (%)	PI (%)	LI
Oven Dried	65	48	25	23	1.7
Natural	60	69	25	44	0.8

Note:

- Representative values from two exploration programs.
- Clay minerals = montmorillonite > illite > kaolinite and clay contains < 5% organic matter (Ladd et al. 1971)

4 UNDISTURBED SAMPLING & SAMPLE DISTURBANCE

4.1 Sources of Disturbance and Procedures to Minimize

Figure 4.1 illustrates potential sources of sample disturbance via a hypothetical stress path during the process of obtaining a tube sample for laboratory testing. Point 1 is the initial stress state for a low OCR clay and the dashed line from Point 1 to Point A represents in situ undrained shear in triaxial compression. The following describes the different steps of the overall sampling process and recommends procedures to minimize the amount of disturbance.

Step 1. Drilling Boring and Stress Relief: Path 1-2.

Drilling to the sampling depth reduces the total vertical stress (σ_v), and hence subjects the clay at the bottom of the hole to undrained shear in triaxial extension (TE). The point at which σ_v equals the in situ total horizontal stress (σ_{h0}) represents the "perfect sample", i.e., the undrained release of the in situ shear stress with an effective stress of σ'_{ps} . However, if the weight of the drilling mud is too low, the soil at the bottom of the borehole can experience an undrained failure in TE before being sampled. This important fact is illustrated in Fig. 4.2. For the conditions given in the upper right sketch, the bottom three lines show the weight of mud producing failure as a function of the boring and water table depths for typical normally consolidated clays of low, intermediate and high plasticity. The insert gives the relevant clay properties used with the following equation to calculate when $\sigma_{h0} - \sigma_v = 2s_u(E)$

$$\frac{\gamma_m}{\gamma_w} = 1 - \frac{z_w}{z} + (K_0 - 2s_u(E)/\sigma'_{v0})(\frac{\gamma_b}{\gamma_w} + \frac{z_w}{z}) \quad (4.1)$$

The weight of mud required to prevent failure increases significantly with boring depth, i.e., with decreasing z_w/z . Failure occurs when z_w/z is less than 0.15 if the mud does not have a weight 10 ± 10% greater than water at NC clay sites.

Recommendations

To prevent excessive disturbance before sampling, be sure that the borehole remains filled with drilling mud having a weight that falls on Fig. 4.2 at least half way between a state of failure (lower three lines) and perfect sampling (upper three lines). If the clay is overconsolidated, the values of K_0 and $s_u(E)/\sigma'_{v0}$ in Eq. 4.1 can be increased by OCR raised to the power 0.5 and 0.8, respectively. For conditions that deviate from those in Fig. 4.2, make independent calculations.

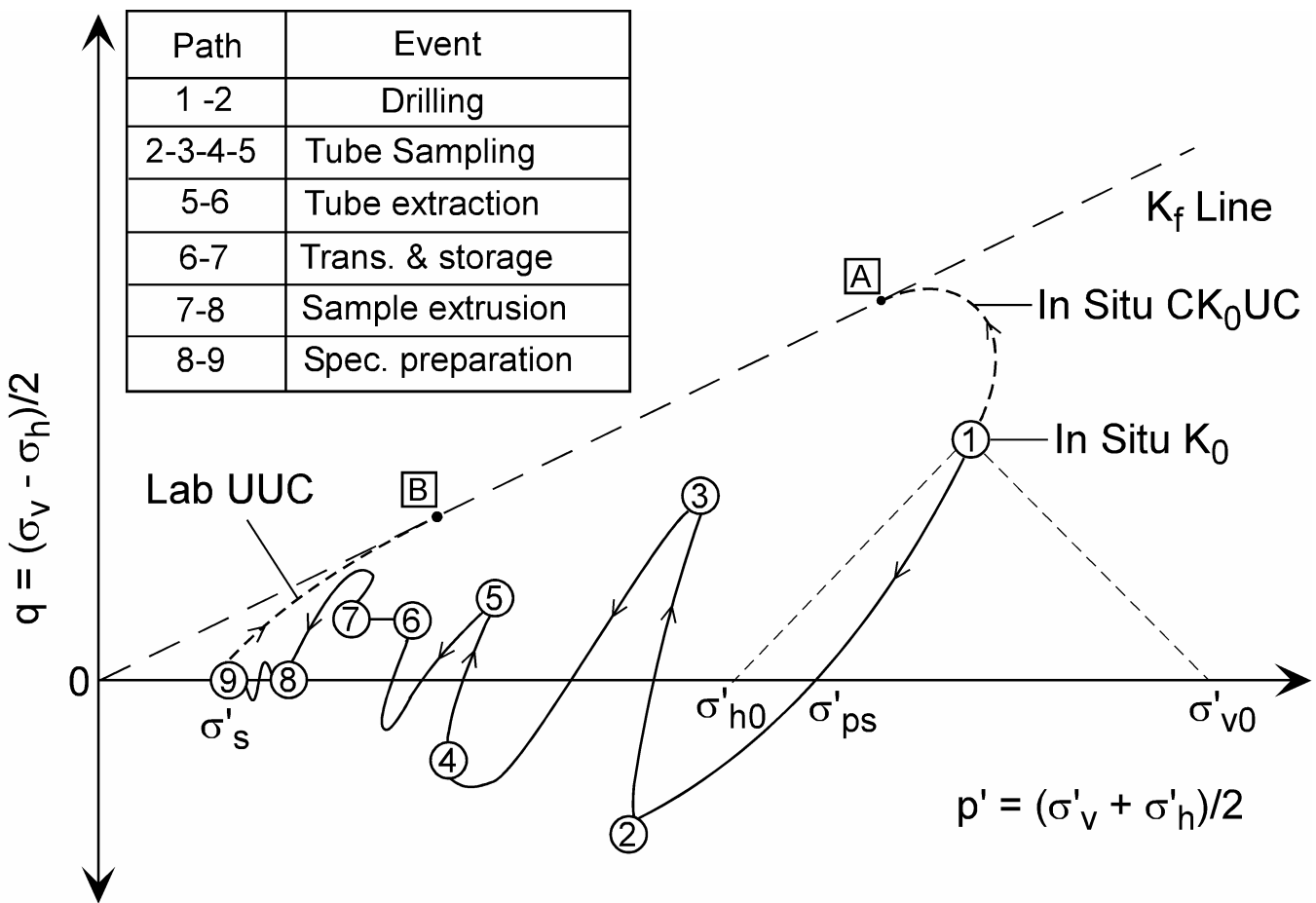


Figure 4.1 Hypothetical Stress Path During Tube Sampling and Specimen Preparation of Centerline Element of Low OCR Clay (after Ladd and Lambe 1963, Baligh et al. 1987)

Step 2. Tube Sampling: Path 2 – 5. Baligh et al. (1987) used the Strain Path Method (Baligh 1985) to show that, for tubes with an inside clearance ratio ($ICR = (D_i - D_e)/D_e$, where D_i and D_e are the inside diameters of the interior tube and its cutting edge, respectively) greater than zero, the centerline soil experiences shear in triaxial compression ahead of the tube (Path 2 – 3), followed by shear in triaxial extension as it enters the tube (Path 3 – 4), and then triaxial compression (Path 4 – 5). The magnitude of the peak axial strain in compression and extension increases with tube thickness (t) to diameter ratio and ICR, and approaches about one percent for the standard 3 in. diameter Shelby tube (ASTM 1587: $D_0 = 76.2$ mm, $t = 1.65$ mm, $ICR < 1\%$). More recent research (Clayton et al. 1998) studied the details of the cutting edge and indicates that a sharp cutting edge with zero inside clearance should give the best quality samples (peak extension $\epsilon_a = 0$) for soft clays since their low remolded strength already provides minimal resistance between the soil and the tube.

Recommendations

Use minimum outside tube diameter $D_0 = 76$ mm, tube wall thickness such that $D_0/t > 45$ with sharp cutting edge, and ICR near zero (certainly less than 0.5%). Use new tubes made of brass, stainless steel or coated (galvanized or epoxy) steel to help minimize corrosion.

Step 3. Tube Extraction: Path 5 – 6. (Note that stress path 5 – 6 shown in Fig. 4.1 is highly speculative). The intact clay just below the bottom of the tube resists removal of the tube sample, both due to its strength and the suction created in the void upon removal. In addition, the pore water pressure in the clay reduces as the tube is brought to the ground surface, which may lead to the formation of gas bubbles due to exsolution of dissolved gas (e.g., Hight 2003). This is a severe problem with some deep water clays, wherein gas voids and cracks form within the tube and the sample actually expands out of the tube if not immediately sealed off.

Recommendations (Non-gaseous clays)

Tube samples should be obtained with a stationary (fixed) piston sampler both to control the amount of soil entering the tube and to better retain the soil upon extraction. Piston samplers usually yield far better recovery and sample quality than push samples. After advancing the tube, allow time for the clay to partially bond to the tube (i.e., consolidation and strengthening of the remolded zone around the sample perimeter), then slowly rotate the tube two revolutions to shear the soil, and finally slowly withdraw the sample. ASTM D6519 describes a hydraulically operated (Osterberg type) sampler. The Acker sampler, which uses a rod to advance the piston, provides better control of the relative position of the piston head, but is more difficult to operate (Germaine 2003). Tanaka et al. (1996) and subsequent experience with the Japanese standard piston sampler (JPN, $D_i = 75$ mm, $t = 1.5$ mm, taper angle = 6° , ICR = 0) indicate excellent sample quality in low OCR clays usually comparable to that of the large diameter (208 mm) Laval sampler. The JPN has one version with extension rods for work on land at relatively shallow depths (< 20 m) and a hydraulic version for larger depths and offshore work (Tanaka 2003).

After obtaining the tube, remove spoil from the top and about 2 cm of soil from the bottom, run Torvane tests on the bottom, and seal the tubes as recommended in ASTM D4220.

Step 4. Transportation and Storage: Path 6 – 7. The path in Fig. 4.1 assumes that the tubes are carefully handled and not subjected to large changes in temperature (especially freezing). Hence the decrease in effective stress occurs solely due to an increase in water content within the central portion of the tube. The more disturbed clay around the perimeter consolidates, which causes swelling of the interior portion. Further swelling can occur if the sample contains relatively permeable zones which become desaturated by the more negative pore pressures (higher soil suction) in the surrounding clay.

Some organizations extrude the sample in the field in order to reuse the tubes and to avoid the development of bonding between the soil and inner wall of the tube. Others (e.g., NGI, Lunne 2003) may use field extrusion with relatively strong clay ($s_u > 25$ kPa) in order to remove the outer highly disturbed clay, and then store the samples in waxed cardboard containers so as to minimize swelling of the interior clay. Both practices require, however, very careful extrusion

and handling techniques to avoid distortion (shear deformation) of the soil that may damage its structure. The authors prefer to deal with the problem of constrained swelling (i.e., by reconsolidation) than to increase the risk of destructuring the soil, which decreases the size of its yield (bounding) surface (e.g., Hight 2003).

Recommendations

Leave the soil in the tubes and pack for shipping (if necessary) following the guidelines set forth in ASTM D4220. The cost of tubes is far less than money wasted by running expensive consolidation and strength tests on disturbed soil.

Line	Plasticity	γ_b/γ_w	K_0	$s_u(E)/\sigma'_{v0}$
L	Low	0.85	0.5	0.14
I	Inter.	0.65	0.6	0.18
H	High	0.45	0.7	0.22

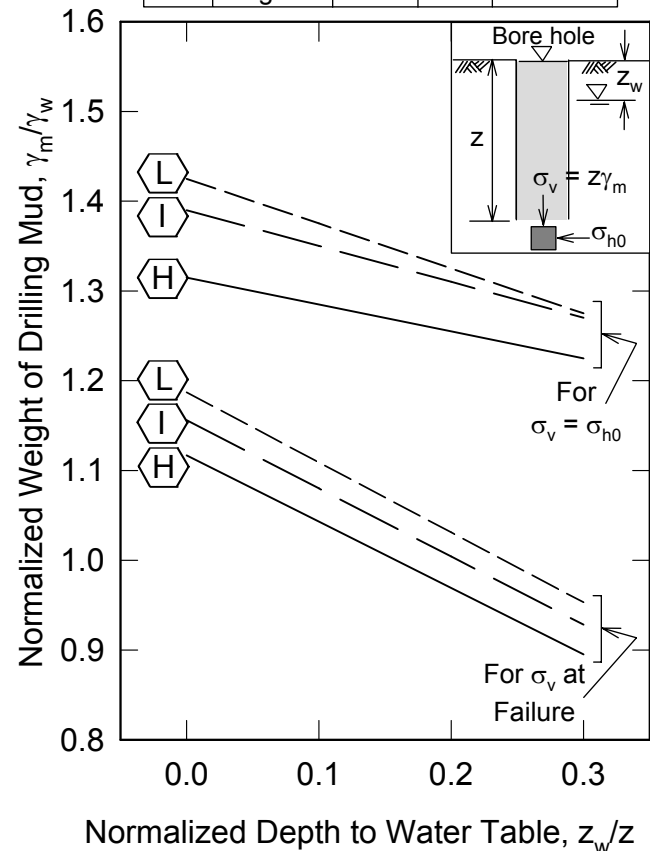


Figure 4.2 Effect of Drilling Mud Weight and Depth to Water Table on Borehole Stability for $OCR = 1$ Clays

Step 5. Sample Extrusion: Path 7 – 8. (stress path also highly speculative). The bond that develops between the soil and the tube can cause very serious disturbance during extrusion. For example, portions of the fixed piston tubes of BBC for the CA/T Special Test Program (Fig. 4.6)

were cut in short lengths for a series of conventional oedometer tests by Haley & Aldrich, Inc. During extrusion of the deep, low OCR samples, disturbance caused cracks to appear on the upper surface, even though the cut tubes were only several centimeters long. The resultant compression curves produced OCRs less than one, whereas subsequent tests on debonded specimens gave reasonable results.

Recommendations

Cut the tubes with a horizontal band saw or by hand using a hacksaw (pipe cutters will distort the tube) with lengths appropriate for each consolidation or shear test. Perform index tests (w_n and strength tests such as Torvane or fall cone) on soil above and below the cut portion as a check on soil quality and variability and then

debond the soil with a piano wire before extrusion as illustrated in Fig. 4.3.

Step 6. Index Tests and Specimen Preparation: Path 8 – 9.

The test specimen may experience a further decrease in effective stress (to end up at σ'_s) due to stress relief (loss of tube confinement), disturbance during trimming and mounting, and suction of water from wet porous stones. Drying would of course increase σ'_s . In any case, the pretest effective stress for reasonable quality samples of non-cemented clays is likely to be in the range of $\sigma'_s/\sigma'_{ps} \approx 0.25$ to 0.5 for relatively shallow soil of moderate OCR and in the range of $\sigma'_s/\sigma'_{ps} \approx 0.05$ to 0.25 for deeper soil with $OCR < 1.5$. (Note: σ'_{ps} roughly approximates the in situ mean (octahedral) effective stress).

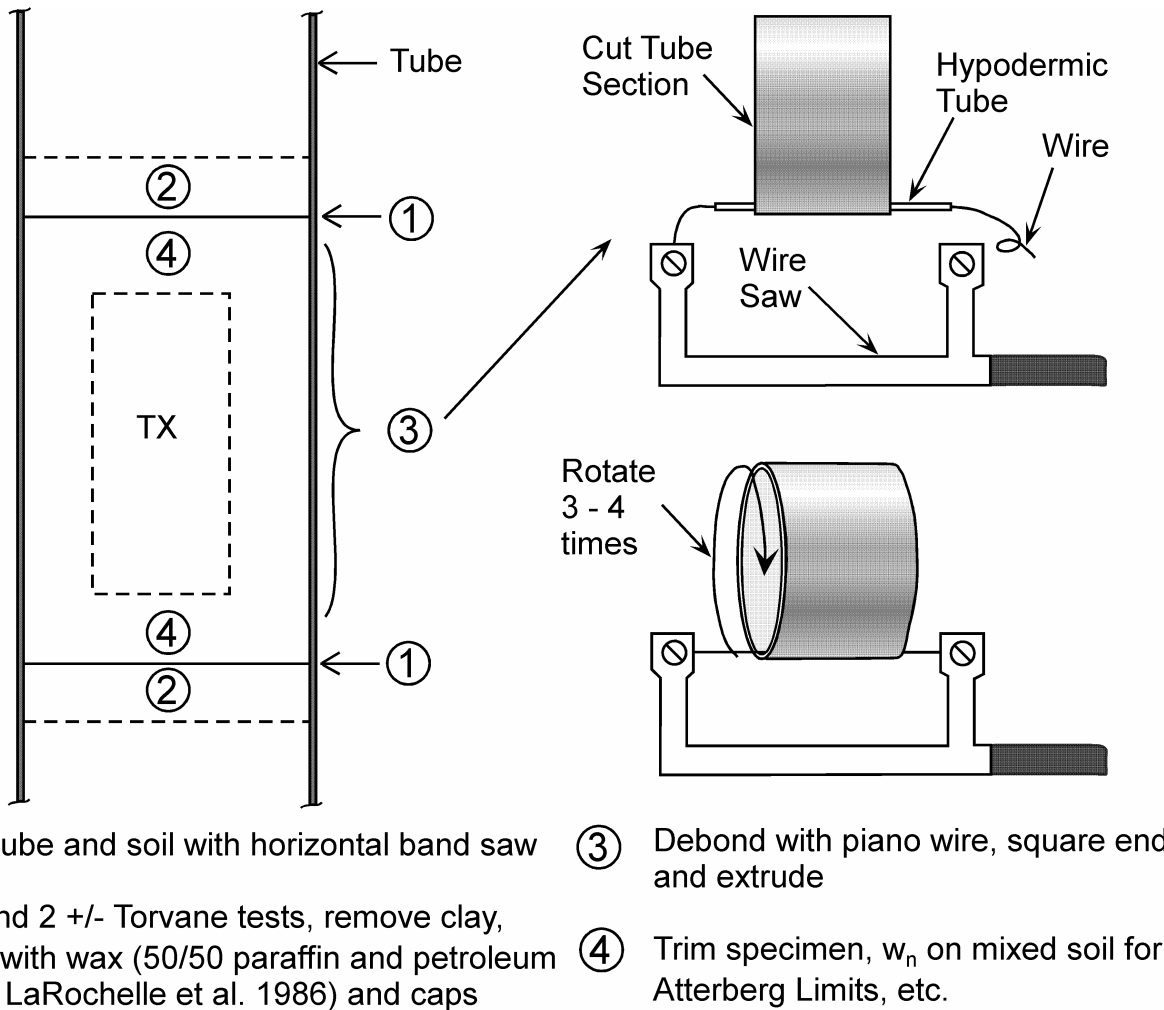


Figure 4.3 MIT Procedure for Obtaining Test Specimen from Tube Sample (Germaine 2003)

Hight et al. (1992) present a detailed study of the variation in σ'_s for the plastic Bothkennar Clay as a function of sampler type (including block samples), sample transport and method of specimen preparation.

Finally Fig. 4.1 shows the expected effective stress path for a UU triaxial compression test starting from Point 9. The large decrease in σ'_s compared to the in situ stresses causes the soil to behave as a highly overconsolidated material.

Recommendations

Prepare test specimens in a humid room (to minimize drying) with a wire saw, perhaps supplemented with a lathe or very sharp cutting ring. Do not use a miniature sampler. Collect soil above and below the specimen for w_n . If running Atterberg Limits, get w_n on well mixed soil. Whether to mount the specimen on wet versus dry stones is controversial. The authors favor moist stones for tests on low OCR clays that require back pressure saturation (e.g., CRSC or CU triaxial).

4.2 Radiography

ASTM D4452 describes the necessary equipment and techniques for conducting X-ray radiography. The ability of X ray photons to penetrate matter depends on the density and thickness of the material and the resulting radiograph records the intensity of photons reaching the film. MIT has been X-raying tube samples since 1978 using a 160 kV generator. The back half of the tube is placed in an aluminum holder (to create a constant thickness of penetrated material) and a scale with lead numbers and letters attached at one inch intervals is used to identify the soil location along the tubes. The applied amperage and exposure time vary with distance, tube diameter and average soil density. Each tube requires two or three films and, at times, the tube is rotated 90° for a second set.

Radiography can identify the following features.

1. Variations in soil type, at least granular vs. cohesive vs. peat.
2. Soil macrofabric, especially the nature (thickness, inclination, distortion, etc.) of any bedding or layering (uniform varved clays produce beautiful photos).
3. The presence of inclusions such as stones, shells, sandy zones and root holes.
4. The presence of anomalies such as fissures and shear planes.
5. The varying degree and nature of sample disturbance, including
 - bending near the tube perimeter

- cracks due to stress relief, such as may result from gas exsolution
- gross disturbance caused by the pervasive development of gas bubbles
- voids due to gross sampling disturbance, especially near the ends of the tube.

Many of these features are well illustrated in ASTM D4452

Radiography is extremely cost effective since it enables one to logically plan a laboratory test program (i.e., where to cut the tubes for each consolidation and shear test) based on prior knowledge of the locations of the best quality material of each representative soil obtained from the site. Radiography greatly reduces the likelihood of running costly tests on poor quality or non-representative soil that produce misleading data.

Recommendations

Radiography is considered essential for projects having a limited number of very expensive samples (e.g., for offshore projects) or that require specialized stress path triaxial tests. For example, NGI has used on-board radiography to immediately assess sample quality for offshore exploration and Boston's CA/T project used radiography for many undisturbed tube samples. The authors believe that each geotechnical "community" should have access to a regional radiography facility that can provide economical and timely service.

4.3 Assessing Sample Quality

No definitive method exists to determine the absolute sample quality vis-à-vis the "perfect sample". It is especially difficult to distinguish between decreases in σ'_s due solely to constrained swelling versus that caused by shear distortions. The former should have minimal effect on consolidation properties (Section 6) or undrained shear if the soil is reconsolidated to the in situ stresses (Section 8). In contrast, the latter produces irreversible destructuration (disturbance of the soil fabric, breaking of cementation and other interparticle bonds, etc.) that alters basic behavior depending upon the degree of damage to the soil structure (e.g., Lunne et al. 1997a, Santagata and Germaine 2002, Hight and Leroueil 2003). Nevertheless, one still should attempt to assess sample quality using the approaches described below.

1. Radiography. The distinct advantages of this non-destructive method should be obvious (Section 4.2).

2. Strength Index Tests. Disturbance decreases the unconsolidated-undrained (UU) strength so that Torvane, lab vane, fall cone and similar tests will reflect relative changes in s_u within and between tube samples. Figure 4.3 shows how index tests can be used for each specimen selected for consolidation and CU shear tests.

Figures 4.4 and 4.5 illustrate how MIT used index tests to help assess the effects of disturbance on consolidation testing to measure the stress history of a offshore Venezuelan CH clay. Azzouz et al. (1982) describe the nature of the deposit and the sampling and testing procedures at the site having a water depth of 78 ft. Radiography of the top foot of a deep sample showed gross disturbance above marker U (the UUC test was purposely run on disturbed soil), whereas Oed. No. 12 was run on presumed (from the X-ray) good quality soil with a much higher Torvane strength (Fig. 4.4). Although the compression curve (Fig. 4.5) looked reasonable, the estimated σ'_p indicated that the deposit was "underconsolidated". A second test (No. 18) was run as a check and, although only two inches deeper, it gave $OCR = 1.2$, plus a S-shaped curve with a significantly higher maximum CR. The Torvane strength also was much higher and equal to that measured onboard. Based on this

experience, the location of the first engineering test was subsequently guided by both the X-ray and Torvane data. It is also useful to compare strengths normalized by σ'_{v0} (e.g., see example in Fig. 7.9).

3. Pretest Effective Stress (σ'_s). Measurement of σ'_s requires a fine porous stone (air entry pressure greater than the soil suction = σ'_s) connected to a fully saturated, rigid system. For relatively unstructured clays (e.g., little or no cementation), decreases in σ'_s generally will correlate with decreases in s_u from UU type tests. For example, samples of NC resedimented Boston Blue Clay (BBC) subjected to varying degrees of disturbance (see Fig. 7.7) showed a unique correlation between $\log[s_u(UUC)/\sigma'_s]$ and $\log[\sigma'_{v0}/\sigma'_s]$ as per the SHANSEP equation (Santagata and Germaine 2002). However, UU tests are not recommended for design (Section 7.2) and thus the real question is whether σ'_s reflects the degree of damage to the soil structure that will alter consolidation and reconsolidated strength test results. The answer is maybe yes and maybe no depending on the soil type and the relative contributions of constrained swelling versus shear distortions on the value of σ'_s .

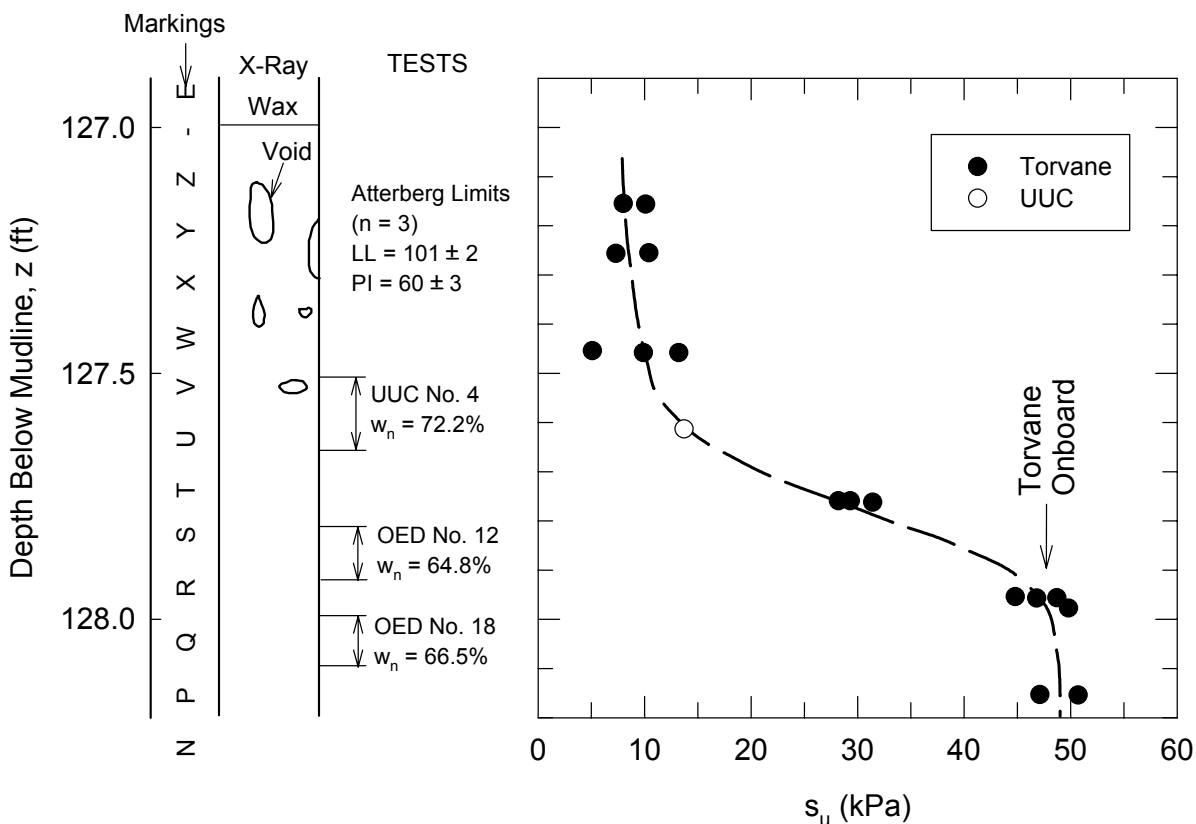


Figure 4.4 Results of Radiography and s_u Index Tests on Deep Tube Sample of Offshore Orinoco Clay (from Ladd et al. 1980)

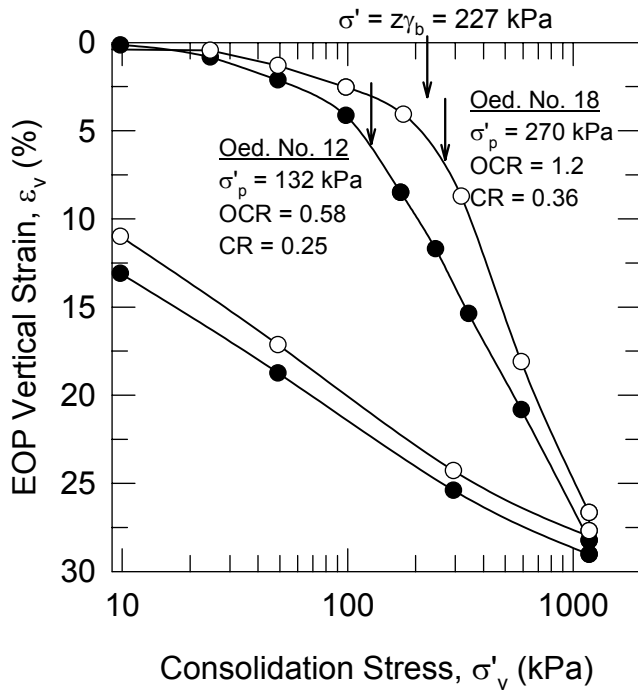


Figure 4.5 Results of Oedometer Tests on Deep Tube Sample of Offshore Orinoco Clay (from Ladd et al. 1980)

4. Vertical Strain at Overburden Stress (ε_{v0}).

This quantity equals the vertical strain measured at σ'_{v0} in 1-D consolidation tests. Andresen and Kolstad (1979) proposed that increasing sample disturbance should result in increasing values of ε_{v0} . Terzaghi et al. (1996) adopted this approach, coined the term Specimen Quality Designation (SQD) with sample quality ranging from A (best) to E (worst), and suggested that reliable lab data required samples with SQD of B or better for clays with $OCR < 3 - 5$. Figure 4.6 shows the SQD criteria superimposed on elevation vs. ε_{v0} and stress history data for the CA/T South Boston BBC test site described in Section 5.2. While most of the tests within the thick crust met the SQD A – B criteria, almost none did in the deep, low OCR clay even though the non-deleted tests produced excellent S-shaped compression curves, i.e., decreasing CR with increase in σ'_v . (Note: values of ε_{v0} for many of the deleted oedometer tests, which were disturbed during extrusion, were not available to plot). Tanaka et al. (2002) also concluded that ε_{v0} cannot be universally correlated to sample quality based on reconsolidation data on tube samples from eight worldwide Holocene clays and the 350 m thick Osaka Bay Pleistocene clay. The latter showed $OCR \approx 1.5 \pm 0.3$ independent of ε_{v0} ranging from 1.8 to 4.2%,

although ε_{v0} did prove useful for at least one of the former sites. Note that NGI recently proposed using $\Delta e/e_0$ rather than ε_{v0} (Lunne et al. 1997a).

5. Variation in Maximum Virgin Compression Ratio (CR_{max}). Clays with an S-shaped virgin compression line indicate that the material is structured and damage to this structure will reduce the value of CR_{max} , and also σ'_p . For example, high quality samples of the deep low OCR BBC at the CA/T test sites generally gave values of CR_{max} ranging from 0.4 to 0.7, whereas $CR_{max} \approx 0.25 \pm 0.05$ from consolidation tests having OCRs less than one (the deleted tests in Fig. 4.6) (Ladd et al. 1999).

Figure 4.7 shows another example from oedometer tests run on tube samples (extruded in the field) of a highly plastic organic clay for a major preload project on a 15 m thick Nigerian swamp deposit. The engineer simply selected a mean CR from all the tests, whereas the data from less disturbed samples with an $OCR \geq 1$ clearly show that CR_{max} increases significantly with natural water content. This relationship was then used with the variation in w_n with depth to select more realistic values of CR for design.

Recommendations

1. Strength index tests (Torvane, lab vane, etc.) should be run above and below all specimens being considered for engineering tests in order to assess relative changes in sample quality. Also evaluate s_u normalized by σ'_{v0} .
2. All consolidation and CK_0U tests should report the vertical strain (ε_{v0}) at the effective overburden stress to help assess relative changes in sample quality at comparable depths and perhaps as a rough measure of absolute quality.
3. Compare values of CR_{max} since structural damage will reduce this parameter (and also σ'_p), especially for soils with S-shaped virgin compression curves.
4. Radiography is strongly recommended as it provides an excellent method for identifying the best quality soil for consolidation and CU strength tests.
5. Measurements of σ'_s on representative samples can be useful if a suitable device is readily available.

Note that items 1, 2 and 3 (and perhaps 5) involve little or no extra cost and that radiography is highly cost effective.

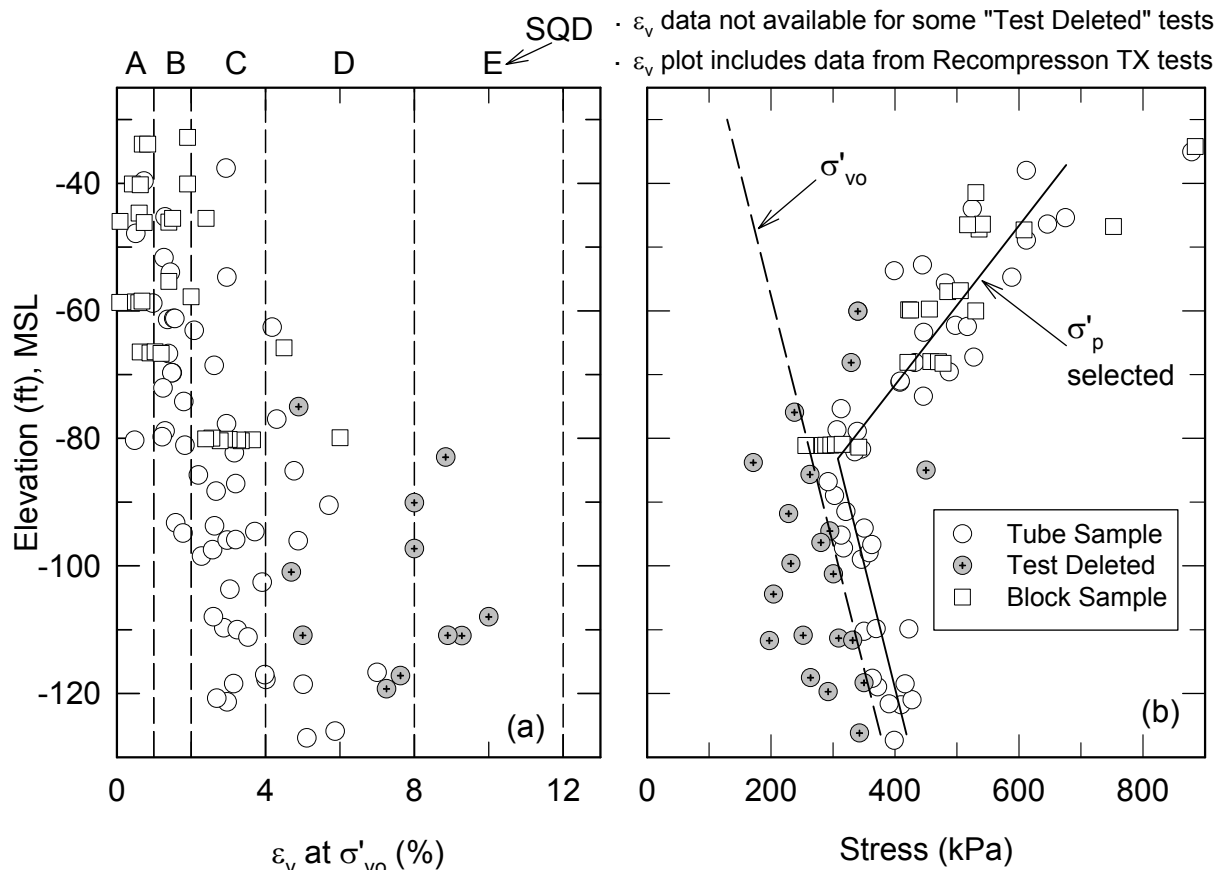


Figure 4.6 (a) Specimen Quality Designation and (b) Stress History for Boston Blue Clay at CA/T South Boston (after Ladd et al. 1999 and Haley and Aldrich 1993)

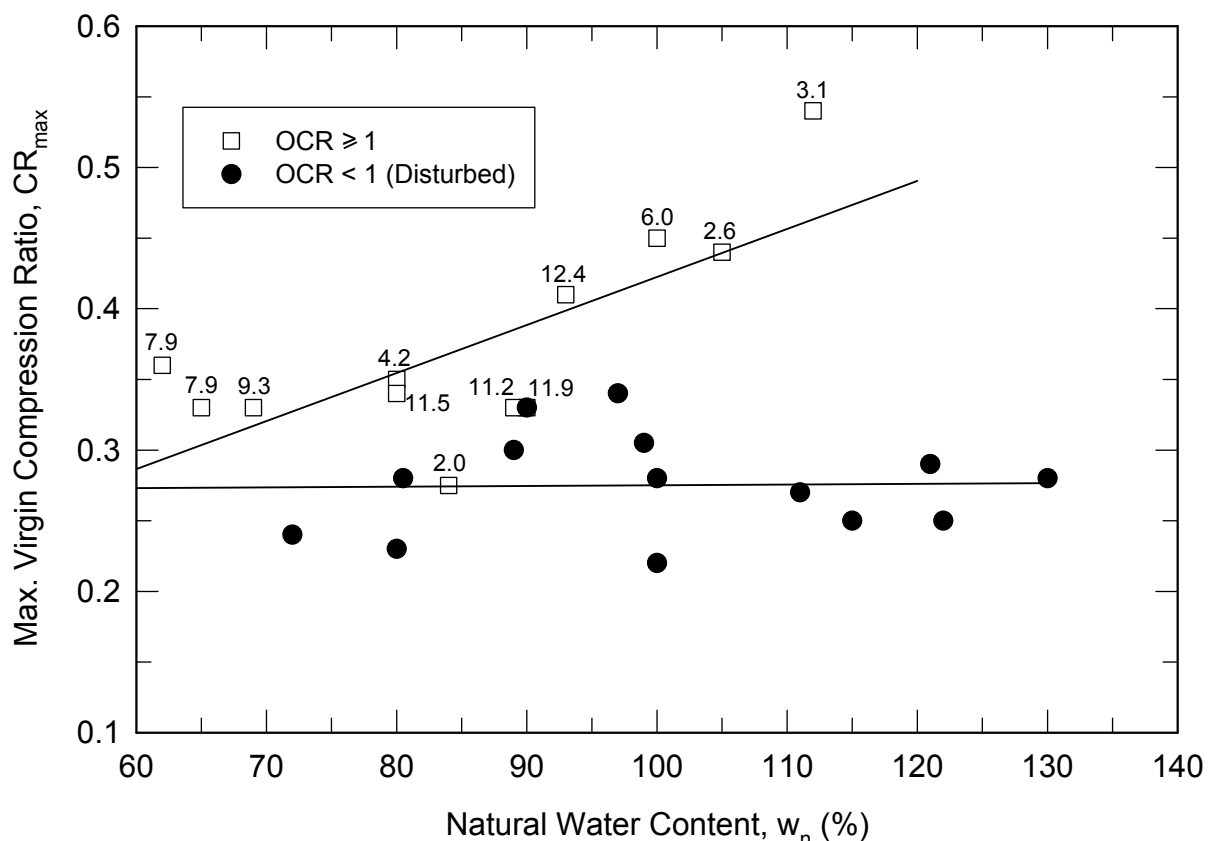


Figure 4.7 Effects of Sample Disturbance on CR_{max} from Oedometer Tests (LIR = 1) on Highly Plastic Organic Clay (numbers are negative elevation (m) for $OCR \geq 1$; GS El. = + 2m)

5 IN SITU TESTING

This section discusses the use of the field vane test (FVT) and the piezocone (CPTU) for the purpose of measuring spatial variations in undrained shear strength and stress history. It also evaluates the ability of these tests to obtain design values of s_u and OCR as opposed to only relative changes in these parameters.

5.1 Field Vane Test

Testing Technique The preferred approach for measuring $s_u(FV)$ in medium to soft clays ($s_u \leq 50$ kPa) has the following features.

- Equipment: four blades of 2 mm thickness with sharpened square ends, diameter (d) = 50 to 75 mm and height (h) = 2d; a gear system to rotate the vane and measure the torque (T); and the ability to account for rod friction. The SGI-Geonor device (designation H-10, wherein the vane head is encased in a sheath at the bottom of the casing and then extended to run a test) and the highly portable Nilcon device (wherein a rod pushes the vane into the ground) are recommended. The Acker (or similar) device with thick tapered blades which are rotated via a handheld torque wrench is not recommended due to increased disturbance during insertion followed by shearing at a rate that is much too fast (failure in seconds rather than minutes).
- Procedure: push vane tip to at least 5 times d (or borehole diameter); after about one minute, rotate at $6^\circ/\text{min}$ to obtain the peak strength within several minutes; then rotate vane 10 times prior to measuring the remolded strength. Compute the peak and remolded strengths using

$$s_u(FV) = \frac{T}{\pi \left(\frac{d^2 h}{2} + \frac{d^3}{6} \right)} = \frac{6T}{7\pi d^3} \quad (\text{for } h = 2d) \quad (5.1)$$

which assumes full mobilization of the same shear stress on both the top and sides of a cylindrical failure surface.

Interpretation of Undrained Shear Strength. It is well established that the measured $s_u(FV)$ differs from the $s_u(\text{ave})$ appropriate for undrained stability analyses due to installation disturbances, the peculiar and complex mode of failure and the fast rate of shearing (e.g., Art. 20.5 of Terzaghi et

al. 1996). Hence the measured values should be adjusted using Bjerrum's (1972) empirical correction factor (μ) vs. Plasticity Index derived from circular arc stability analyses of embankment failures [$\mu = 1/\text{FS}$ computed using $s_u(FV)$]. Figure 5.1 shows this correlation, the data used by Bjerrum and more recent case histories. The coefficient of variation (COV) ranges from about 20% at low PI to about 10% at high PI for *homogeneous* clays (however, Fig. 20.21 of Terzaghi et al. 1996 indicates $\text{COV} \approx 20\%$ independent of PI). Note that the presence of shells and sandy zones can cause a large increase in $s_u(FV)$, as shown by the "FRT" data point (very low μ) for a mud flat deposit.

Bjerrum's correction factor ignores three-dimensional end effects, which typically increase the computed FS by $10 \pm 5\%$ compared to plane strain (infinitely long) failures (Azzouz et al. 1983). Hence the μ factor should be reduced by some 10% for field situations approaching a plane strain mode of failure or when the designer wants to explicitly consider the influence of end effects (see Section 7).

Interpretation of Stress History. Table VI and Fig. 8 of Jamiolkowski et al. (1985) indicate that the variation in $s_u(FV)/\sigma'_{v0}$ with overconsolidation ratio can be approximated by the SHANSEP equation

$$\frac{s_u(FV)}{\sigma'_{v0}} = S_{FV}(\text{OCR})^{m_{FV}} \quad (5.2a)$$

where S_{FV} is the NC undrained strength ratio for clay at $\text{OCR} = 1$. Chandler (1988) adopted Bjerrum's (1972) correlation between $s_u(FV)/\sigma'_{v0}$ for $\text{OCR} = 1$ "young" clays vs. Plasticity Index and $m_{FV} = 0.95$ in order to predict OCR from field vane data, i.e.,

$$\text{OCR} = \left(\frac{s_u(FV)/\sigma'_{v0}}{S_{FV}} \right)^{1.05} \quad (5.2b)$$

Figure 5.2 compares measured values of S_{FV} and m_{FV} for ten sites having homogeneous clays (no shells or sand) and $\text{PI} \approx 10$ to 60% with Chandler's proposed correlation. The agreement in S_{FV} is quite good (error = 0.024 ± 0.017), and excluding the three cemented Canadian clays (for which $m_{FV} > 1$), $m_{FV} = 0.89 \pm 0.08$ compared to $1/1.05 = 0.95$ selected by Chandler (1988). Less well documented experience suggests that Eq. 5.2b and Fig. 5.2 also yield reasonable predictions

of OCR for highly plastic CH clays with $PI > 60\%$. It is interesting to note that the decrease in μ and increase in S_{FV} with PI vary such that $\mu S_{FV} =$

0.21 ± 0.015 for $PI > 20\%$, which is close to the 0.22 recommended by Mesri (1975) for clays with m near unity.

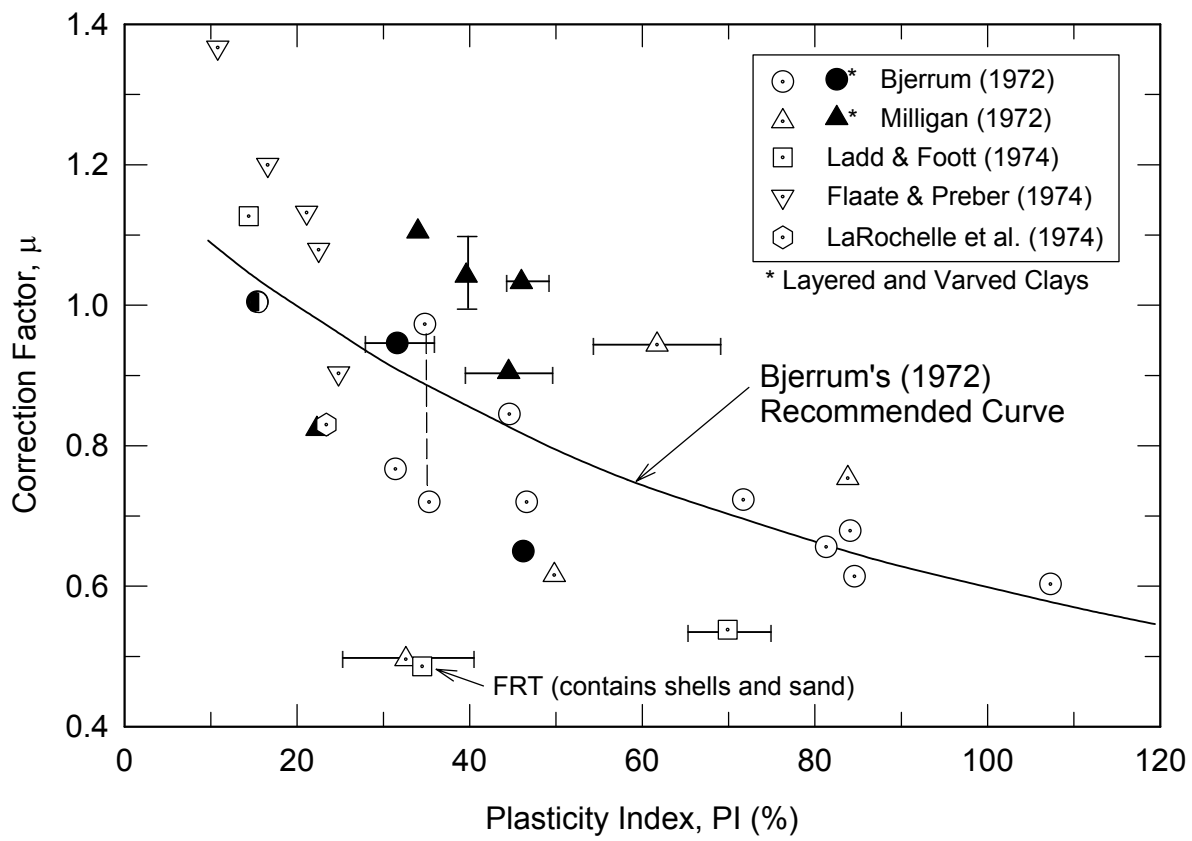


Figure 5.1 Field Vane Correction Factor vs. Plasticity Index Derived from Embankment Failures (after Ladd et al. 1977)

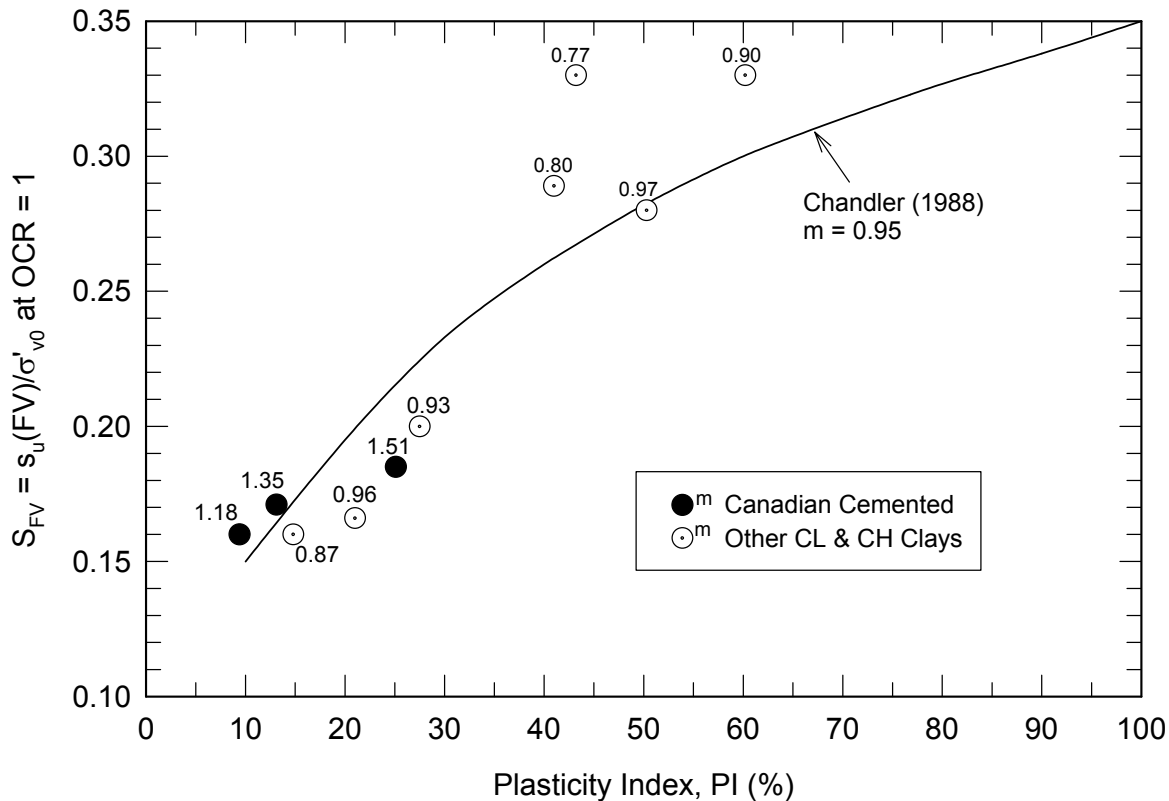


Figure 5.2 Field Vane Undrained Strength Ratio at $OCR = 1$ vs. Plasticity Index for Homogeneous Clays (no shells or sand) [data points from Lacasse et al. 1978 and Jamiolkowski et al. 1985]

Case History. Figure 5.3 shows the location of approach abutments with preload fills for two bridges that are part of a highway reconstruction project founded on 40 m of a varved to irregularly layered CH deposit in Northern Ontario. Construction of the preload fills started on the East side in early October, 2000. Massive failures occurred almost simultaneously at both abutments when the steeply sloped reinforced fill reached a thickness of about 4 m. The sliding mass extended to the opposite (West) bank of the river. The figure also shows the location of three preconstruction CPTU soundings and two borings (B95-9 and B97-12) with 75 mm push tube samples and FV tests. Boring B01-8 on the West side was made after the failure, but before any filling, and did not include FV tests. Subsequent discussion focuses on the upper 15 to 20 m of clay since it is most relevant to the stability and settlement of the preload fills.

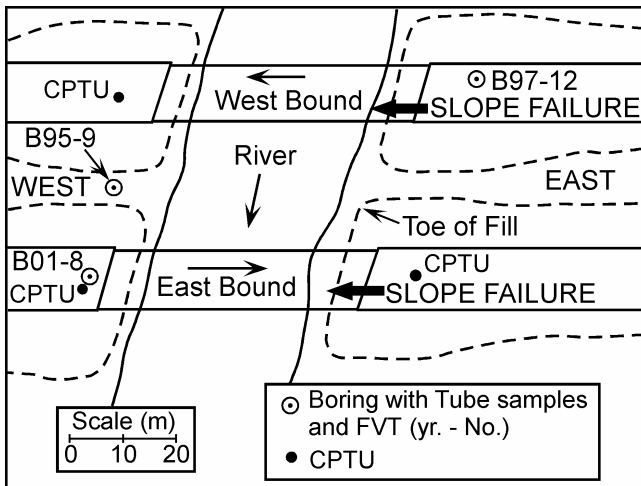


Figure 5.3 Location Plan of Bridge Abutments with Preload Fill and Preconstruction Borings and In Situ Tests

Figure 5.4 presents summary plots of water contents, measured FV strengths and stress history prepared by the first author, who was hired to investigate the failure by the design-build contractor. The clay has an average PI of about 50% and a Liquidity Index near unity. The two $s_u(FV)$ profiles on either side of the river are very similar, with an essentially linear increase with depth. The scatter is relatively small considering the fact that the tests were run with thick, Acker type blades and a torque wrench. However, the recorded sensitivity of only $S_t = 3 - 6$ is too low based on the high Liquidity Index of the clay. It is interesting to note that the two CPTU soundings on the West side predicted strengths some 25% and 80% higher than the one sounding on the East

side, i.e., much larger differences than shown by the field vane data. The preconstruction site investigation included only two consolidation tests within the upper 15 m. The range in σ'_p shown in Fig. 5.4 reflects uncertainty in the location of the break in the S-shaped compression curves because the tests doubled the load for each increment (LIR = 1).

Chandler's (1988) method was used with $S_{FV} = 0.28$ in Eq. 5.2b (for PI = 50%) to predict the variation in $\sigma'_p(FV)$ with depth. The results are plotted in Fig. 5.5 and show good agreement with the two lab tests. Because the agreement may have been fortuitous, and due to uncertainty in virgin compressibility and an appropriate design s_u/σ'_{vc} for the layered deposit, tube samples from boring B97-12 were sent to MIT for testing. The tubes were X-rayed and clay extruded using the cutting-debonding technique illustrated in Fig. 4.3 for several CRS consolidation and SHANSEP CK₀U direct simple shear (DSS) tests. In spite of using 4-year old samples, the test results were of exceptional quality, e.g., see the CRS consolidation data in Fig. 6.5. Four values of σ'_p from the MIT tests are plotted in Fig. 5.5, leading to the conclusion that the $\sigma'_p(FV)$ profiles were reasonable for virgin clay (Note: three DSS tests on NC clay gave $s_u/\sigma'_{vc} = 0.205 \pm 0.004$ SD).

5.2 Piezocone Test

Testing Technique. Figure 5.6 illustrates the bottom portion of a 10 to 20 metric ton capacity 60° piezocone having a base area of 10 cm^2 (15 cm^2 is less common), a base extension of $h_e \approx 5 \text{ mm}$, a filter element of $h_f \approx 5 \text{ mm}$ to measure penetration pore pressures (denoted as u_2 for the filter located at the cylindrical extension of the cone), a dirt seal at the bottom of the friction sleeve and an O-ring to provide a water tight seal. A temperature compensated strain gage load cell measures the force (Q_c) required to penetrate the cone (cone resistance $q_c = Q_c/A_i$, A_i = internal area of recessed top of cone) and a pressure transducer measures u_2 . The porous filter element (typical pore size $\leq 200 \mu\text{m}$) is usually plastic and filled with glycerin or a high viscosity silicon oil (ASTM D5778). Since the u_2 pressure acts around the recessed top rim of the cone, the corrected actual tip resistance is

$$q_t = q_c + u_2(1-a) \quad (5.3)$$

where a = net area ratio = A_i/A_{cone} (should approach 0.8, but may be only 0.5 or lower, and must be measured in a pressure vessel).

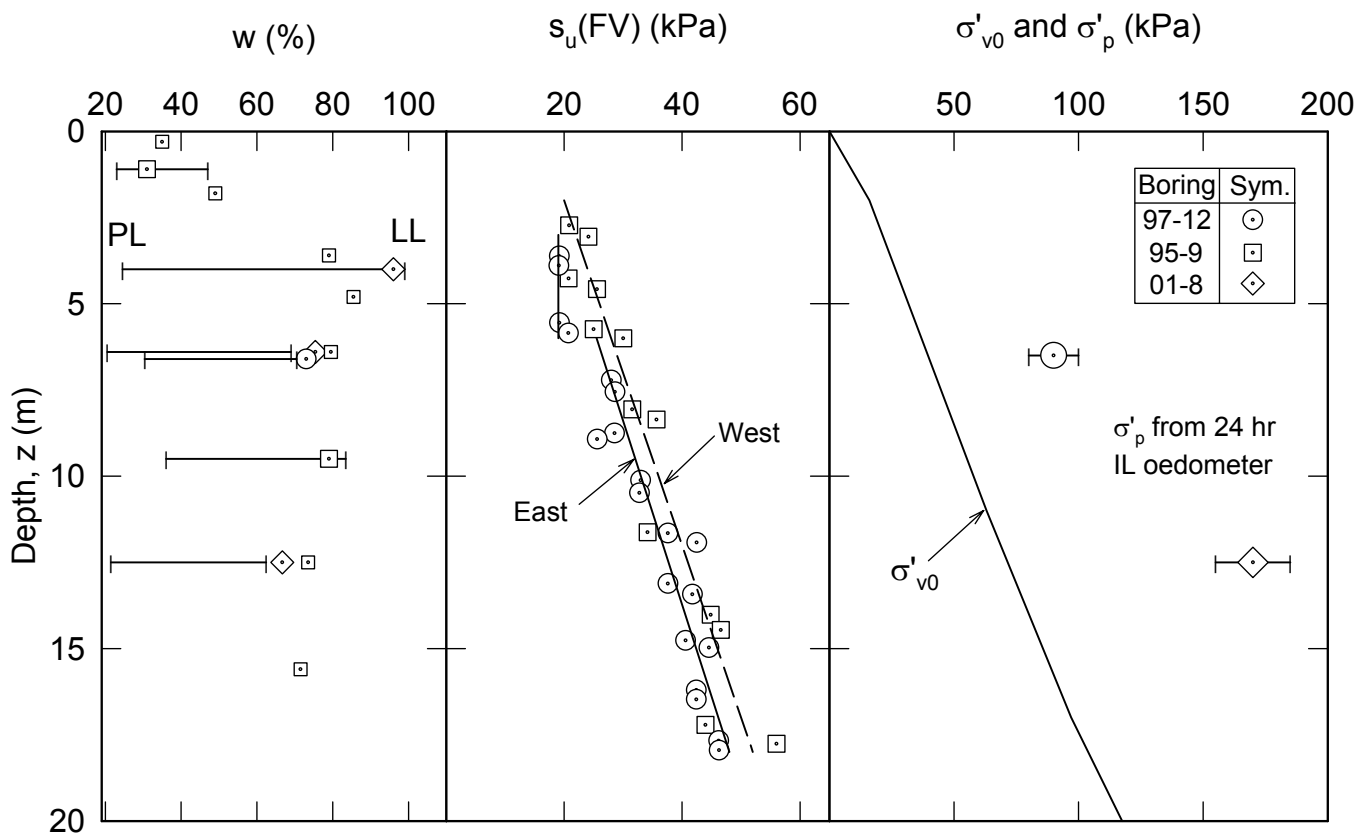


Figure 5.4 Depth vs. Atterberg Limits, Measured $s_u(FV)$ and Stress History for Highway Project in Northern Ontario

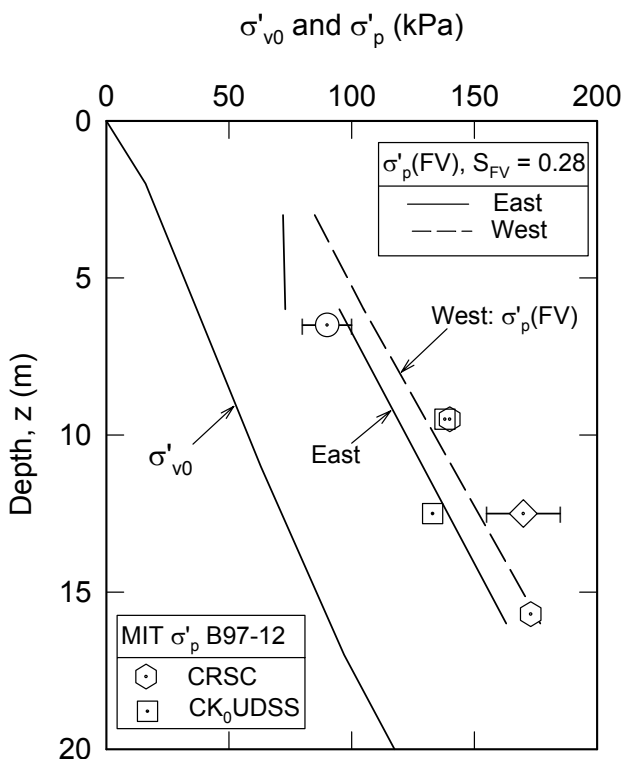


Figure 5.5 Revised Stress History with $\sigma'_p(FV)$ and MIT Lab Tests

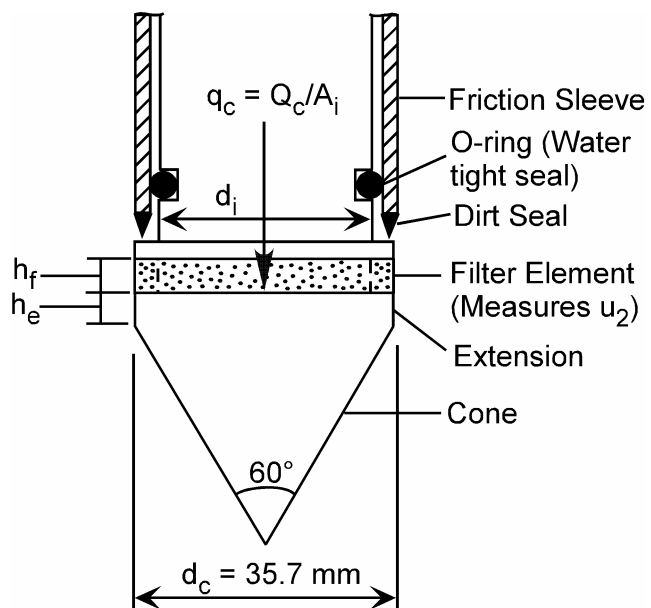


Figure 5.6 Illustration of Piezocone (CPTU) with Area = 10 cm^2 (adapted from ASTM D5778 and Lunne et al. 1997b)

The cone is hydraulically penetrated at 2 cm/s with records of q_c , sleeve friction (f_s) and u_2 at minimum depth intervals of 5 cm. Penetration stops each minute or so to add 1-m lengths of high tensile strength push rods (this affects the data, which should be noted or eliminated). It also is stopped to run dissipation tests, i.e., decrease in u_2 with time, by releasing the force on the push rods.

Quantitative interpretation of piezocone data in soft clays requires very accurate measurements of q_c , u_2 and q_t (f_s approaches zero in sensitive soils). ASTM D5778 recommends load cell and pressure transducer calibrations to 50% of capacity at the start and finish of each project and zero readings before and after each sounding. System overload, rod bending, large temperature changes (inclinometers and temperature sensors are wise additions) and failure of the O-ring seal, as examples, can cause erroneous readings. Desaturation of the pore pressure system is a

pervasive problem since relatively coarse filters can easily cavitate during handling or during penetration in soil above the water table and in dilating sands below the water table. Hence ASTM recommends changing the filter element after each sounding (from a supply of carefully deaired filters stored in saturated oil). However, it still may be difficult to detect u_2 readings in soft clays that are too low, which in turn reduces the value of q_t . Figure 5.7 illustrates an extreme, but typical, example from pre-bid CPTU soundings for the I-15 reconstruction design-build project in Salt Lake City. Poor saturation and possible cavitation in sand layers caused values of u_2 to be even less than the initial in situ pore pressure (u_0) in underlying low OCR clays. The resulting erroneous q_t data negated development of site specific correlations for using the very extensive piezocone soundings for s_u and stress history profiling during final design.

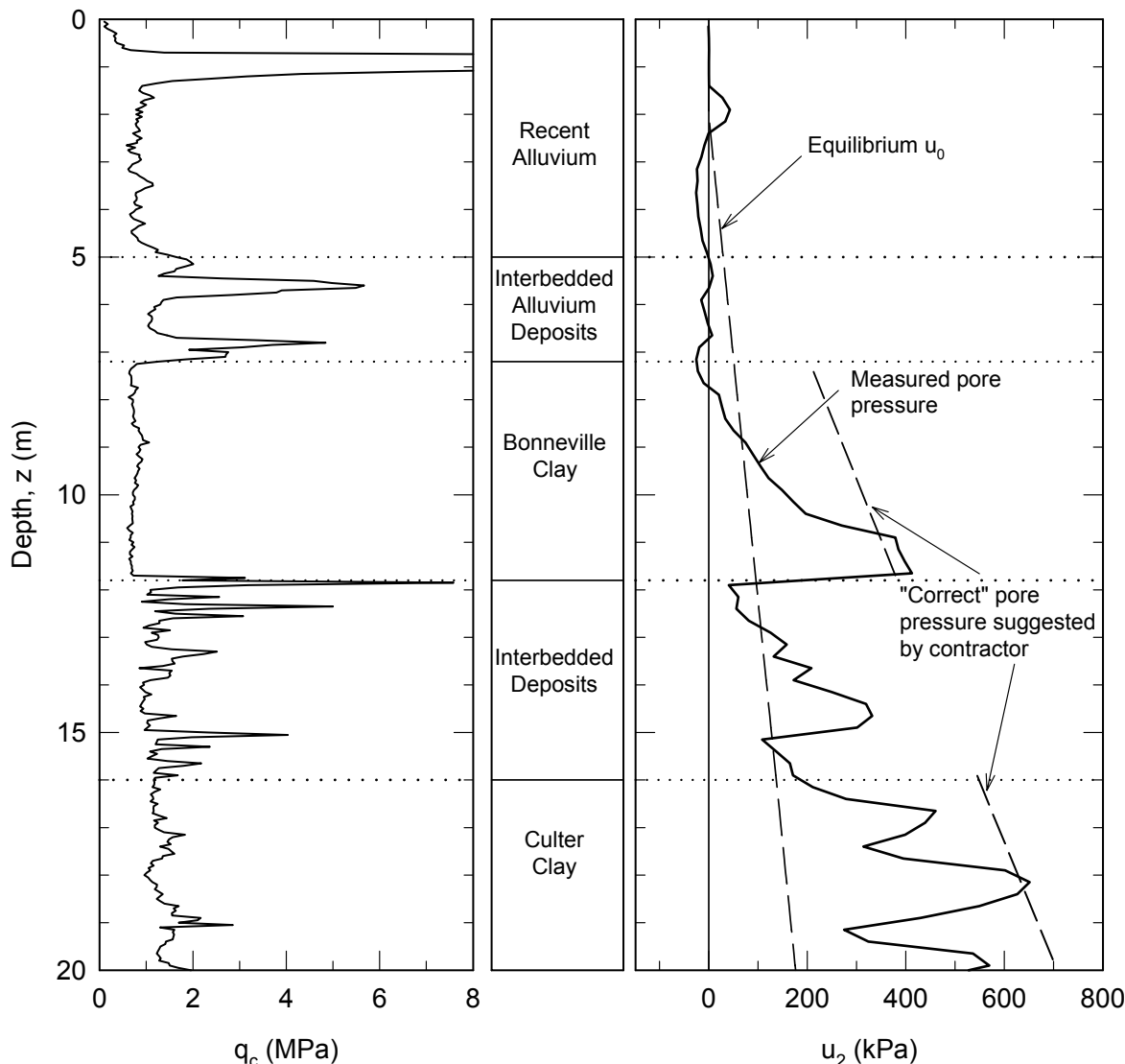


Figure 5.7 Example of Very Low Penetration Pore Pressure from CPTU Sounding for I-15 Reconstruction, Salt Lake City (record provide by Steven Saye)

Interpretation of Undrained Shear Strength.

The undrained shear strength from the piezocone test, $s_u(\text{CPTU})$, relies on empirical correlations between $q_{\text{net}} = (q_t - \sigma_{v0})$ and reference strengths determined by other testing methods. This approach gives values of the cone factor, N_{kt} , equal to q_{net} divided by the reference s_u ; hence

$$s_u(\text{CPTU}) = (q_t - \sigma_{v0})/N_{kt} = q_{\text{net}}/N_{kt} \quad (5.4)$$

For undrained stability analyses, the reference strength should equal $s_u(\text{ave})$, such as estimated from corrected field vane data (for homogeneous clays) or from laboratory CK_0U testing (as discussed in Sections 7 and 8). Reported values of N_{kt} typically range from 10 to 20 (e.g., Aas et al. 1986), which presumably reflect differences in the nature of the clay (e.g., lean and sensitive vs. highly plastic) and its OCR, the reliability of the reference strengths, and the accuracy of q_{net} .

The large variation in cone factor precludes direct use of CPTU soundings for calculating design strengths. One needs a site specific correlation for each deposit. But be aware that N_{kt} may vary between different piezocone devices and operators (e.g., see Gauer and Lunne 2003). Moreover, even with the same system, one can encounter serious discrepancies, as illustrated at two Boston Blue Clay sites.

One site is at the CA/T Project Special Test

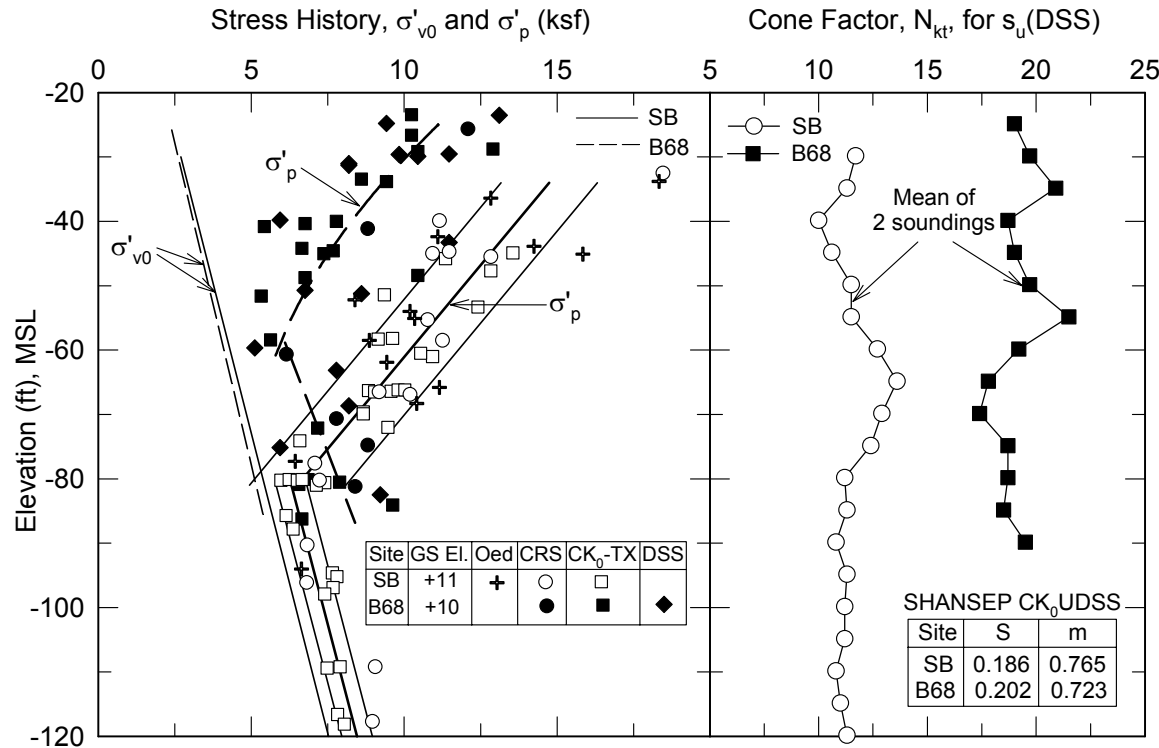


Figure 5.8 Comparison of Stress History and CPTU Cone Factor for Boston Blue Clay at CA/T South Boston and MIT Bldg 68: Reference $s_u(\text{DSS})$ from SHANSEP $CK_0\text{UDSS}$ Tests (after Ladd et al. 1999 and Berman et al. 1993)

Program location in South Boston (Ladd et al. 1999) and the other at Building 68 on the MIT campus (Berman et al. 1993). The marine clay at both sites is covered by 30 ft of fill and either organic silt or marine sand and has a thick desiccated crust overlying low OCR clay. Figure 5.8 shows the well defined stress history profiles developed from several types of 1-D consolidation tests, mostly run at MIT. The SB deposit has a thicker crust and extends deeper than the B68 deposit. SB also tends to be more plastic: typical $LL = 50 \pm 7\%$ and $PI = 28 \pm 4\%$ versus $LL = 40 \pm 10\%$ and $PI = 18 \pm 8\%$ at B68. The same company performed two CPTU soundings at South Boston and four at MIT using the same device ($A = 10 \text{ cm}^2$, $a = 0.81$, 9 mm thick oil saturated Teflon filter resting 3 mm above the cone base) in holes predrilled to the top of the clay. The reference strength profiles were calculated using the mean stress history and values of S and m from extensive CK_0U direct simple shear (DSS) testing by MIT at both sites. Figure 5.8 plots the back calculated value of N_{kt} , which differ by almost two fold. The B68 cone factor is essentially constant with depth, although the mean PI decreases with depth. Hence the variation in N_{kt} is not thought to be caused by differences in the plasticity of BBC. The reason for the discrepancy is both unknown and worrisome.

Interpretation of Stress History. Numerous OCR correlations have been proposed based on q_{net}/σ'_{v0} , $\Delta u/\sigma'_{v0}$, $B_q = \Delta u/q_{net}$ and various combinations of these parameters. Because the penetration excess pore pressure ($\Delta u = u - u_0$) varies significantly with location of the filter element, especially near the base of the cone where u_2 is located, the authors prefer correlations using q_{net} . Lunne et al. (1997b) recommend

$$OCR = k(q_{net}/\sigma'_{v0}) \quad (5.5)$$

with $k = 0.3$ and ranging from 0.2 to 0.5.

If the deposit has large variations in OCR, a SHANSEP type equation is preferred for site specific correlations.

$$OCR = \left(\frac{q_{net}/\sigma'_{v0}}{S_{CPTU}} \right)^{1/m_{CPTU}} \quad (5.6)$$

Figure 5.9 plots the CPTU Normalized Net Tip Resistance versus OCR for the same two BBC sites just discussed. As expected, the two sites have very different values of S_{CPTU} , since this parameter equals N_{kt} times $s_u(CPTU)/\sigma'_{v0}$ for normally consolidated clay. Note, however, that $m_{CPTU} = 0.77 \pm 0.01$ from the two data sets, whereas Eq. 5.5 assumes that m is unity.

Case History. This project involves construction of a 800-m long breakwater for the Terminal Portuario de Sergipe (TPS) harbor facility located 2.5 km off the coastline of northeast Brazil. The site has a water depth of 10 m and a soil profile consisting of 4 m of silty sand and 7 to 8 m of soft plastic Sergipe clay overlying

dense sand. Construction of the initial design with a small stability berm, as shown by the cross-section in Fig. 5.10, started in October, 1988. A failure occurred one year later when the first 100 m length of the central core had nearly reached its design elevation. Geoproyectos Ltda. of Rio de Janeiro developed a "Redesign" with the crest axis moved 39 m seaward and a much wider 5-m thick stability berm. Figure 5.11 shows the locations of the access bridge, the initial failure, the plan of the Redesign, and the locations of relevant borings and CPTU soundings.

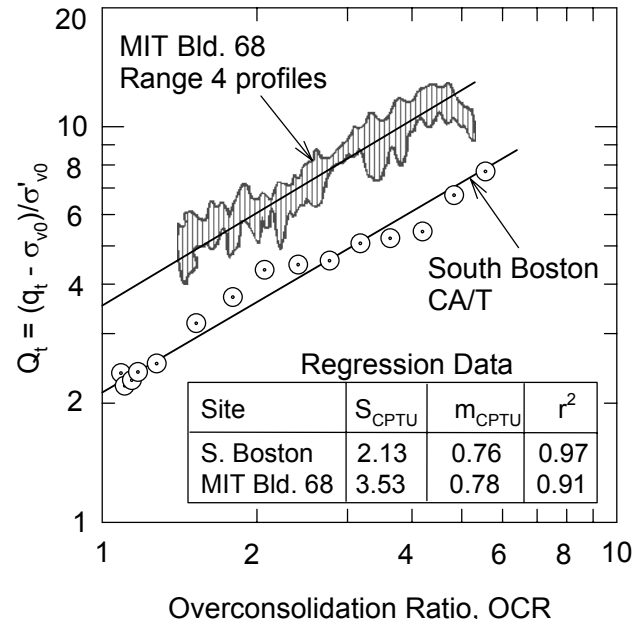


Figure 5.9 Comparison of CPTU Normalized Net Cone Resistance vs. OCR for BBC at South Boston and MIT Bldg 68

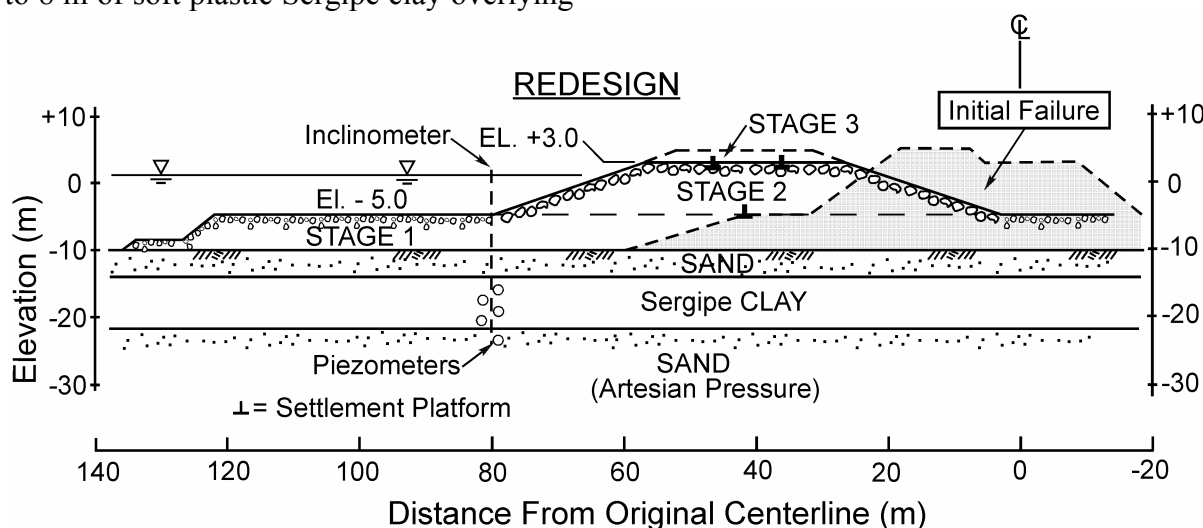


Figure 5.10 Cross-Section of TPS Breakwater Showing Initial Failure, Redesign, and Instrumentation at QM2

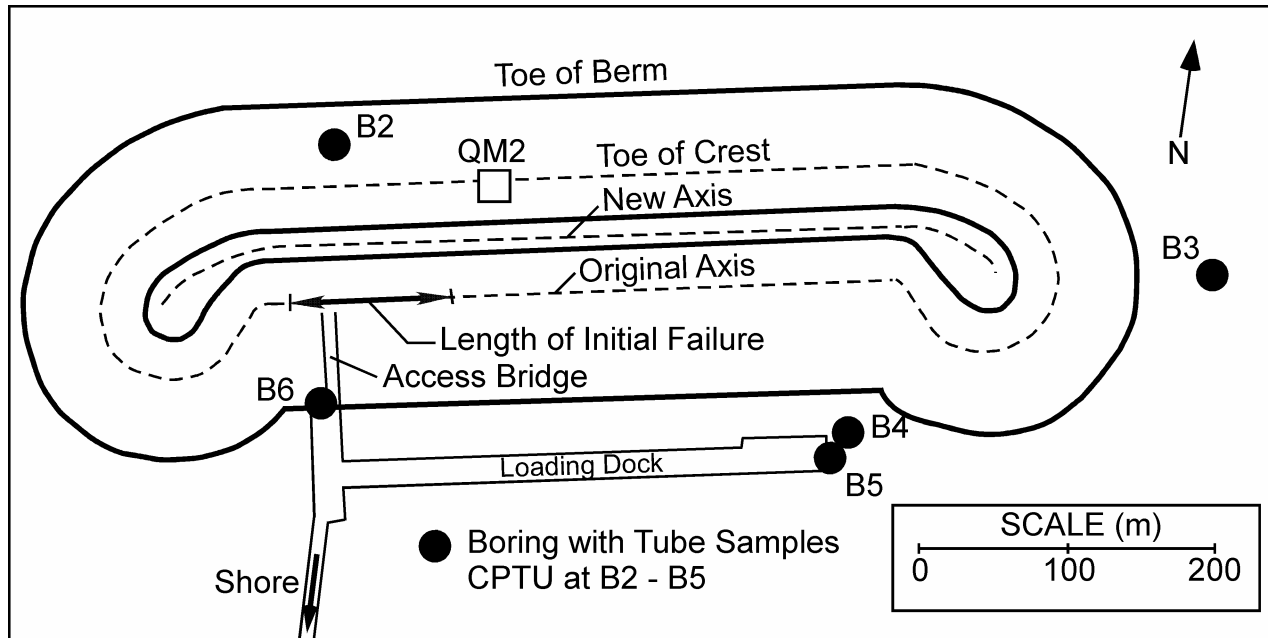


Figure 5.11 TPS Location Plan (Adapted from Geoproyectos, Ltda.)

The Stage 1 rockfill for the new berm was placed by barges during 1990 and construction of the central core (via trucks from the access bridge) reached El. + 3.0 m (Stage 2) by mid-1991. Construction was then halted due to "large" lateral displacements (e.g., 15 cm by the inclinometer at QM2) and results of stability analyses by three independent consultants. The contractor hired MIT in January, 1992 to ensure "99.9%" safety during Stage 3 construction to a final design grade of about El. + 5.5 m. In cooperation with Geoproyectos, two sets of 125 mm Osterberg fixed piston samples were immediately taken at location B6, one for testing in Brazil (6A) and the other by MIT (6B).

Figure 5.12 plots typical water content data and those values of σ'_p judged to be reasonable for the soil profile selected by MIT for Redesign consolidation and stability analyses. The upper 5 m of the CH Sergipe clay has PI = $37 \pm 7\%$ and water contents near the Liquid Limit, while the lower portion becomes less plastic with depth. The nine prior IL (open) and CRS (shaded) consolidation tests had values of vertical strain at the overburden stress of $\varepsilon_{v0} \approx 4 \pm 1\%$ and $\sigma'_p \approx 80 \pm 10$ kPa. The 18 new consolidation data, which included 10 automated SHANSEP CK₀U triaxial and DSS tests, generally had lower values of ε_{v0} and higher values of σ'_p (and also CR, especially for the 6B tests run at MIT).

Selection of a design stress history from the data in Fig. 5.12 posed three problems: very little data within the top 3 m of clay (the upper B6 samples unfortunately were generally quite

disturbed); considerable scatter in σ'_p within the lower portion of the deposit; and insufficient information to assess the potential variation in stress history across the site. Extensive field vane data were available, but these showed large scatter (in part due to the presence of shells and sandy zones) and large discrepancies between the five different programs conducted during 1985 – 1991. Fortunately COPPE (Federal Univ. of Rio de Janeiro) performed four CPTU soundings (at the B2 through B5 locations shown in Fig. 5.11) and these gave very consistent profiles of $q_{net} = q_t - \sigma'_{v0}$, e.g., the coefficient of variation at each elevation was only $5.5 \pm 2.2\%$. Figure 5.13 shows the lab σ'_p values (open and shaded symbols for the IL and continuous loading tests) and how Eq. 5.6 and the q_{net} data were used to develop a σ'_p (CPTU) profile. For the 0.6 m depth interval centered at El. -18.5 m, $\sigma'_p = 83 \pm 7$ kPa from 10 tests (excluding the 109 value), $q_{net} = 279 \pm 13$ kPa, and $\sigma'_{v0} = 48.5$ kPa. For an assumed $m_{CPTU} = 0.8$, one calculates $S_{CPTU} = 3.74$. Thus

$$\sigma'_p(\text{kPa}) = (q_{net}/3.74)^{1.25} (\sigma'_{v0})^{-0.25} \quad (5.7)$$

which led to the solid circles in Fig. 5.13 (the bands denote the SD in σ'_p from the SD in q_{net}). The vertical solid lines equal the selected σ'_p for consolidation analyses (as discussed in Section 8.3). In retrospect, given the small variation in OCR for the deposit (1.4 to 2.0), the more simple Eq. 5.5 could have been used with $k = 83/279 = 0.30$.

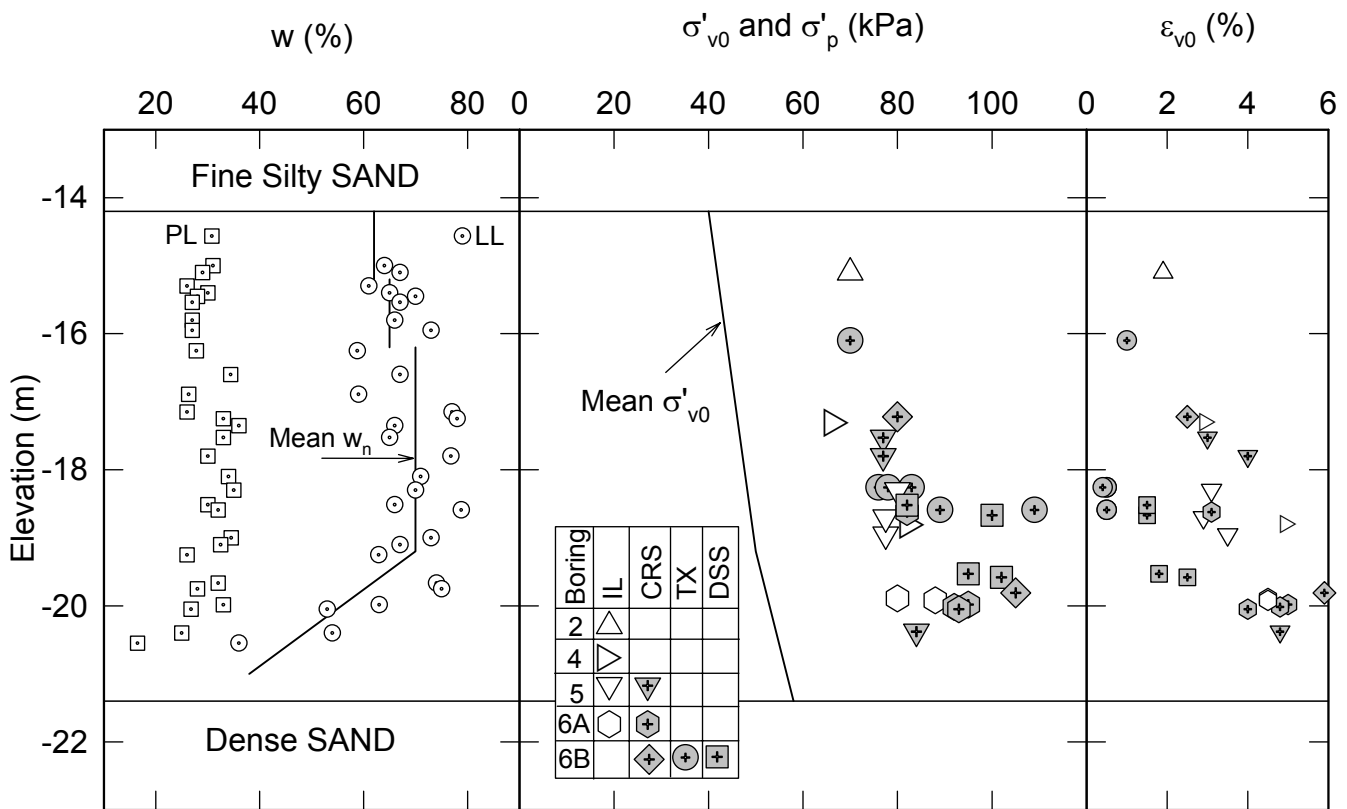


Figure 5.12 Atterberg Limits and Stress History of Sergipe Clay (Ladd and Lee 1993)

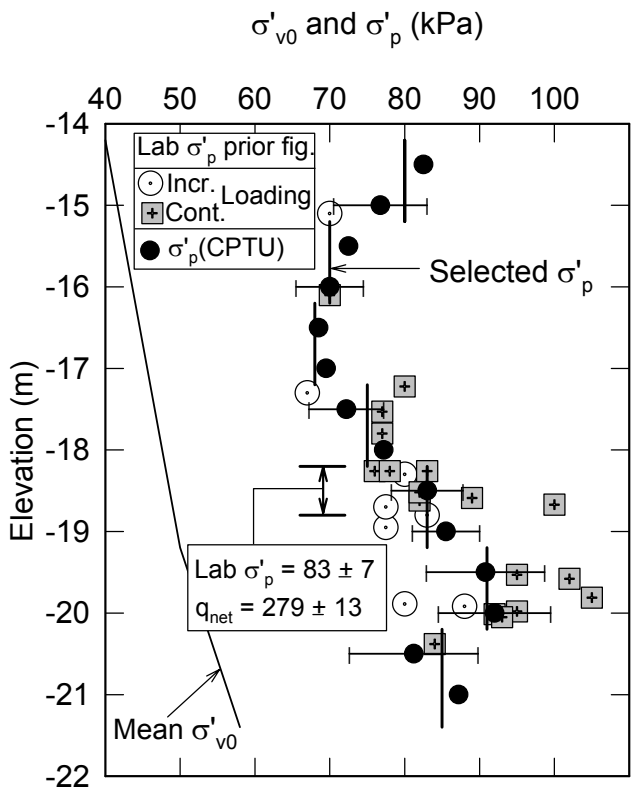


Figure 5.13 Selected Stress History of Sergipe Clay Using CPTU Data from B2 - B5 Soundings (Ladd and Lee 1993)

5.3 Principal Recommendations

The FVT is the most reliable in situ test for estimating values of $s_u(\text{ave})$ via Bjerrum's (1972) correction factor (Fig. 5.1) and for estimating variations in OCR via Chandler's (1988) correlation (Fig. 5.2), both of which require knowledge of the PI of the soil. This conclusion applies to homogeneous deposits (minimal shells and sand zones) and vane devices with thin rectangular blades that are rotated with a gear system at 6°/min. and account for rod friction.

The CPTU is the best in situ test for soil profiling (determining stratigraphy and *relative* changes in clay stiffness) and for checking ground water conditions (Fig. 3.1 and Section 3). However, in spite of ASTM standards and ISSMGE guidelines, details of the cone design may vary significantly, which affects recorded values of q_t and u_2 . Desaturation of the porous filter after penetrating relatively dense sand layers also can be a major problem. Thus the CPTU cannot be used for reliable estimates of $s_u(\text{ave})$ and OCR based on universal correlations. Even deposit specific correlations can vary due to problems with measurement precision and accuracy (e.g., results in Figs. 5.8 and 5.9). However, high quality CPTU data can be very

helpful in defining spatial variations in both stress history (e.g., case history in Figs. 5.10 – 5.13) and undrained strength.

6 LABORATORY CONSOLIDATION TESTING

The one-dimensional consolidation test is typically performed using an oedometer cell with application of incremental loads (IL). This equipment is widely available and the test is relatively easy to perform. However, the constant rate of strain (CRS) test (Wissa et al. 1971) has significant advantages over that of IL equipment as it produces continuous measurement of deformation, vertical load, and pore pressure for direct calculation of the stress-strain curve and coefficients of permeability and consolidation. Furthermore, recently developed computer-controlled flow pumps and load frames allow for automation of most of the test. Capital investment in CRS equipment is higher than IL equipment, but in the broader picture, the improved data quality and test efficiency can result in significant cost benefits.

This section describes laboratory methods and interpretation techniques for determining consolidation design parameters. A brief overview of consolidation behavior fundamentals is followed by a discussion and recommendations for determining consolidation compression curves and flow characteristics. General requirements for the IL test are covered by ASTM D2435 and for the CRS test by ASTM D4186.

6.1 Fundamentals

The one-dimensional compression behavior of soft clays changes dramatically when the load exceeds the preconsolidation stress. This transition stress, which separates small, mostly elastic strains from large, mostly plastic strains, is more appropriately referred to as a vertical loading "yield" stress (σ'_{vy}), although in this paper the more familiar σ'_p notation is used. Jamiolkowski et al. (1985) divided the mechanisms causing the preconsolidation stress for horizontal deposits with geostatic stress conditions into four categories.

- A: Mechanical due to changes in the total overburden stress and groundwater conditions.
- B: Desiccation due to drying from evaporation and freezing.
- C: Drained creep (aging) due to long term secondary compression.

D: Physico-chemical phenomena leading to cementation and other forms of interparticle bonding.

Categories A, B and C are well understood and should be closely correlated to the geological history of the deposit. Although Category D mechanisms are poorly understood, there is no doubt that they play a major role in some deposits, a prime example being the sensitive, highly structured Champlain clay of eastern Canada. The authors hypothesize that various forms of cementation may be primarily responsible for the S-shaped virgin compression curves exhibited by many (perhaps most) natural soft clays. Cementation also can cause significant changes in σ'_p over short distances (i.e., even at different locations within a tube sample). For example, it is thought to be responsible for the large scatter in σ'_p shown in Fig. 5.8 for the deep BBC below El. – 60 ft at the MIT Building 68 site. In any case, very few natural clay deposits are truly normally consolidated, unless either recently loaded by fill or pumping if on land or by recent deposition if located under water.

Figure 6.1 illustrates the significant changes in compressibility and flow properties when a structured clay is loaded beyond the preconsolidation stress. S-shaped virgin compression curves in ϵ_v - $\log\sigma'_v$ space have continuous changes in CR with stress level, with the maximum value (CR_{max}) located just beyond σ'_p . As the loading changes from recompression (OC) to virgin compression (NC), c_v and C_a also undergo marked changes. For undisturbed clay, $c_v(OC)$ is typically 5 to 10 times the value of $c_v(NC)$, which is mostly due to a lower coefficient of volume change ($m_v = \Delta\epsilon_v/\Delta\sigma'_v$) in the OC region. The rate of secondary compression increases as σ'_v approaches σ'_p and often reaches a peak just beyond σ'_p . This change in C_a is uniquely related to the slope of the compression curve as clearly demonstrated by Mesri and Castro (1987), such that C_a/CR is essentially constant for both OC and NC loading (Note: here "CR" equals $\Delta\epsilon_v/\Delta\log\sigma'_v$ at all stress levels). For most cohesive soils $C_a/CR = 0.04 \pm 0.01$ for inorganic and 0.05 ± 0.01 for organic clays and silts (Table 16.1, Terzaghi et al. 1996). The vertical permeability decreases with an increase in σ'_v with an approximate linear relationship between e and $\log\sigma'_v$ such that

$$k_v = k_{v0}(10)^{\frac{e - e_0}{C_k}} \quad (6.1)$$

where k_{v0} = vertical permeability at the in situ void ratio e_0 . The coefficient $C_k = \Delta e / \Delta \log k_v$ is empirically related to e_0 such that for most soft clays, $C_k \approx (0.45 \pm 0.1)e_0$ (Tavenas et al. 1983, Terzaghi et al. 1996).

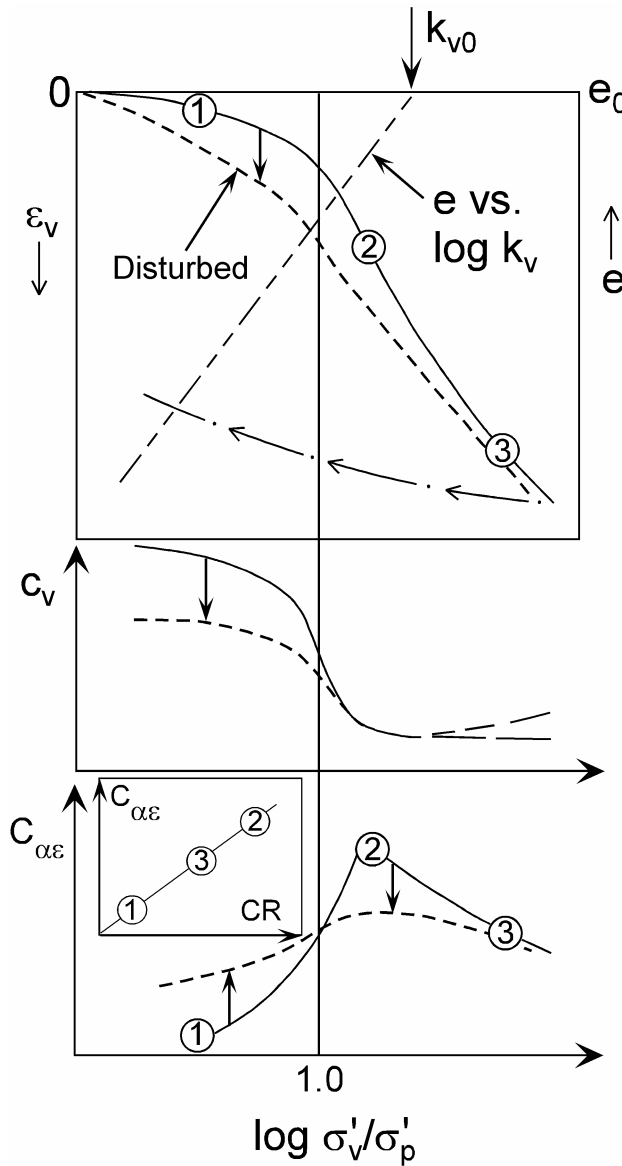


Figure 6.1 Fundamentals of 1-D Consolidation Behavior: Compression Curve, Hydraulic Conductivity, Coefficient of Consolidation and Secondary Compression vs. Normalized Vertical Effective Stress

Most of the aforementioned one-dimensional consolidation properties are adversely influenced by sample disturbance, as also illustrated in Fig. 6.1. Sample disturbance results in a more rounded compression curve with greater ϵ_v at all stress levels. The increased compressibility in the OC range (higher RR) and decreased compressibility in the NC range (lower CR) tend to obscure and usually lower σ'_p , especially for S-shaped

compression curves (with much lower values of CR_{max} , e.g., Fig. 4.7). During recompression, $c_v(OC)$ is usually much lower and $C_\alpha(OC)$ is higher. The only parameters not significantly affected by sample disturbance are $c_v(NC)$ well beyond σ'_p and the e - $\log k_v$ relationship, unless there is severe disturbance.

The potential existence of secondary compression (or drained creep) during primary consolidation is controversial with two opposing theories (Ladd et al. 1977). Hypothesis A (Mesri et al. 1994) assumes that secondary compression occurs only after the end-of-primary (EOP) consolidation, whereas Hypothesis B (Leroueil 1994) assumes that secondary compression also occurs during primary consolidation. Proponents on both sides present convincing data for validating one hypothesis over the other. There is little difference between the hypotheses for interpretation of standard laboratory incremental load consolidation tests using thin specimens. But very significant practical differences occur when predicting field consolidation settlements with $\sigma'_{vf}/\sigma'_p < 2 - 3$ for thick clay layers having long durations for dissipation of excess pore pressures, i.e., large values of t_p . Without dwelling on the details of this controversy, which are beyond the scope of this paper, design calculations using either hypothesis require essentially the same information from the site characterization program (i.e., σ'_p , CR , c_v , C_α , etc.). It is, however, noted that all clays exhibit significant one-dimensional strain rate effects at fast rates (e.g., Leroueil 1994), which has important implications for CRS testing as further discussed below.

6.2 Compression Curves

IL oedometer and CRS tests are usually conducted by first loading the specimen beyond the preconsolidation stress (σ'_p) to a maximum stress sufficient to define the virgin compression line, followed by unloading to the seating load. In some cases an unload-reload cycle is used to better define the OC behavior (i.e., RR), although for most soft ground construction problems this is not an important design issue. During initial set-up, a seating load of approximately 3 to 5 kPa should be applied prior to determining the reference zero reading for displacement measurements. The authors prefer using moist filter stones (as opposed to dry, e.g., Sandbækken et al. 1986) and adding water after application of the seating load. The specimen should be monitored to check for swelling and additional load applied, as necessary, to prevent swelling.

Traditional IL tests employ 15 – 20 mm thick specimens, a load increment ratio (LIR) of one and 24 hour load increments. For many soft clays, particularly those with S-shaped compression curves, doubling the load is too high to properly define the compression curve. Furthermore, 24 hour increments include secondary compression deformations, which result in lower estimates of σ'_p by about $15 \pm 5\%$. Better definition of the compression curve can be achieved using a reduced LIR (e.g., $\frac{1}{2}$) at σ'_v increments bracketing σ'_p and EOP data. For consistent definition of the EOP compression curve, it is best to plot data for all increments at one constant time of consolidation (t_c). The selected value of t_c should be based on the maximum t_p estimated from increments in the NC region, which typically ranges from 10 to 100 min.

Better definition of consolidation properties are obtained from CRS tests for which continuous data are collected. In the CRS test, the drainage is one-way and the base excess pore pressure (u_e) is measured with a pressure transducer. The measured ε_v - σ_v - u_e data are used with a linear CRS theory (e.g., Wissa et al. 1971) to compute continuous values of ε_v , e , σ'_v , k_v , and c_v . The strain rate for CRS tests needs to be selected such that the normalized base excess pore pressure (u_e/σ_v) is within acceptable limits. Too slow a rate will result in $u_e = 0$ and secondary compression strains, while too fast a rate will result in high excess pore pressures leading to significant variations of void ratio and σ'_v in the specimen. The selected strain rate should give $u_e/\sigma_v \approx 10 \pm 5\%$ in the NC range (e.g., Mesri and Feng 1992). Note that ASTM D4186 allows excess pore pressures that can be too high, especially during virgin compression. Mesri and Feng (1992) present an equation to compute a strain rate which gives the same compression curve as the EOP curve from IL tests. They also recommend using a rate ten times larger than this so that sufficient excess pore pressure develops to measure k_v and c_v . For typical soft clays, this gives a strain rate of about 0.5 to 1.0 %/hr that should produce u_e/σ_v less than 15%. However, the resulting σ'_p will be about 10% greater than the EOP σ'_p due to strain rate effects (Mesri et al. 1994). NGI uses a strain rate of 0.5 to 1%/hr for most CRS tests (Sandbækken et al. 1986).

Figure 6.2 compares CRS and IL (with LIR = 1) data for tests conducted on Sherbrooke block samples of Gloucester Clay from Ottawa, Canada and Boston Blue Clay from Newbury, MA. The CRS tests were run at a strain rate of 1%/hr resulting in normalized base excess pore pressures

(u_e/σ_v) that were greater than 1%, but well below 10% for the majority of the tests to minimize rate effects on σ'_p . The IL EOP data were determined using a constant t_c taken from t_p in the NC region. The Gloucester data in Fig. 6.2a shows that the IL EOP curve results in values of σ'_p and CR_{max} that are far too low. For the BBC tests, the IL 24 hr data gives values of σ'_p and CR_{max} that are too low. The EOP IL data, using $t_c = 40$ min. throughout the test, produced a more realistic compression curve, but with a CR_{max} value that is still too low. However, the good agreement between the EOP IL and CRS σ'_p values was fortuitous in that the selected load increments for the IL test just happen to result in one of the load increments close to σ'_p . If the clay had a different value of σ'_p , or a different load increment schedule was used, the comparison would not be as favorable.

Figure 6.3 plots the vertical strain – time data for three increments of the BBC IL test in Fig. 6.2b and highlights the difficulty with interpreting such curves for an increment near σ'_p . The three increments span the CRS $\sigma'_p = 193$ kPa. The time curves for the 100 kPa and 400 kPa increments have distinct breaks and are easily interpreted using the Casagrande log time method to estimate t_p (the break is not visible for the 100 kPa increment in Fig 6.3 only because of the scale used for the vertical axis). The 200 kPa increment almost coincides with σ'_p and contains a significant amount of secondary compression during the 24 hr loading period. The large amount of secondary compression is consistent with the sharp increase in CR near σ'_p (i.e., C_a/CR is a constant). Neither the log time method nor the root time method can be used to estimate the EOP for this increment. This problem is a prime reason for recommending the use of a constant t_c (based on maximum t_p in the NC range) for plotting EOP strains for all increments.

At strain rates around 1%/hr, a typical CRS test with back pressure saturation takes about 3 to 4 days (without an unload-reload cycle), which is much faster than the traditional IL test with 24 hr load increments. Test durations comparable to the CRS test are feasible for IL testing, but load increments must be applied soon after primary consolidation for each increment. This can be achieved using automated computer controlled equipment (e.g., Marr 2002) or frequent manual application of loads. Estimates of C_a from CRS tests are feasible if the test is stopped during loading and maintained at constant σ'_v for a long enough duration (e.g., at the maximum stress prior to unloading), although definition of C_a is less

reliable than from IL oedometer tests due to an ill-defined zero time. The measured C_a/CR ratio can be used to estimate C_a at other stress levels having different values of CR.

As an added advantage of automation, computer controlled CK_0 stress path triaxial tests for specimens consolidated beyond σ'_p give reliable data for determining the compression curve (i.e., σ'_p , CR). The automated K_0 consolidation also measures K_0 for NC clay and provides sufficient data for estimating the in situ K_0 using the method of Mesri and Hayat (1993). More details on triaxial equipment and test procedures are given in Section 8.

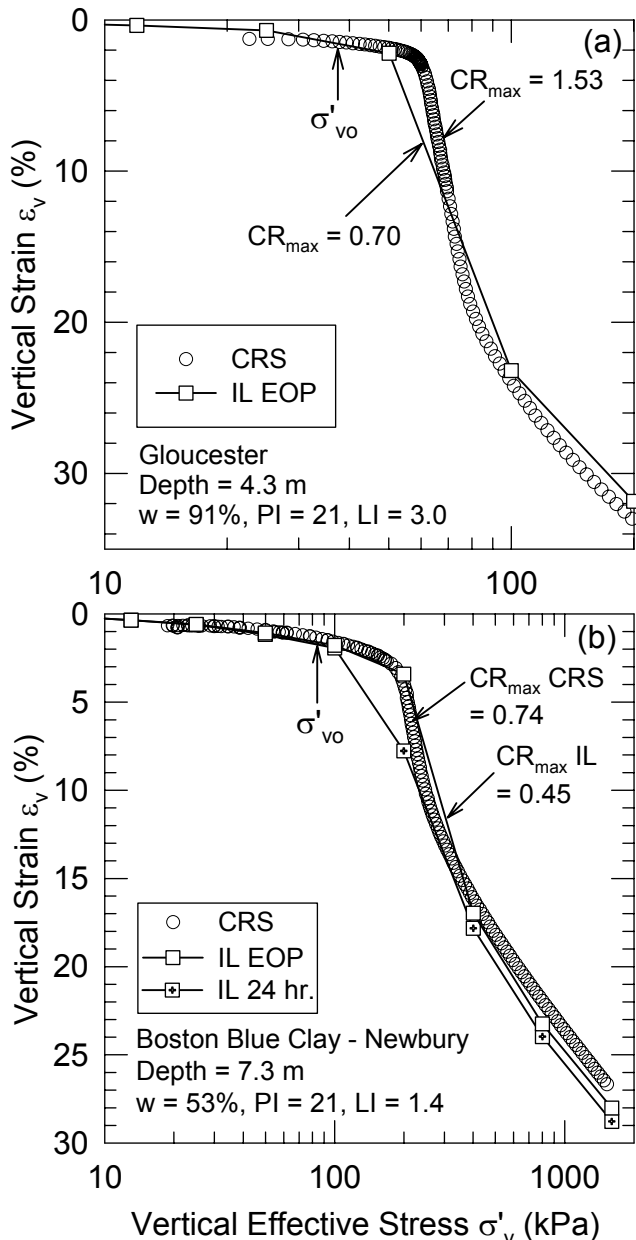


Figure 6.2 Comparison of Compression Curves from CRS and IL Tests on Sherbrooke Block Samples (CRS tests run with $\Delta\epsilon/\Delta t = 1\%/\text{hr}$): (a) Gloucester Clay, Ottawa, Canada; (b) Boston Blue Clay, Newbury, MA

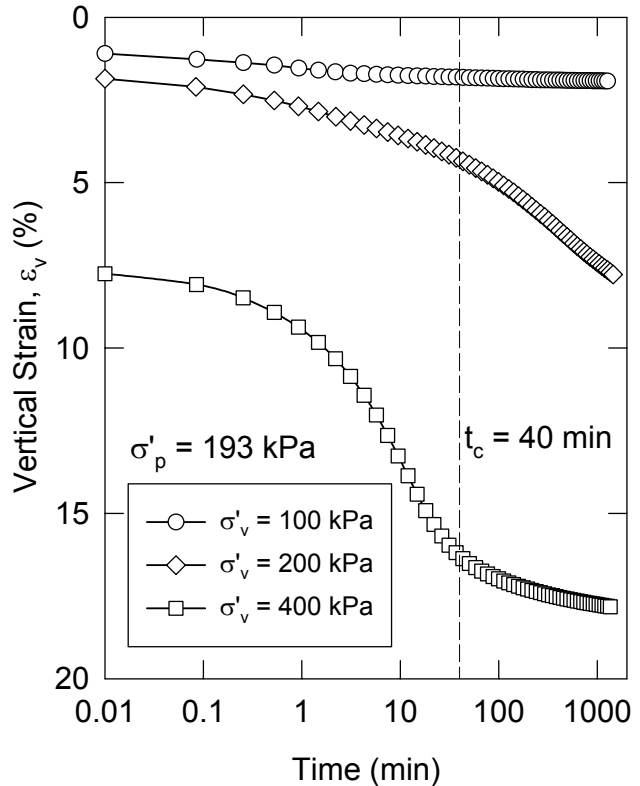


Figure 6.3 Vertical Strain – Time Curves for Increments Spanning σ'_p from the IL Test on BBC Plotted in Fig. 6.2b.

Numerous methods have been proposed for estimating σ'_p , but they all depend on reliable data from good to high-quality samples. The compression curve used for interpretation should be from CRS tests conducted at an acceptable strain rate (say 0.5 to 1.0 %/hr, with perhaps a 10% reduction in σ'_p as noted previously) or consistent end of primary data from IL tests with appropriate LIRs. The maximum load must be sufficient to prove that CR is either constant or decreasing. Casagrande's method is the oldest, simplest, and most widely used technique for estimating σ'_p . However, it can be quite subjective and is difficult to apply with relatively stiff soils having rounded compression curves. The strain energy method of Becker et al. (1987) uses work per unit volume as the criterion for estimating σ'_p from a plot of strain energy versus σ'_v in linear scales (Fig. 6.4). The method is easy to use and typically results in more reliable and consistent estimates of σ'_p as compared to Casagrande's procedure, especially for stiffer clays with more rounded compression curves. For application of the strain energy method it is important to note that the method uses the natural strain to compute the strain energy and that the maximum slope of

the strain energy vs. σ'_v plot in the NC range should be used for the interpretation, rather than the average slope.

6.3 Flow Characteristics

The secondary compression that occurs in conventional 24 hr IL tests causes the soil to initially behave as an overconsolidated material with high c_v during the next load increment. Hence derived values of c_v depend upon the graphical construction method selected to estimate c_v . For example, for one day tests with $LIR = 1$, $c_v(\sqrt{t}) \approx (2 \pm 0.5)$ times $c_v(\log t)$. The problem gets worse at lower LIRs, such that c_v may become indeterminate, unless one also reduces the time increment in order to reduce the amount of secondary compression. CRS testing not only avoids this problem, but also produces continuous values of k_v and c_v versus ε_v and σ'_v .

Figure 6.5 shows computer generated plots from a CRS test run at MIT on the lacustrine clay for the case history presented at the end of Section

5.1. The results are typical of CRS tests on structured clays (e.g., S-shaped compression curve, with well-defined σ'_p and large decreases in CR, minimum u_e/σ_v near σ'_p and large drop in c_v as σ'_v approaches σ'_p) except for the e-log ε_v data. The initial k_v data usually plot to the right of the linear relationship, rather than to the left as shown in Fig. 6.5.

6.4 Principal Recommendations

Test Selection. The CRS test should largely replace the conventional 24 hr IL oedometer test for measuring the consolidation properties of soft clays because it

- Gives a continuous compression curve, which is especially important for structured clays with S-shaped virgin compression lines.
- Provides continuous unambiguous values of k_v and c_v .
- Can be completed in far less time. A strain rate of 0.5 to 1.0 %/hr is suitable for most clays in order to achieve $u_e/\sigma_v \approx 10 \pm 5\%$.

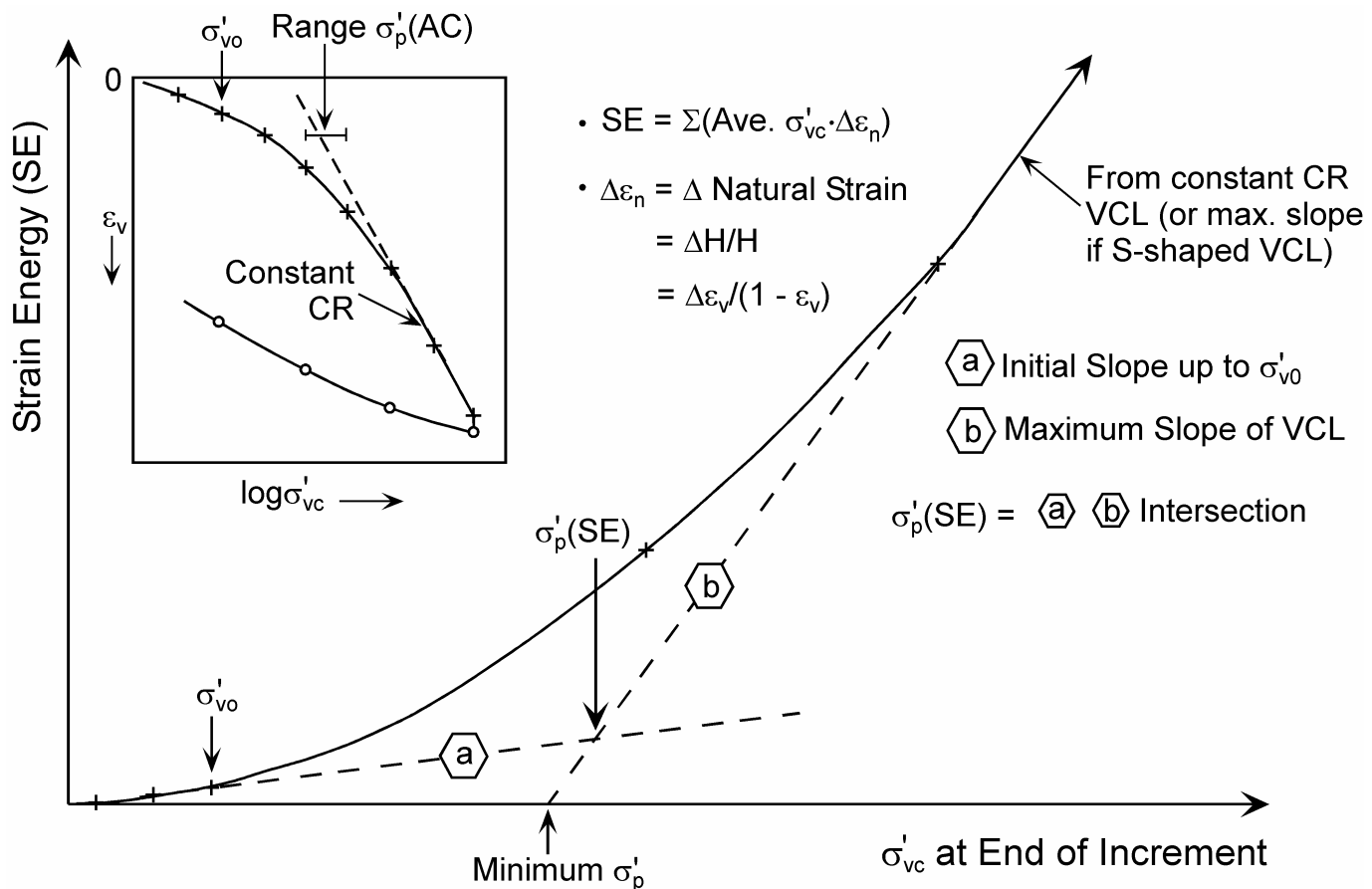


Figure 6.4 Estimation of Preconsolidation Stress Using the Strain Energy Method (after Becker et al. 1987)

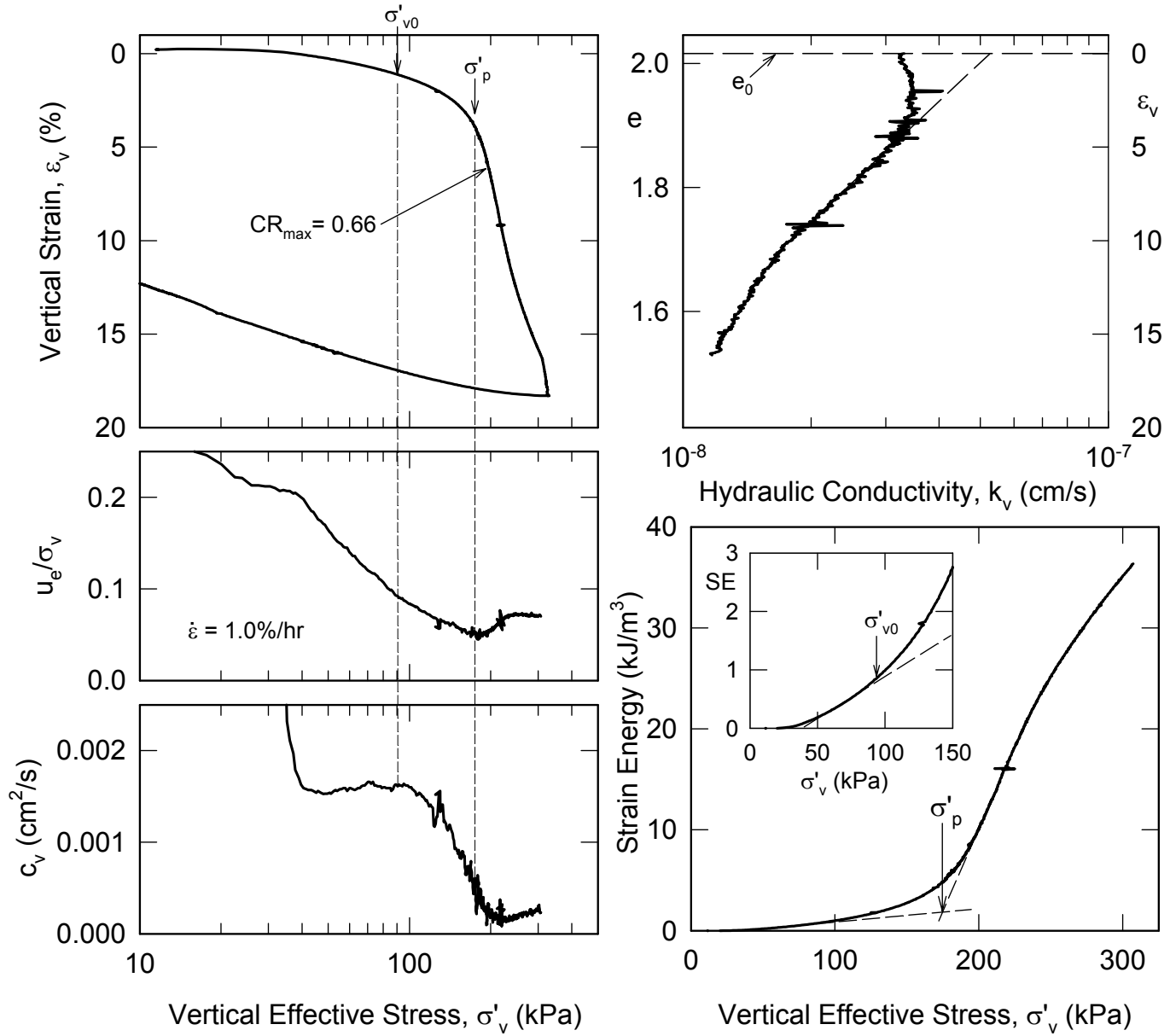


Figure 6.5 Results of CRS Test on Structured CH Lacustrine Clay, Northern Ontario, Canada ($z = 15.7 \text{ m}$, $w_n = 72\%$, Estimated LL = $75 \pm 10\%$, PI = $47 \pm 7\%$)

However, the IL test is better suited for measuring C_α as a function of OCR for projects where surcharging is used to reduce long term secondary compression settlements. For structured clays, the LIR should be reduced (say to one-half) in the vicinity of σ'_p . The time t_c for each increment also can be reduced (but at the expense of losing $c_v(\log t)$ and C_α).

Atterberg limits should be run for each test specimen (at least for the first test series), plus some specific gravity tests to obtain an average G_s for the soil. Hydrometer analyses are less important.

Individual Test Results. An appropriate sheet should document the results of each IL test (e.g., dimensions, location, index properties, load and time increments, ε_v and e , strain energy, t_{50} and t_{90} , c_v , C_α and C_α/CR). Recommended plots for each test include ε_v vs. $\log \sigma'_v$ (at a constant $t_c \approx$ the NC t_p) showing σ'_{v0} and σ'_p , and strain energy vs. σ'_v , plus at least representative \sqrt{t} and $\log t$ curves for increments exceeding σ'_p . Although void ratio is useful for research and some consolidation computer programs, strain is far better suited for practice in order to standardize scales for the compression curves and to obtain RR and CR. Moreover, values of C_c have little

meaning without knowing e_0 . For CRS tests, plots such as those in Fig. 6.5 are recommended. Report ε_v at σ'_{v0} and use both the Casagrande and strain energy methods to estimate σ'_p . Consider reducing σ'_p from CRS tests of excellent quality by 10%. Finally, the results from all consolidation tests should be summarized in a table that includes at least a qualitative assessment of sample quality (e.g., excellent, good, fair or poor).

Selecting Design Parameters. Selection of the stress history profile is the most important and often the most difficult task. Always include a plot showing the soil profile and elevation vs. σ'_{v0} (document how obtained), the measured lab σ'_p data with quality assessments, and the selected stress history profile(s). The latter should consider the local geology, spatial variation in index properties (w_n , AL and LI) and CR_{max} , and results from in situ tests. As covered in Section 5, σ'_p profiles estimated from field vane data, and perhaps CPTU soundings, can be very helpful in developing best estimates of spatial variation in σ'_p both with depth and across the site.

CR is the most important compressibility parameter. With structured clays, one usually wants values of CR_{max} for design, unless CR becomes significantly lower at the in situ σ'_{vf} . If CR_{max} is highly variable, both due to natural variability and because of sample disturbance, a site specific correlation between w_n and values of CR_{max} from better quality tests can be very useful, as discussed in connection with Fig. 4.7.

The design value of $c_v(NC)$ is critical for preloading and staged construction without vertical drains. Navfac DM-7.1 (1982) provides a very useful correlation between c_v and Liquid Limit (Fig. 4, p. 7.1-144). Reported values of $c_v(NC)$ that deviate by more than a factor of two from the mean trend line should be questioned. For projects with vertical drains, one needs $c_h = r_k c_v$, where $r_k = k_h/k_v$. The value of r_k for marine clays is essentially one and for lacustrine varved clays may approach 5 to 10 (e.g., Tavenas et al. 1983, Mesri and Feng 1994, DeGroot and Lutenegger 2003). For these clays, r_k can be estimated most easily in the laboratory via permeability or CRSC tests on vertical and horizontal specimens, whereas in situ testing (CPTU dissipation, piezometers, etc.) is better suited for deposits with irregular layers of more permeable soil (Ladd 1991). Note, however, that soil disturbance caused by installation of displacement drains (e.g., wick drains) will lower

the effective c_h at close drain spacings (Saye 2003).

Selection of $C_\alpha(NC)$ is best done by first establishing C_α/CR for the deposit and then applying this ratio to the design values of CR. For the reduction in C_α with OCR due to surcharging, see Fig. 6 and 7 of Saye et al. (2001).

7 UNDRAINED SHEAR BEHAVIOR AND STABILITY ANALYSES

7.1 Review of Behavioral Fundamentals

This section reviews five major factors affecting the undrained shear behavior of cohesive soils 1) the stress history of the soil; 2) the stress system applied during shear (mainly effects of anisotropy); 3) the influence of progressive failure and strain compatibility; 4) the influence of the rate of shearing; and 5) the effects of sample disturbance. Except for the last item, the discussion focuses on results from K_0 consolidated-undrained shear (CK_0U) tests as these replicate the behavior of in situ clay under horizontal ground.

Stress History. The increase in undrained strength ratio of clays with increasing overconsolidation ratio can be modeled by the SHANSEP equation

$$s_u/\sigma'_{vc} = S(OCR)^m \quad (7.1)$$

as illustrated in Fig. 7.1 for two clays, each with three modes of shearing (triaxial compression and extension and direct simple shear). The CK_0U tests were run using the SHANSEP reconsolidation technique for the plastic, insensitive AGS clay and using the Recompression technique for the lean, highly sensitive James Bay clay (these techniques are described in Section 8.2). The strength increase with OCR for the AGS clay is mainly due to changes in the shear induced pore pressure from contractive (positive) to dilative (negative) with increasing OCR, as is typical of most non-structured soils. In contrast, the shape of the yield (bounding) surface is mainly responsible for the strength increase for the highly structured and cemented James Bay clay. The value of m for most cohesive soils equals 0.8 ± 0.1 . The shear strain required to reach the peak strength (γ_f) either remains approximately constant or increases with OCR.

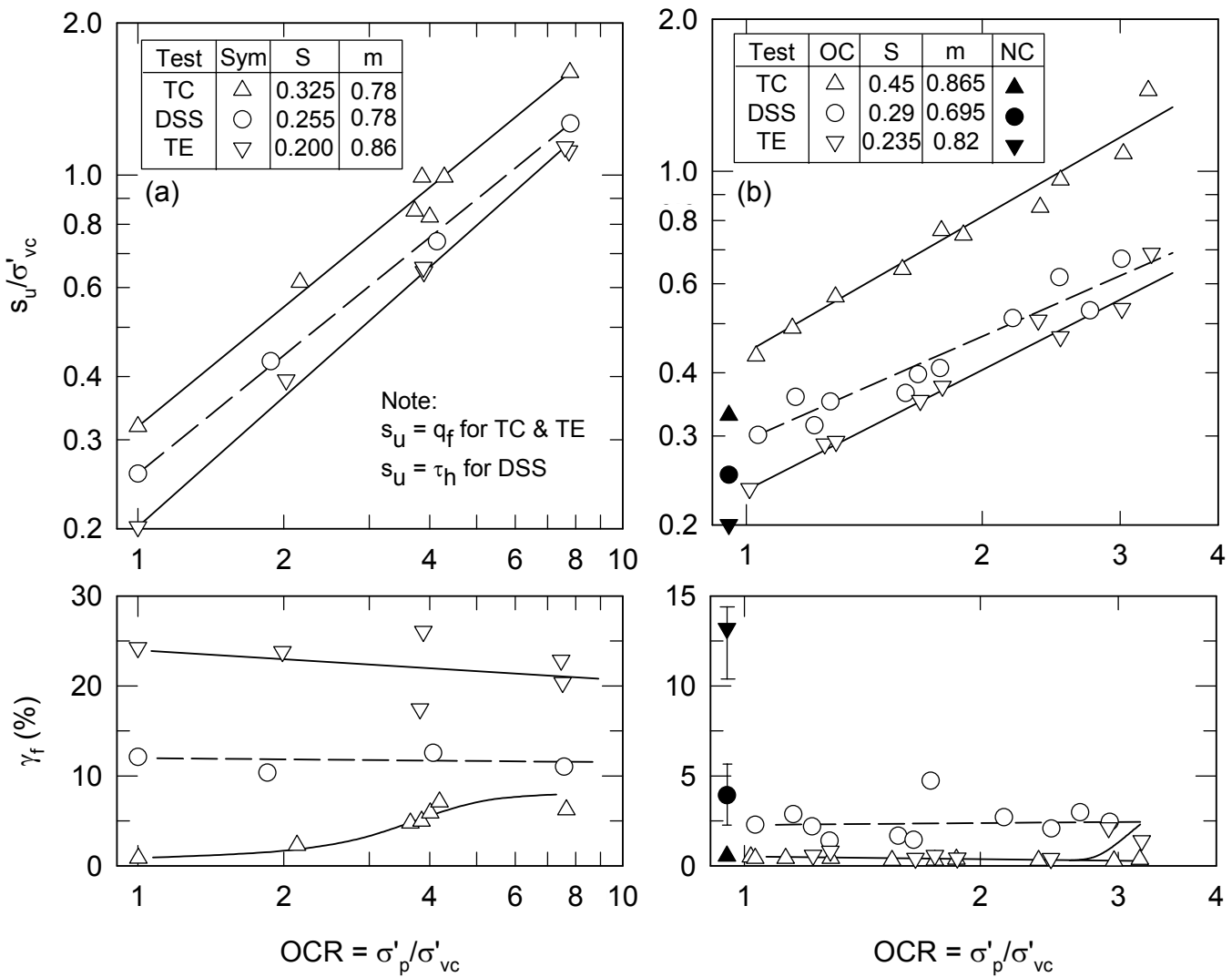


Figure 7.1 OCR versus Undrained Strength Ratio and Shear Strain at Failure from CK₀U Tests: (a) AGS Plastic Marine Clay (PI = 43%, LI = 0.6) via SHANSEP (Koutsoftas and Ladd 1985); and (b) James Bay Sensitive Marine Clay (PI = 13%, LI = 1.9) via Recompression (B-6 data from Lefebvre et al. 1983) [after Ladd 1991]

Stress System and Anisotropy. Two variables usually suffice to describe the basic differences in the applied stress system during CK₀U shearing:

- The relative magnitude of the intermediate principal stress as defined by $b = (\sigma_2 - \sigma_3)/(\sigma_1 - \sigma_3)$, and
- The direction of the applied major principal stress at failure relative to the vertical (depositional) direction denoted by the δ angle.

Changes in the values of b and δ lead to different stress-strain responses due to the effects of σ_2 and anisotropy, respectively.

Figure 7.2 shows the combinations of b and δ that can be achieved by laboratory shear devices, these being triaxial compression and extension

(TC/TE), plane strain compression and extension (PSC/PSE), direct simple shear (DSS), the true triaxial apparatus (TTA), the torsional shear hollow cylinder (TSHC), and the directional shear cell (DSC). Jamiolkowski et al. (1985) and Ladd (1991) provide additional details and references. Ideally, one would like to vary δ at constant b (e.g., plane strain with $b \approx 0.3$ to 0.4) in order to directly measure the effects of anisotropy as δ increases from 0° to 90°. Although both the DSC and the TSHC have this capability (at least in theory), they remain research tools. The plane strain device correctly measures s_u at $\delta = 0^\circ$ and 90°, but its availability is rather limited. Hence, for most jobs, CK₀U testing is limited to the triaxial (TX) apparatus and perhaps the DSS.

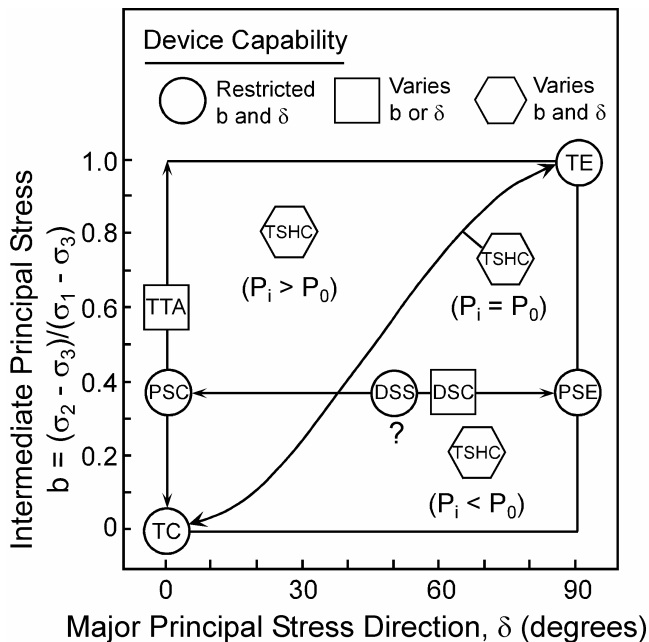


Figure 7.2 Stress Systems Achievable by Shear Devices for CK₀U Testing (modified from Germaine 1982) [Ladd 1991]

Triaxial tests measure undrained strengths that are too low relative to shear in plane strain, as illustrated by the following results quoted in Ladd (1991), where $q_f = 0.5(\sigma_1 - \sigma_3)$ at failure:

Mode of Shearing	$q_f(PS)/q_f(TX)$	Remarks
Compression ($\delta = 0^\circ$)	1.09 ± 0.06	Several clays
Extension ($\delta = 90^\circ$)	1.22 ± 0.03	Only 4 clays
Average	≈ 1.15	

The DSS device does shear the soil in plane strain, but with an indeterminate and non-uniform state of stress as further discussed in Section 8.1.

Figure 7.3 plots peak undrained strength ratios versus Plasticity Index from CK₀U TC, TE and Geonor DSS tests run on various normally consolidated clays and silts (but excluding varved deposits). The data show a constant ratio in TC; generally much lower DSS strengths that tend to decrease with lower PI; and even smaller ratios for shear in TE, especially at low PI. Although TX tests underestimate plane strain strengths (due to the b effect just described), these data and the literature clearly demonstrate that most OCR = 1 soils exhibit significant s_u anisotropy that generally becomes more important in lean clays, especially if also sensitive. Varved clays represent a special case wherein horizontal (DSS) shearing

gives an unusually low peak τ_h/σ'_{vc} of only 0.15 to 0.18 for northeastern U.S. deposits (Ladd 1991).

Overconsolidated clays also can exhibit pronounced anisotropic behavior, as illustrated by the data in Fig. 7.1. For relatively non-structured soils such as the AGS clay, the degree of anisotropy usually decreases with increasing OCR, i.e., the value of m is larger in extension than for compression. By contrast, OCR may have little effect on the anisotropy of sensitive, cemented soils such as the James Bay clay.

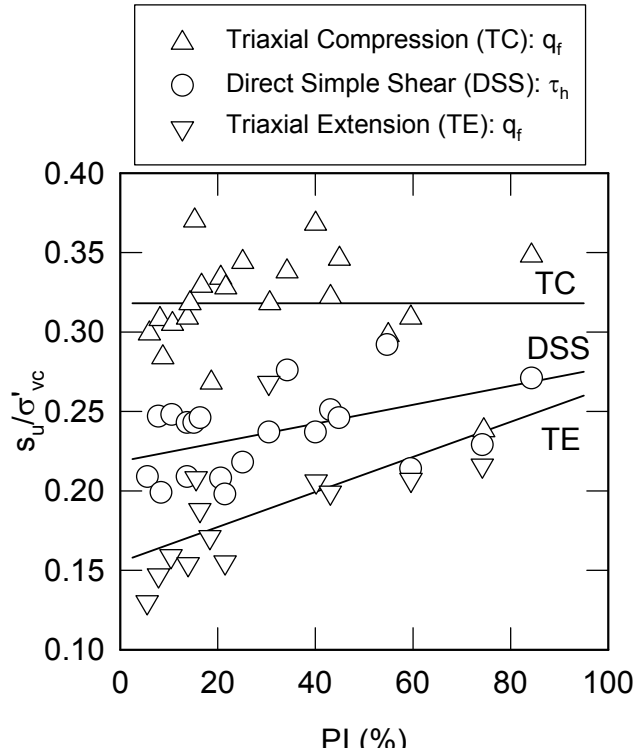


Figure 7.3 Undrained Strength Anisotropy from CK₀U Tests on Normally Consolidated Clays and Silts (data from Lefebvre et al. 1983; Vaid and Campanella 1974; and various MIT and NGI Reports) [Ladd 1991]

Progressive Failure and Strain Compatibility. For low OCR clays, the peak strength for shear in compression occurs at a low strain (typically < 1 to 2%) and is almost always followed by strain softening (i.e., smaller resistance at larger strains). Also the strain required to reach the peak strength for modes of shearing with $\delta > 0^\circ$ is larger than that for compression (e.g., Fig. 7.1). Hence for failure surfaces where δ ranges from 0° to 90° , the average strength mobilized along this surface will be less than the average of the peak strengths. The *strain compatibility* technique was developed as an approximate methodology to account for this form of progressive failure.

Figure 7.4 illustrates application of the strain compatibility technique via a plot of normalized shear stress versus shear strain from CK₀U PSC, DSS and PSE data on NC AGS clay (see Section 4.9 of Ladd 1991 for further details). Assuming equal portions of the three modes of shearing along a potential failure surface, τ_{ave} equals the average shear stress mobilized as a function of the value of γ along the surface. $s_u(ave)$ occurs at the "design" shear strain giving the maximum value of τ_{ave} . The design γ may be only 1–2% for lean sensitive (brittle) clays and increases to $\gamma = 10$ –15% for insensitive plastic clays and silts. The strain compatibility technique produces values of $s_u(ave)$ that are 10±5% lower than the average of the peak strengths. The reduction is largest for lean, sensitive clays such as the Champlain clays, and smallest for highly plastic clays of low sensitivity.

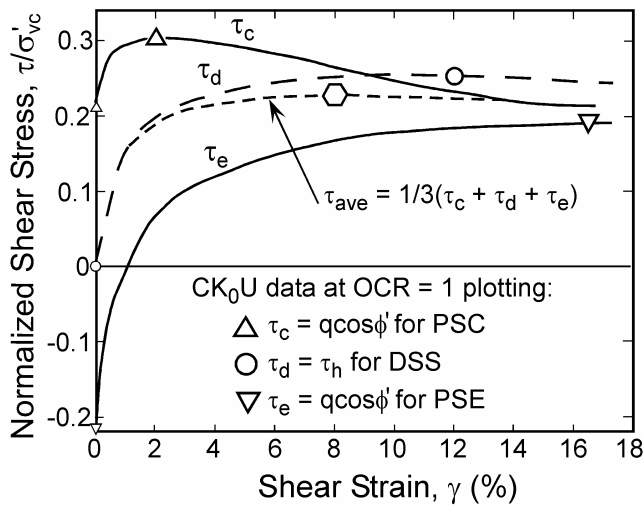


Figure 7.4 Normalized Stress-Strain Data for AGS Marine Clay Illustrating Progressive Failure and the Strain Compatibility Technique (after Koutsoftas and Ladd 1985) [Ladd 1991]

Strain Rate Effects. All cohesive soils exhibit an undrained strain rate sensitivity at fast rates of undrained shearing. The magnitude of the rate sensitivity can be expressed by the parameter

$$\rho_{\dot{\epsilon}_{a0}} = [(\Delta s_u/s_{u0})/\Delta \log \dot{\epsilon}_a] \quad (7.2)$$

where s_{u0} = value of s_u at the reference axial strain rate $\dot{\epsilon}_a = \dot{\epsilon}_{a0}$. Most reported values of $\rho_{\dot{\epsilon}_{a0}}$ come from isotropically consolidated TC tests (CIUC) run on NC clays, although some data exist from CAUC tests and even less for overconsolidated clay. Sheahan et al. (1996) present the only systematic study of the variation in $\rho_{\dot{\epsilon}_{a0}}$ as a

function of OCR and strain rate. The program ran CK₀UC tests with lubricated end caps on resedimented Boston Blue Clay (LL ≈ 45%, PI ≈ 24%) at OCR = 1, 2, 4 and 8 and $\dot{\epsilon}_a$ ranging from 0.05 to 50%/hr. Figure 7.5 plots s_u/σ'_{vm} (σ'_{vm} = maximum vertical consolidation stress) versus $\log \dot{\epsilon}_a$ and shows the resulting values of $\rho_{0.5}$ (i.e., for a reference $\dot{\epsilon}_a = 0.5\%/\text{hr}$). For very fast shearing ($\dot{\epsilon}_a = 5$ to 50%/hr), the rate sensitivity is essentially independent of OCR, with $\rho_{0.5} = 9.5\% \pm 2.0$ SD. However, at lower strain rates, $\rho_{0.5}$ decreases with OCR from 6.5±0.5% for NC clay, to 4.5±1.0% at OCR = 2, and finally to zero at OCR = 8. (Note: most reported data from UUC and CIUC tests on highly overconsolidated clay show a moderate to high rate sensitivity. However, this is mainly caused by softening (swelling) of the clay at slower rates due to migration of water from the ends to the center of the test specimens).

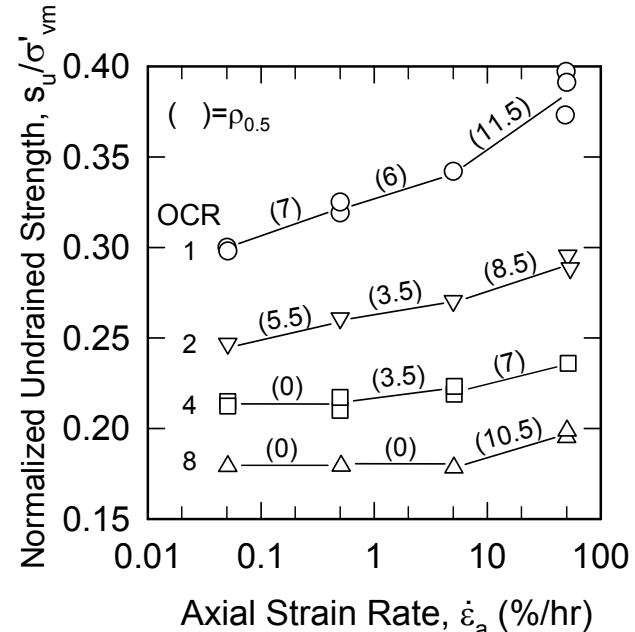


Figure 7.5 Normalized Undrained Shear Strength versus Strain Rate, CK₀UC Tests, Resedimented BBC (Sheahan et al. 1996)

Based on the results in Fig. 7.5, data from the literature and considerable judgment, Fig. 7.6 was developed to illustrate how rate effects could influence the strength measured in different in situ and laboratory shear tests for a hypothetical low OCR clay. For the assumed values of $\rho_{1.0}$ and t_f , the sketch shows, that relative to a lab CK₀U test,

- Extremely fast shearing ($t_f \approx 5$ sec), such as occurs in CPTU and lab strength index tests, increases s_u by almost 50%.

- Fast shearing ($t_f \approx 5$ min), such as occurs in the FVT and lab UUC tests, increases s_u by about 15%.
- Very slow shearing ($t_f \approx 2$ weeks), such as might occur in the field, reduces s_u by almost 10%.

These percentages (which assume adjustment to the same mode of shearing) are very approximate and undoubtedly will vary with soil type and its stress history, and possibly temperature (e.g., Arctic soils with near freezing temperature can be extremely rate sensitive). But there is little question that fast shearing rates associated with in situ and lab strength index and UUC tests produce strengths that are too high for design, all else being equal. (Note: the field vane correction factor μ plotted in Fig. 5.1 is thought to mainly reflect strain rate effects with increasing PI).

Sample Disturbance. Sample disturbance reduces the effective stress of the soil to values of σ'_s less than that for the perfect sample (σ'_{ps}) due to a combination of internal swelling and shear

distortions (as discussed in connection with Fig. 4.1). Figure 7.7 illustrates how the reduction in σ'_s affects the undrained shear behavior of UUC tests (run at a slower rate than usual, with measurements of pore pressure) for specimens of NC resedimented BBC subjected to increasing degrees of disturbance by varying the magnitude of the undrained cyclic strain to simulate sampling with different tube geometries. The figure shows that, as σ'_s decreases from σ'_{ps} , the behavior changes from contractive to dilatant, s_u decreases and the strain to failure (ε_f) increases. Even perfect sampling caused a 15% decrease in strength and a large increase in ε_f relative to in situ shearing. And the s_u after "sampling" with $\varepsilon_c = 5\%$ ($\sigma'_s/\sigma'_{ps} < 0.1$) is only about half of the in situ value.

Although increases in sample disturbance will certainly reduce the s_u measured in all types of UU tests (i.e., tests sheared at the sample water content), the effects of disturbance on CU tests that are reconsolidated to the in situ stresses are less clear. This topic is addressed in Section 8.2.

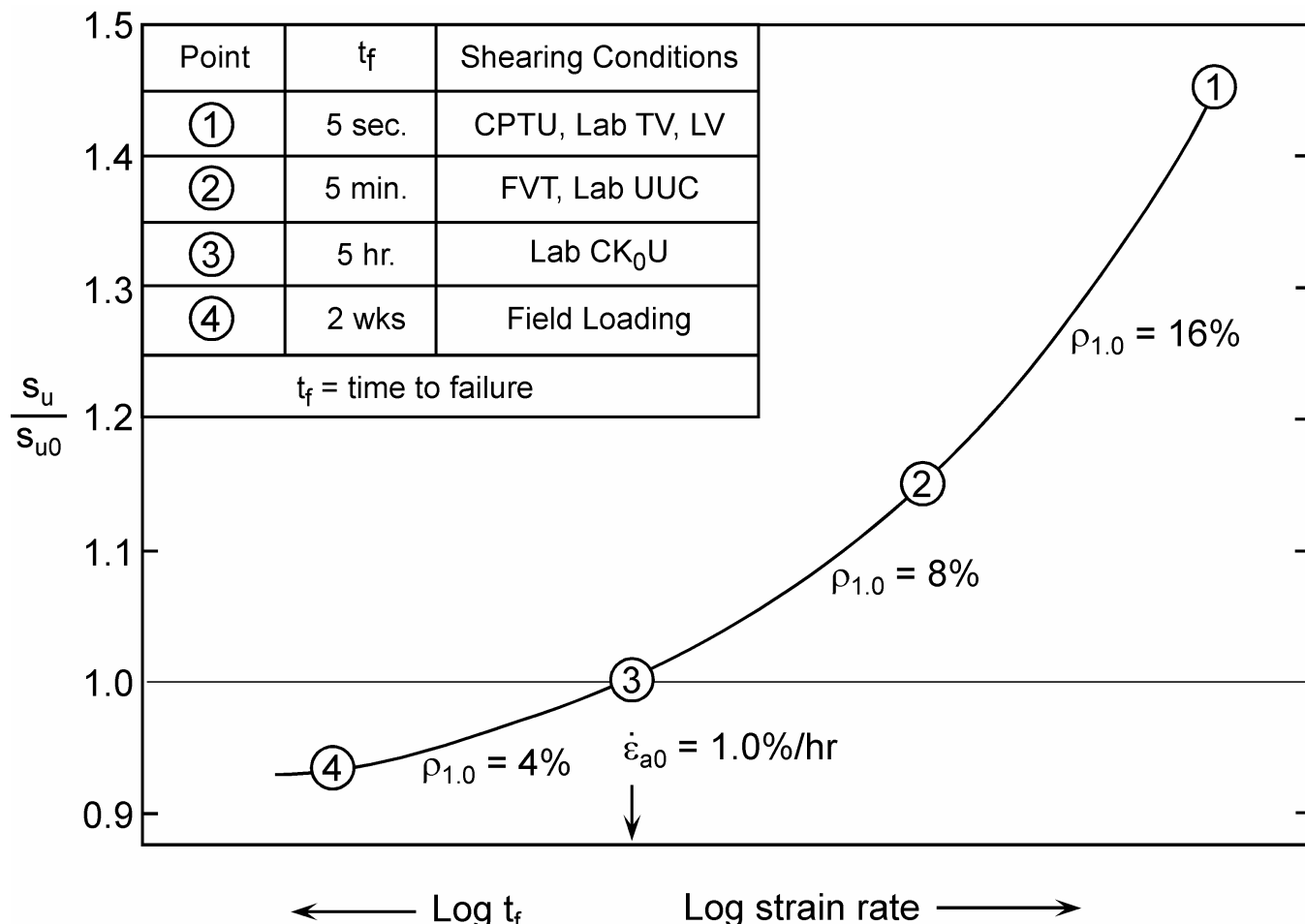


Figure 7.6 Schematic Illustration of Effect of Rate of Shearing on Measured s_u from In Situ and Lab Tests on Low OCR Clay

Notes: PS = Perfect Sample; $(\varepsilon_c, \%)$ = plus-minus axial strain cycle in compression, extension and compression; undrained shear at $\dot{\varepsilon}_a = 0.5 - 1.0 \text{ \%}/\text{hr}$

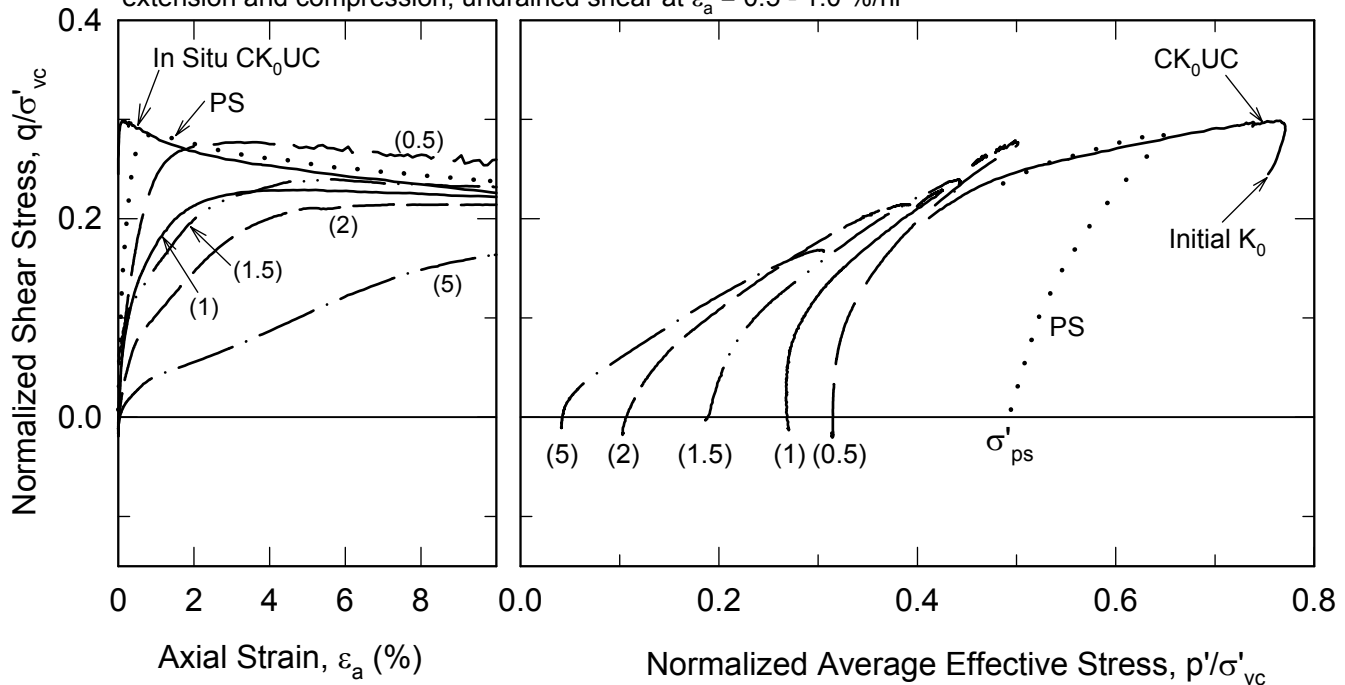


Figure 7.7 Effects of Sample Disturbance on Stress-Strain-Effective Stress Paths from UUC Tests on NC Resedimented BBC (Santagata and Germaine 2002)

Conclusion. Laboratory strength testing for estimating the in situ undrained stress-strain behavior of soft clays should ideally meet the following criteria:

1. Test specimens from high quality samples which retain the in situ structure of the soil, i.e., minimal disturbance of the fabric and interparticle bonding.
2. Reconsolidation to the in situ stresses in order to start shearing from the correct state of stress. This is especially important for assessing the effects of anisotropy.
3. Undrained shearing with values of b and δ (Fig. 7.2) that replicate the modes of shearing that will occur in the field.
4. Undrained shearing at a strain rate that approaches the conditions in the field.
5. Consideration of how strain compatibility will affect the strength that can be mobilized in the field.

However, it is not feasible to meet all of these criteria in practice. Section 7.3 suggests how one can adjust the scope of the lab strength testing program to fit the needs of the project (i.e., its importance and complexity) and Section 8 covers recommended testing procedures and interpretation of undrained shear data to obtain design parameters.

7.2 Problems with Conventional UUC and CIUC Tests

UU Triaxial Compression (UUC) Test: ASTM D2850. UUC tests are widely used in practice throughout the world to obtain design values of s_u for undrained stability analyses of loads on soft clay. Such tests often exhibit large scatter, especially with increasing depth. But more fundamentally, reliance on UUC tests to estimate $s_u(\text{ave})$ depends on a fortuitous cancellation of three errors:

1. The fast rate of shearing (60%/hr) causes an increase in the measured s_u ;
2. Shearing in triaxial compression also causes an increase in s_u since it ignores the effects of anisotropy, which lowers s_u with increasing δ angle;
3. Sample disturbance causes a decrease in s_u .

These compensating errors cannot be controlled and only pure luck will yield a strength equal to $s_u(\text{ave})$, i.e., such that disturbance offsets the higher strength due to fast shearing in triaxial compression. If one runs UUC tests on high quality samples, the s_u values can be too high (unsafe) by more than 25 to 50% (e.g., Table 7 of Germaine and Ladd 1988). And UUC strengths from low quality samples can easily be 25 to 50% too low.

In essence, UUC tests generally are a waste of time and money and have little advantage (except possibly within crusts) over less costly strength index tests like the Torvane, lab vane and fall cone. The cost savings will be better spent on consolidation tests and Atterberg Limits, which can then be used with a Level C (Ladd 1991) estimate of S and m in order to directly calculate $s_u(\text{ave})$ (see Section 7.3) or to check strengths estimated from in situ vane or piezocone tests.

CIU Triaxial Compression (CIUC) Test: ASTM D4767. CIUC tests are frequently used to estimate both the initial strength of soft soils (UU Case) and how it increases with consolidation (CU Case). Estimates of the initial $s_u(\text{ave})$ based on the measured strength from CIUC tests reconsolidated to the in situ σ'_{v0} for low OCR clays are almost always unsafe because:

1. $K_c = \sigma'_{hc}/\sigma'_{vc} = 1$ leads to a water content that is too low, which increases s_u ;
2. Shearing in triaxial compression ($\delta = 0^\circ$) ignores anisotropy and hence overestimates $s_u(\text{ave})$.

The only possible exception is with poor quality samples of cemented clays wherein reconsolidation may not offset the strength decrease due to destructureation.

Similar problems occur when CIUC tests are used to predict $s_u(\text{ave})$ versus σ'_{vc} , especially if the

design undrained strength ratio is taken as $q_f(C)/\sigma'_c$. For NC clays, this ratio typically equals 0.33 ± 0.05 SD (Mayne 1980) and hence is 50% higher than appropriate for design. (Note: Section 6.2 of Ladd (1991) describes the "QRS" methodology used by the U.S. Army Corps of Engineers for calculation of design strengths during staged construction from CIUC test data. It depends on compensating errors and is not recommended).

Since CIUC tests do not give correct design strengths for undrained stability analyses, they should be replaced by CK_0U tests.

Conclusion. The wide spread practice of running UUC and CIUC tests for soft ground construction projects should be discontinued. Funds allocated to lab testing are better spent on consolidation and CK_0U strength tests.

7.3 Strength Testing for Undrained Stability Analyses

Table 7.1 lists three examples of stability evaluations having increasing levels of sophistication regarding the method of stability analysis and the nature of the strength input parameters. These examples will be used to illustrate an appropriate scope of strength testing for each case.

Table 7.1 Levels of Sophistication for Evaluating Undrained Stability

Ex. No.	Stability Case	Method of Analysis	Strength Input	Strength Testing	Stress History	Typical* Design FS
1	UU	Circular Arc (Isotropic s_u)	$s_u(\text{ave})$ vs. z	FVT (no shells) or Estimated S and m (Level C)	Desirable Required	≥ 1.5
2	CU	Circular Arc (Isotropic s_u)	$s_u(\text{ave})$ vs. z for each zone	CK_0U TC & TE or CK_0UDSS (Level B)	Essential	1.3 – 1.5
3	CU	Non-circular Surface (Anisotropic s_u)	$s_u(\alpha)$ vs. z for each zone	CK_0U TC, TE & DSS (Level A)	Essential	1.25 – 1.35

*Design FS should be a function of the uncertainty in the "best estimate" FS, the consequences of failure, and the level of monitoring during construction. For major projects, a reliability analysis is recommended to help select a suitable FS (e.g., Christian et al. 1994).

Test Program for UU Case: Circular Arc Analyses with Isotropic Strengths. Example 1 is typical of a small project requiring a stability evaluation for the UU Case (i.e., assuming no drainage during application of the full load) such as for a storage tank or preload fill. One needs to develop a profile of the initial in situ $s_u(\text{ave})$ versus depth for circular arc stability analyses using isotropic strengths. That is, the input values of s_u do not vary with inclination of the failure surface, but they should account for undrained strength anisotropy and strain compatibility.

After determining the soil profile from CPTU tests and/or borings with Standard Penetration Tests (or even from prior experience if the site has a uniform stratigraphy), one can then identify the location of cohesive layers for which z versus $s_u(\text{ave})$ will be needed for the stability analyses.

For clays without shells or sand lenses-layers, FV tests with Bjerrum's correction should give fairly reliable results, with the PI measured on split-spoon samples or estimated from prior experience. Strengths obtained from CPTU q_t data are generally less reliable, unless N_{kt} has been established from prior experience for the deposit with the same piezocone device (Section 5.2).

If one has little experience with the soft soil at the site, several consolidation tests (with Atterberg Limits) are highly recommended in order to compute $s_u(\text{ave})$ via the SHANSEP equation with values of S and m estimated from

empirical correlations with soil type. Table 7.2 summarizes these so-called Level C correlations, which are described more fully in Section 5.3 of Ladd (1991). For most soil types, $S = 0.22 \pm 0.03$ and $m = 0.8 \pm 0.1$. These "point" values of $s_u(\text{ave})$ should be compared with $\mu s_u(FV)$ or q_{net}/N_{kt} .

If the project requires settlement analyses, and if the consolidation test program shows a reasonably well defined stress history profile, then the design strengths can be computed based on Level C estimates of S and m . The authors have more confidence in these strengths than those obtained from CPTU data or from FVT data that did not follow the recommended test procedures in Section 5.1.

Since the scope of the above testing program is fairly modest, a relatively high design factor of safety (FS) is warranted.

Test Program for CU Case: Circular Arc Analysis with Isotropic Strengths. (Note: if construction involves fairly wide berms and a relatively thin layer of soft soil, then one should also evaluate non-circular failure surfaces for the stability analyses). The cross-section in Fig. 7.8 is used to illustrate this CU Case, where prefabricated vertical drains (PVD) are installed beneath most of the embankment. One first has to establish a maximum safe height for Stage 1 (usually treated as a UU Case) in order to achieve the maximum benefit from consolidation prior to

Table 7.2 Level C Values of S and m for Estimating $s_u(\text{ave})$ via SHANSEP Equation (slightly modified from Section 5.3 of Ladd 1991).

Soil Description	S	m^a	Remarks
1. Sensitive cemented marine clays (PI < 30%, LI > 1.5)	0.20 Nominal SD = 0.015	1.00	Champlain clays of Canada
2. Homogeneous CL and CH sedimentary clays of low to moderate sensitivity (PI = 20 to 80%)	$S = 0.20 + 0.05(\text{PI}/100)$ or Simply 0.22	$0.88(1 - C_s/C_c)$ $\pm 0.06 \text{ SD}$ or simply 0.8	No shells or sand lenses-layers
3. Northeastern US varved clays	0.16	0.75	Assumes that DSS mode of failure predominates
4. Sedimentary deposits of silts and organic soils (Atterberg Limits plot below A-line) and clays with shells	0.25 Nominal SD = 0.05	$0.88(1 - C_s/C_c)$ $\pm 0.06 \text{ SD}$ or simply 0.8	Excludes peat

^a $m = 0.88(1 - C_s/C_c)$ based on analysis of CK₀UDSS data on 13 soils with max. OCR = 5 - 10

Stage 2 construction. This means that the vertical consolidation stress (σ'_{vc}) profile under Stage 1 must significantly exceed the initial σ'_p profile within the weakest soils. Consequently, lab consolidation tests are essential, although they usually should be supplemented by in situ testing to help assess spatial variations in the initial stress history (as per Sections 2 and 5). Consolidation analyses are also needed to predict the rate of consolidation within the PVD zone (i.e., \bar{U}_h vs. t_c) since the Stage 2 stability analyses will typically want the FS as a function of fill height and \bar{U}_h within Zone 2. In any case, one must develop a reliable initial stress history as this is needed to compute strength profiles using the SHANSEP equation for both the Stage 1 UU Case and the Stage 2 CU Case.

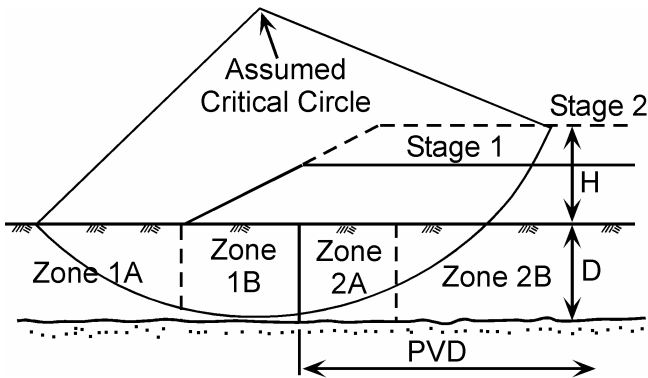


Figure 7.8 Hypothetical Cross-Section for Example 2: CU Case with Circular Arc Analysis and Isotropic s_u

This example assumes the use of isotropic strengths. For the UU Case, using $s_u(\text{ave})$ is clearly valid since the critical failure surface will involve modes of shearing ranging from compression to extension. But for the CU Case (refer to Fig. 7.8), the failure mode within Zone 1 varies from DSS to extension and thus using $s_u(\text{ave})$ will overpredict the actual strength. Conversely, the failure mode within the strengthened Zone 2 varies from compression to DSS and using $s_u(\text{ave})$ will underpredict the actual strength. However, since Zone 2 is stronger than Zone 1, using $s_u(\text{ave})$ throughout usually leads to a FS that errs on the safe side.

The recommended CK₀U test program can use either DSS tests or a combination of TC and TE tests. DSS testing requires less effort and $s_u(D) = \text{maximum } \tau_h$ generally provides a good estimate of $s_u(\text{ave})$. The more costly CK₀UC/E program requires either very considerable time or automated stress path triaxial equipment (Section 8.1). But it has the advantage of giving

information regarding s_u anisotropy, which can be used to input different undrained strength ratios within portions A and B of Zones 1 and 2, as discussed in Section 8.3. However, the triaxial option is not suitable for varved deposits because the lowest strength occurs for shear parallel to the varves.

Example 2 is typical of projects of intermediate complexity. However, the design FS can be lower than for the first example since the strength parameters are better defined and field instrumentation will (or should) be used to monitor the degree of consolidation and preferably also lateral deformations.

Test Program for CU Case: Non-circular Analyses with Anisotropic Strengths. Example 3 represents a highly complex stability problem that justifies the use of non-circular failure surfaces and anisotropic values of s_u that vary with inclination of the failure surface, $s_u(\alpha)$. In addition to in situ testing to assess spatial variability and extensive consolidation tests, the CK₀U strength testing program now includes both triaxial and direct simple shear tests. In fact, one may even want to include some plane strain tests to check the triaxial data and CAUDSS tests to assess the benefit of consolidation with a horizontal shear stress (e.g., see Fig. 19 of Ladd 1991). Section 8.3 describes how one can interpret triaxial and DSS tests to develop design values of $s_u(\alpha)/\sigma'_{vc}$ versus failure plane inclination. The case history in Section 8.3 also illustrates its application in practice.

Case History. This example is for a bridge replacement project located north of Boston, MA. The general soil profile consists of: coarse sand, organic soil, fine to coarse sand, and then Boston Blue Clay (BBC) from El. -4.2 to -50 m (Fig. 7.9). The clay was subjected to significant weathering since deposition some 14,000 years ago (Kenney 1964), resulting in a stiff overconsolidated clay crust at the top of the deposit. The initial geotechnical investigation consisted of SPT, 75 mm fixed piston tube sampling for lab tests, and field vane testing (tapered blade). The borehole was advanced using a hollow stem auger with all testing and sampling conducted in the same borehole. All SPT data were weight of rod below El. -9.6 m. Subsequently, UMass Amherst conducted a CPTU sounding with u_2 pore pressure measurements. This case history is used to illustrate how one can develop reasonable stress history and s_u profiles when faced with misleading data from a poorly executed site investigation

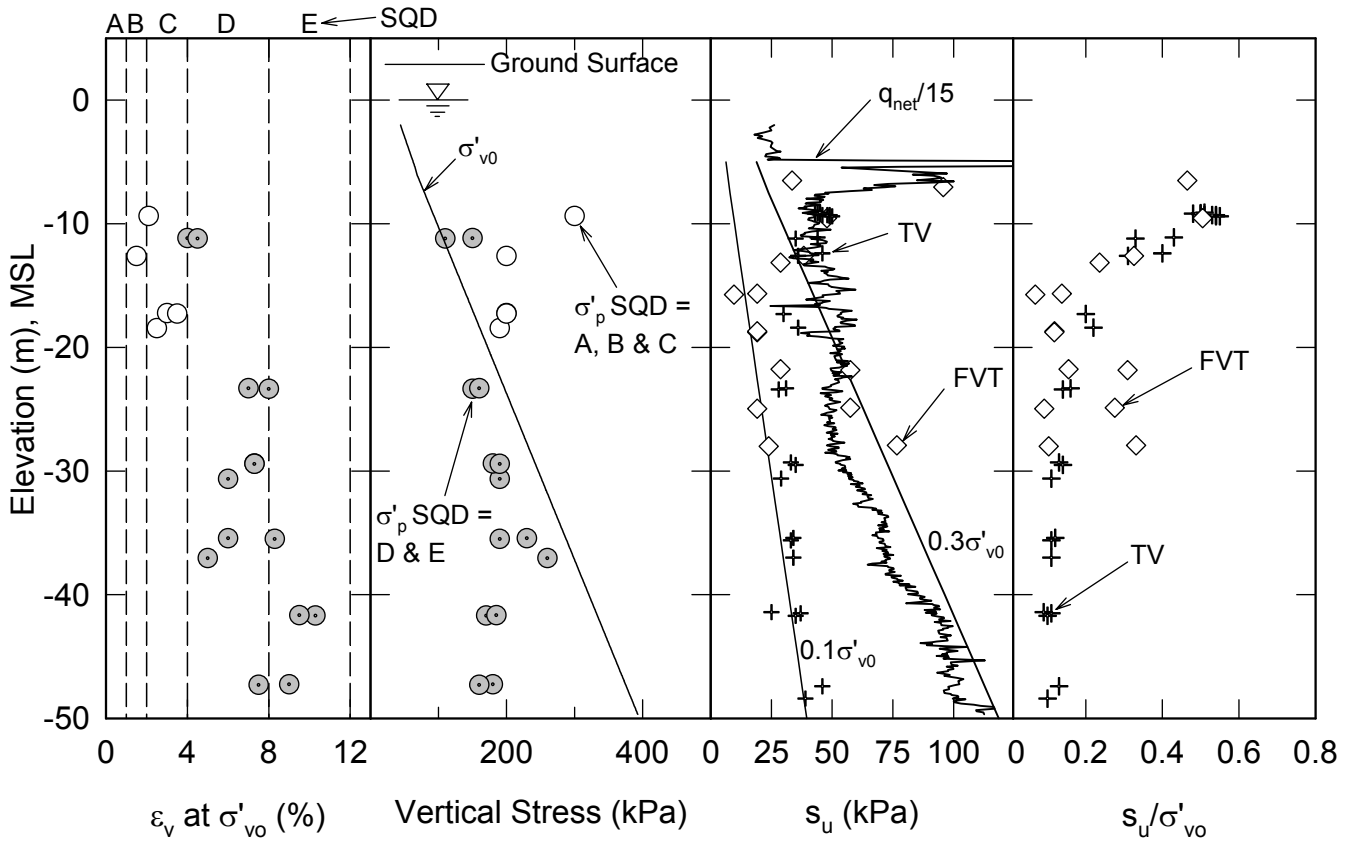


Figure 7.9 Elevation vs. Stress History From IL Oedometer Tests, Measured and Normalized s_u (FV) and s_u (Torvane) and CPTU Data for Bridge Project Located North of Boston, MA

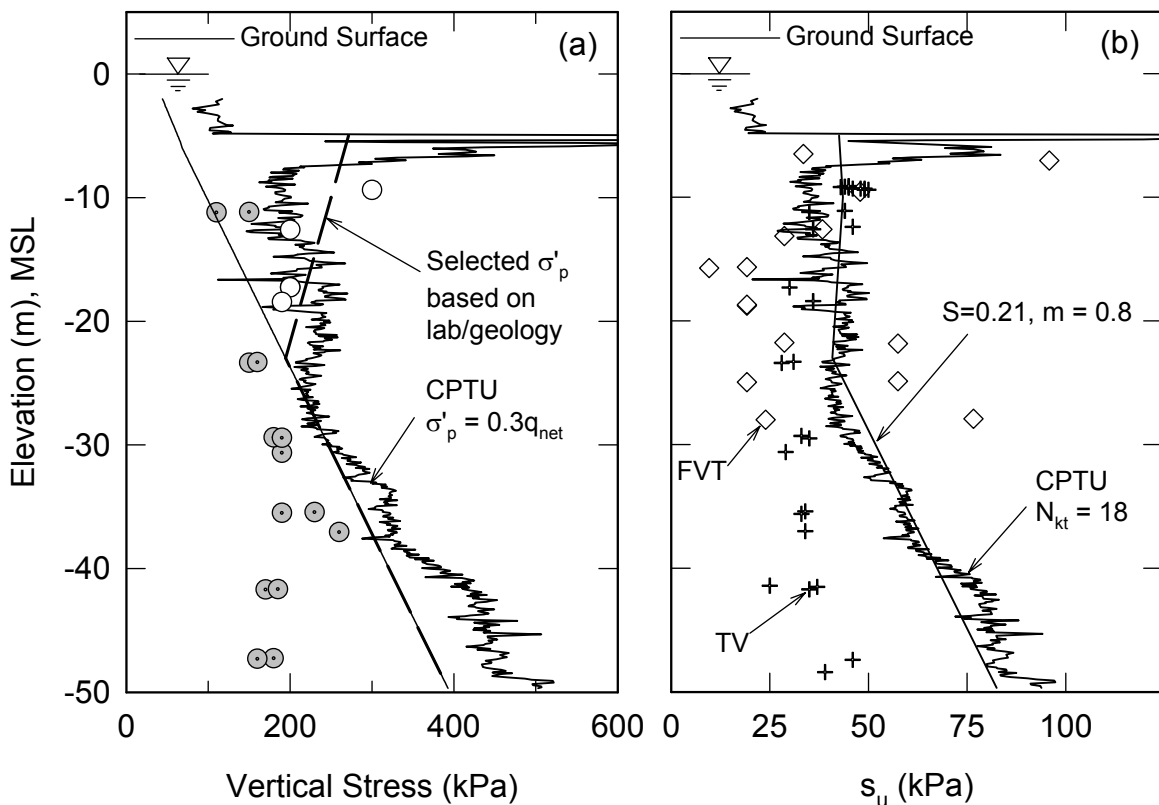


Figure 7.10 Interpreted Stress History and Predicted Undrained Shear Strength Profiles Using a Level C Prediction of SHANSEP Parameters

program (except for the CPTU sounding). Note that the approach will assume no prior experience with the deposit other than its geology.

Atterberg limits for this CL marine clay are approximately constant with depth with LL = 45% and PI = 20%. The Liquidity Index is less than one in the crust and then becomes near unity.

Figure 7.9 plots stress history and SQD data from IL consolidation tests and s_u data from the field vane (FV), Torvane (TV) and CPTU (using $N_{kt} = 15$; middle value of typical range of 10 to 20 as reported in Section 5.2) tests. The IL consolidation test samples were debonded and extruded from the tubes using the procedure in Fig. 4.3, with adjacent Torvane tests. The σ'_p data indicate an overconsolidated soil near the top of the BBC deposit and an apparent underconsolidated soil below El. -23 m. However, the geological history of the region (Kenney 1964) indicates the soil should not be underconsolidated and only a slight 1.5 m artesian condition exists in the underlying glacial till (Ladd et al. 1994). The apparent underconsolidation is therefore undoubtedly the result of sample disturbance causing a significant decrease in the measured σ'_p , especially since all tests below -23 m have an SQD of D and E, compared to A and B recommended by Terzaghi et al. (1996) for reliable estimates of σ'_p .

The FV data are highly scattered and many tests had unusually low undrained strength ratios, i.e., $s_u(FV)/\sigma'_{vo}$ only about 0.1. The $s_u(TV)$ data show very little scatter and the $s_u(TV)/\sigma'_{vo}$ ratios clearly show a transition from the crust to the softer clay at depth. However, the ratios for the deep clay also are very low. The poor quality tube samples (hence very low lab values of σ'_p and s_u) and unreliable FV data are believed to be largely due to making a hollow stem auger borehole without a proper weight drilling mud (see beginning of Section 4.1).

The approach used a Level C prediction of SHANSEP parameters. With a PI averaging 20%, Table 7.2 gives $S = 0.21$ and $m = 0.8$. An estimate of the stress history profile was not possible based only on IL data. However, from the site geology, the soil deposit at depth is likely to be normally to lightly overconsolidated. A *practical* and safe approach is to assume normally consolidated soil starting at a depth where the oedometer σ'_p values are less than σ'_{vo} , i.e., approximately elevation -23 m. An estimate of the OCR profile for the crust was made using the measured σ'_p data from the four better quality shallow samples. Figure 7.10a plots this interpretation of the stress history and Fig. 7.10b plots the resulting s_u values computed

via the SHANSEP equation with $S = 0.21$ and $m = 0.8$. The CPTU data provide corroborating evidence for these profiles. Figure 7.10a plots the CPTU data interpreted using Eq. 5.5 with $k = 0.3$. And CPTU estimates of s_u using Eq. 5.4 with $N_{kt} = 18$ gives a reasonable match to the SHANSEP s_u profile plotted in Fig. 7.10b.

7.4 Three Dimensional End Effects

Conventional slope stability analyses assume a plane strain condition, i.e., that the failure has an infinite length. Azzouz et al. (1983) show that the increase in FS due to actual 3-D failures, compared to infinitely long failures, can be closely approximated by

$$FS(3D)/FS(2D) = 1 + 0.7(D/L) \quad (7.3)$$

where D = maximum thickness of the failure zone and L = maximum longitudinal length of the zone of failure. They also showed that end effects increase the $FS(2D)$ by 1.10 ± 0.04 SD based on analysis of 17 embankment failures. Consequently, "precise" conventional plane strain (2D) stability analyses overestimate the actual in situ $s_u(ave)$ backcalculated from observed failures by roughly $10 \pm 5\%$ (as previously mentioned in Section 5.1 regarding Bjerrum's FV correction factor). Thus when conducting stability analyses, one should know whether the input values of s_u already include end effects [e.g., using $s_u(ave) = \mu s_u(FV)$] or that the strengths represent plane strain values. For the later case, the results from 2-D analyses can be adjusted using Eq. 7.3 to obtain a more realistic factor of safety by explicitly considering end effects.

7.5 Principal Recommendations

The test program selected to develop undrained strength parameters for stability analyses should account for the major factors that affect the stress-strain response of soft clays. These are the effects of anisotropy and sample disturbance (which require that test specimens first be anisotropically reconsolidated and then sheared with representative mode(s) of failure) and the rate of shearing. Table 7.1 suggests three levels of sophistication for the scope of the strength testing program as a function of the complexity of the stability problem. Level A calls for CK_0U triaxial compression (TC) and extension (TE) and direct simple shear (DSS) tests to develop anisotropic strength parameters, $s_u(\alpha)$, for the CU Case (staged construction) with non-circular slope stability analyses. Level B uses either CK_0U TC/TE or DSS tests to obtain $s_u(ave)$ for the CU

Case with circular arc analyses. And Level C for the UU Case (undrained loading) suggests using corrected field vane strengths to estimate $s_u(\text{ave})$ or consolidation tests and values of the SHANSEP S and m parameters estimated from empirical correlations with soil type presented in Table 7.2.

UU and CIU triaxial compression tests are not recommended. UUC tests depend on a fortuitous cancellation of errors, i.e., a strength decrease due to sample disturbance that offsets the strength increase due to fast shearing in triaxial compression in order to end up with $s_u(\text{ave})$. CIUC produce unsafe values of s_u much higher than $s_u(\text{ave})$. The cost savings from deleting these tests are better spent on consolidation and CK_0U tests.

8 LABORATORY CONSOLIDATED-UNDRAINED SHEAR TESTING

The numerous devices that have been developed to measure the stress-strain-strength behavior of soft clays range from simple-to-use equipment to sophisticated ones that are only suitable for research purposes. Comprehensive reviews of the capabilities of laboratory shear testing equipment include Ladd et al. (1977), Saada and Townsend (1981), Jamiolkowski et al. (1985), and Ladd (1991). This section reviews experimental capabilities and recommended procedures for conducting laboratory shear tests in practice, evaluates laboratory reconsolidation options, and discusses interpretation of shear test data for selection of design parameters.

8.1 Experimental Capabilities and Testing Procedures

Section 7.1 briefly reviewed the capabilities of the various shear devices illustrated in Fig. 7.1, leading to the conclusion that equipment realistically available for most practice is limited to triaxial compression (TC) and extension (TE) and direct simple shear (DSS) tests. This section discusses recommended procedures for conducting CK_0U triaxial and DSS tests.

Triaxial Testing. Baldi et al. (1988), Germaine and Ladd (1988), and Lacasse and Berre (1988) give thorough recommendations on use of triaxial equipment and test procedures. The key steps in the process are specimen set-up, saturation, consolidation, and undrained shear. Tests specimens should be trimmed down from the tube sample diameter to allow for removal of sample perimeter soil that is usually more disturbed. Backpressure saturation is essential for accurate

measurement of volume change during consolidation and pore pressure changes during undrained shear. It should ideally take place at the measured or estimated sampling effective stress to minimize specimen volume changes and without allowing swelling to occur. A final backpressure of approximately 200 to 300 kPa is typically sufficient to obtain saturation of most soft clays, although Skempton's B value should always be checked to ensure that saturation has occurred (e.g., $B > 95\%$ within one minute).

Realistic measurement of the effects of undrained strength anisotropy requires consolidation to a preshear state of stress that closely approximates the anisotropic in situ stress condition. A K_0 state of stress exists for virgin horizontal ground and thus CK_0U tests should be run to provide s_u data for the UU Case (i.e., stability analyses for initial undrained loading). For staged construction corresponding to the CU Case, the consolidation stress state under the loaded area becomes far more complex (see Fig. 12 of Ladd 1991). However, CK_0U undrained strength ratios applied to the estimated vertical consolidation stress (σ'_{vc}) should give safe estimates of s_u for stability analyses (Section 4.11 of Ladd 1991). Hence the text will now focus on consolidation procedures to achieve a preshear K_0 condition.

As subsequently described, computer automated stress path triaxial equipment makes the task of achieving K_0 consolidation much simpler and more efficient than manual methods. This is especially true for tests run on NC soil because manual consolidation requires the application of many small increments of vertical and radial stress in order to avoid excessive undrained shear deformations and to check that $K_c = \sigma'_{hc}/\sigma'_{vc}$ is close to K_0 (i.e., equal axial and volumetric strains). Hence for practice with manual equipment, CAU tests are often used (e.g., Lacasse and Berre 1988) wherein test specimens are consolidated along a horizontal stress path and then σ'_v is slowly increased to the estimated K_0 condition in one or more steps depending on the preshear value of σ'_{vc}/σ'_p .

One-dimensional reconsolidation to the overburden stress of OC clays results in a value of K_0 that is typically much lower than exists in situ (e.g., Mesri and Hayat 1993 and data in Fig. 8.1). Consequently, one first has to estimate K_0 and then either follow a linear stress path to σ'_{v0} and $\sigma'_{h0} = K_0\sigma'_{v0}$ with automated triaxial equipment or use the simplified CAU procedure for manual reconsolidation.

The rate of strain for undrained shear should be selected taking into account the strain rate sensitivity of clays and typical field loading rates. A strain rate of $d\varepsilon/dt = 0.5$ to 1.0% per hour for CK_0U triaxial tests on soft clays is a commonly recommended rate (Germaine and Ladd 1988). Triaxial cells should be equipped with internal load cells to eliminate uncertainty about piston friction (together with perfect alignment of the specimen, piston and applied load); this is especially important for conducting reliable extension tests. See Germaine and Ladd (1988) for a detailed treatment of triaxial testing errors due to piston friction (for external load cells), membrane and filter paper resistance, membrane leakage and related problems.

Direct Simple Shear. The direct simple shear (DSS) device is used to simulate shearing along a horizontal plane and also to obtain $s_u(\text{ave})$ for isotropic stability analysis. Bjerrum and Landva (1966), Ladd and Edgers (1972), and DeGroot et al. (1992) provide comprehensive reviews of DSS test equipment, data reduction and interpretation, and typical results for a wide variety of cohesive soils. The test procedure is also covered in ASTM D6528. The DSS device has limitations due to an indeterminate and non-uniform state of stress. The horizontal shear stress at the peak strength ($\tau_{h\max}$) probably lies between $q_f = 0.5(\sigma_1 - \sigma_3)_f$ and $\tau_{ff} = q_f \cos\phi'$ and inclination of σ_{1f} probably equals $\delta \approx 45 \pm 15^\circ$. The device also produces excessive strain softening at $\gamma > 10 - 15\%$ (DeGroot et al. 1992, 1994). However, the measured maximum τ_h using the Geonor device is thought to give very reasonable estimates of $s_u(\text{ave})$ [excluding varved clays] and the test requires less soil and less time and effort than CK_0U triaxial tests.

In the Geonor DSS device, a circular specimen is trimmed into a wire-reinforced rubber membrane and loaded either incrementally or continuously to produce a K_0 compression curve that is the same as those measured in other 1-D consolidation tests. Undrained shear is usually performed by running constant volume tests at approximately $dy/dt = 5\%/\text{hour}$, with the peak shear stress for most clays being reached within 1 to 3 hours. Recompression tests that reconsolidate OC clay to σ'_{vo} typically require the use of stones with embedded pins to prevent slippage. Unfortunately, these stones are difficult to fully seat and they create an unknown degree of disturbance to the specimen. Another issue for Recompression tests is the lack of sufficient horizontal stress developed during recompression

to σ'_{vo} , such that the resulting laboratory K_0 is typically much lower than exists in situ (Dyvik et al. 1985). This can produce measured results that are markedly different from the correct behavior corresponding to the in situ OCR. Therefore specimens must first be loaded up to a stress level beyond σ'_{vo} and unloaded back to σ'_{vo} to develop additional horizontal stress, which can be a tricky procedure. As a guideline, NGI typically loads to approximately 80% of the best estimate of σ'_p and then unloads back to σ'_{vo} prior to undrained shear. Obviously, this cannot be done for very low OCR soils.

Computer Automation. Significant advances have been made since the mid-1980s in computer automation of triaxial and DSS equipment. Triaxial stress path cells have emerged through computer automation of flow pumps, screw jacks and load frames. CK_0U tests can now be reliably conducted through computer control with a very significant reduction in potential for operator error and with much shorter testing periods as compared to traditional manual procedures. Many of the basic features of top-level triaxial stress path cells and DSS equipment that were developed at research institutions (e.g., Sheahan and Germaine 1992, Sheahan et al. 1994) are now being commercially manufactured, thus making this equipment available to geotechnical laboratories. Although the capital investment in automated equipment is not trivial, the benefits from improved data quality and test efficiency (both in time and cost) cannot be overstated.

Figure 8.1 plots data from the 1-D consolidation phase of a SHANSEP CK_0U test conducted in one of MIT's automated triaxial stress path cells. An axial strain rate of about $0.1\%/\text{hr}$ is used during consolidation and automated adjustments of the cell pressure (via a flow pump) are made to maintain a K_0 stress state (i.e., the computer control system targets maintaining $\varepsilon_a = \varepsilon_{vol}$). After consolidation to the final target stress or strain (usually about 10% axial strain for SHANSEP NC tests), a constant stress state is then maintained for the desired period (i.e., either one day or 2 hours as discussed in Section 8.2) prior to undrained shear. The system produces continuous compression curves that provide values of σ'_p and CR. Such tests also provide a reliable value of $K_0(\text{NC})$ and the σ'_v versus σ'_h loading data can be used to estimate the in situ K_0 using the procedure of Mesri and Hayat (1993).

The advantages of using computer controlled equipment, especially for triaxial testing, are significant. The authors appreciate that acquiring automated equipment is not feasible for most laboratories in terms of the capital cost and available personnel to run and maintain the equipment. However, the relatively few geotechnical laboratories that do have this capability are not being properly utilized, even though undisturbed tube samples are being shipped to them for "conventional" lab testing. That is, most practitioners will call for UUC and CIUC tests, rather than CK_0U tests, because they do not appreciate or understand the value of reliable strength data. Nevertheless, the authors

advocate the continued establishment of regional specialized testing facilities, both for teaching and to serve practice.

8.2 Reconsolidation Procedure

The Recompression and SHANSEP strength testing techniques were independently developed to address the important soil behavior issues discussed in Section 7.1 (i.e., anisotropy, strain rate effects, and sample disturbance). The methods are identical except for an important difference in how to deal with sample disturbance for the UU stability case. Both approaches use CK_0U tests with shearing in different modes of failure (e.g., TC, DSS, and TE) at appropriate strain rates to account for anisotropy and strain rate effects.

In the Recompression method, Bjerrum (1973) recognized the unreliable nature of the standard UU test and proposed using CU tests, which anisotropically reconsolidate specimens to the in situ state of stress (σ'_{vo} , σ'_{ho}) as shown by point 3 in Fig. 8.2. This procedure assumes that the reduction in water content during reconsolidation to σ'_{vo} is small enough so as to produce s_u data that are representative of in situ conditions. Berre and Bjerrum (1973) recommended that the volumetric strain during recompression should be less than 1.5 to 4 percent.

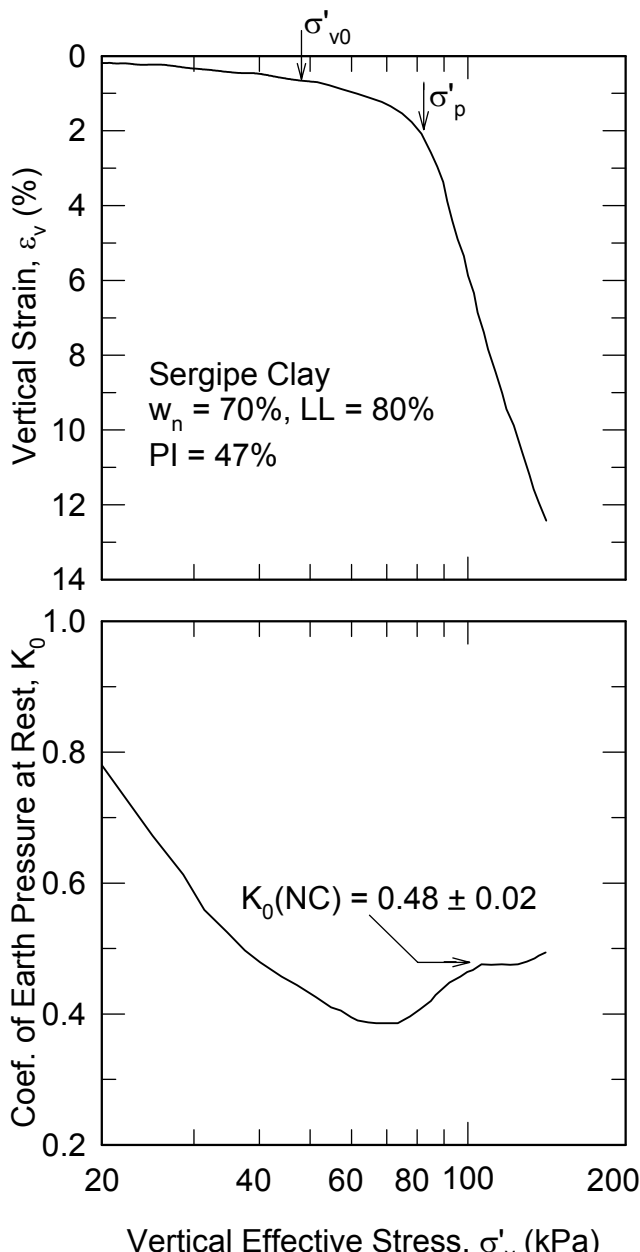


Figure 8.1 Example of 1-D Consolidation Data from MIT's Automated Stress Path Triaxial Cell

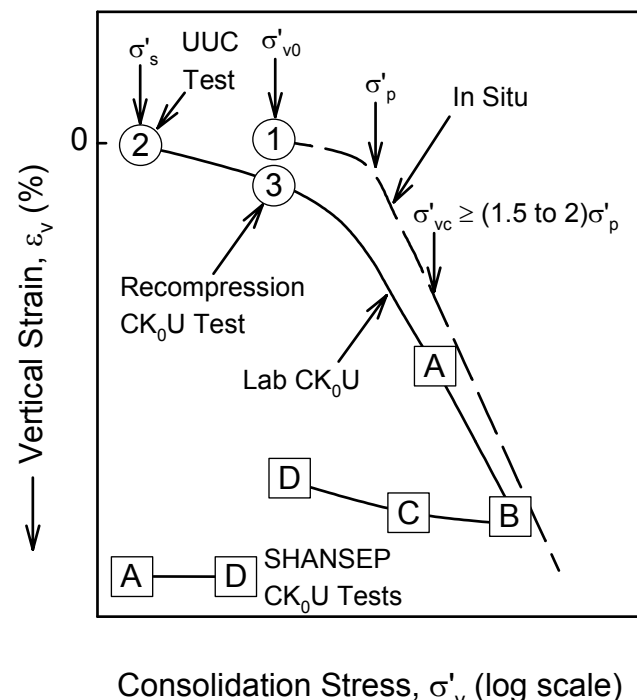


Figure 8.2 Recompression and SHANSEP Consolidation Procedure for Laboratory CK_0U Testing (after Ladd 1991)

The SHANSEP method (Ladd and Foott 1974, Ladd 1991) is based on the experimental observation that the undrained stress-strain-strength behavior of most "ordinary" clays, for a given mode of shear, is controlled by the stress history of the soil deposit. The method assumes that these clays exhibit normalized behavior and uses mechanical overconsolidation to represent all preconsolidation mechanisms. The procedure explicitly requires the stress history profile for the soil to be evaluated and was developed to obtain s_u profiles for both the UU and CU stability cases. Test specimens are K_0 consolidated to stress levels greater than σ'_p to measure the normally consolidated behavior (Points A and B in Fig. 8.2). Additional specimens are also unloaded to varying OCRs (points C and D) to measure overconsolidated behavior. Plots of $\log s_u/\sigma'_{vc}$ vs. $\log \text{OCR}$ are then used (e.g., Fig. 7.1a) to obtain values of S and m for the SHANSEP equation.

For in situ clay deposits that are truly normally consolidated, the SHANSEP procedure is clearly the best method for determining design strengths. Recompression to $\sigma'_{v0} = \sigma'_p$ for NC soils will result in a volumetric strain that is too high and a ε_v - $\log \sigma'_v$ slope that is too low, and thus lead to unsafe results. SHANSEP CK_0U tests for predicting the behavior of in situ OC clay use $t_c = 1$ day so as to allow secondary compression to "restore" some of the clay structure. But for in situ NC soil, the tests should use $t_c = t_p$ (i.e., little or no secondary compression; MIT uses $t_c \approx 2$ hr). Table 8.1 presents data for two plastic soils comparing SHANSEP DSS strengths measured with $t_c = 1$ day versus $t_c = 2$ hours. The effect is significant, producing values of S that are some 10 to 15% less than from tests with $t_c = 1$ day.

Table 8.1 Effect of Consolidation Time on NC s_u/σ'_{vc} from CK_0UDSS Tests

Soil	t_c	τ_{hmax}/σ'_{vc} (SD)	Ratio
Fresh Kills, NY Organic Silt (PI $\approx 50\%$)	1 day	0.296 (0.018)	0.87
	2 hr	0.257 (0.020)	
Sergipe, Brazil Offshore CH ($w_n \approx 65\%$)	1 day	0.238 (0.004)	0.91
	2 hr	0.216 (0.007)	

Note: data are average of two tests for each case

There is no question that the SHANSEP reconsolidation technique "destructures" the OC clay by consolidating test specimens beyond the in situ σ'_p to obtain values of S and m. Furthermore, the mechanical overconsolidation used with SHANSEP will seldom if ever exactly reproduce the undrained stress-strain behavior of natural overconsolidated deposits. Possible reasons for selecting SHANSEP, even though it gives imperfect results (except when the in situ $OCR = 1$ as noted above) include:

1. It forces the user to establish the initial stress history of the soil, which is needed to understand the deposit and is required for settlement analyses and stage construction.
2. With the advent of computer automation, SHANSEP CK_0U triaxial and DSS tests yield continuous compression curves that provide values of σ'_p and CR; automated triaxial tests also measure K_0 vs. σ'_{vc} (Fig. 8.1). These features represent a great advantage compared to Recompression tests.
3. The error in S and m is always on the safe side and is generally small for cohesive soils of low to moderate sensitivity. This is illustrated in Fig. 8.3 for SHANSEP and Recompression triaxial tests on natural BBC. The differences in the measured data are small except for TE at high OCR.

Reasons for selecting the Recompression technique for the UU Case are now discussed. For highly structured clays, such as the Champlain clays, SHANSEP gives values of S that are much too low, for example by 15 to 25% as shown by the solid points in Fig. 7.1b for the James Bay clay. In general SHANSEP will underpredict the in situ undrained stiffness of soils, as illustrated in Fig. 8.4 by the values of E_{50}/σ'_{vc} (Young's modulus at $\Delta q/\Delta q_f = 0.50$) from triaxial tests on natural BBC. The error is likely to increase for more structured soils.

The SHANSEP method is questionable in highly weathered clay crusts in which mechanical overconsolidation does not represent the primary overconsolidation mechanism (although the SHANSEP TC strengths for the BBC crust plotted in Fig. 8.3 are essentially identical to those of the Recompression tests). Figure 8.5 plots SHANSEP and Recompression results from DSS tests conducted on Laval block samples of Connecticut Valley Varved Clay (CVVC) from the UMass Amherst National Geotechnical Experimental Site. Figure 8.6a shows the stress history data for the site, which has a highly weathered crust believed to be due to desiccation and freeze-thaw cycles. The σ'_p data in Fig. 8.6a are from EOP

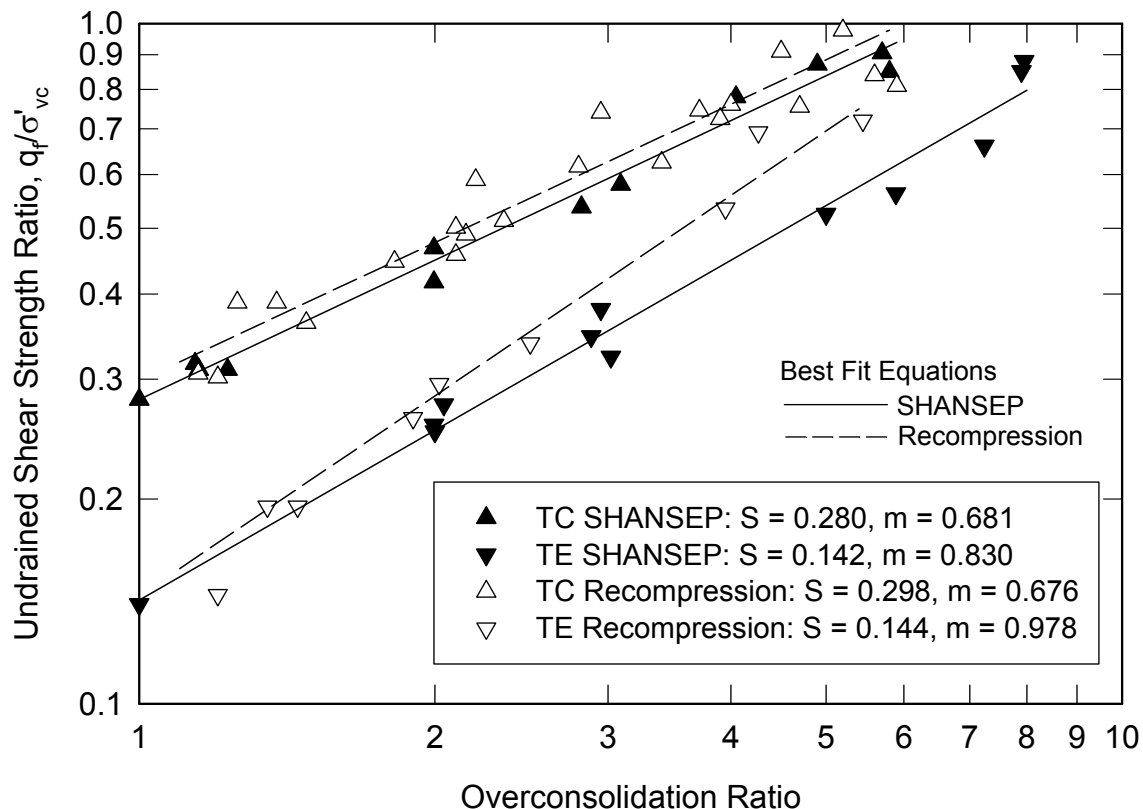


Figure 8.3 Comparison of SHANSEP and Recompression CK_0U Triaxial Strength Data on Natural BBC (after Ladd et al. 1999)

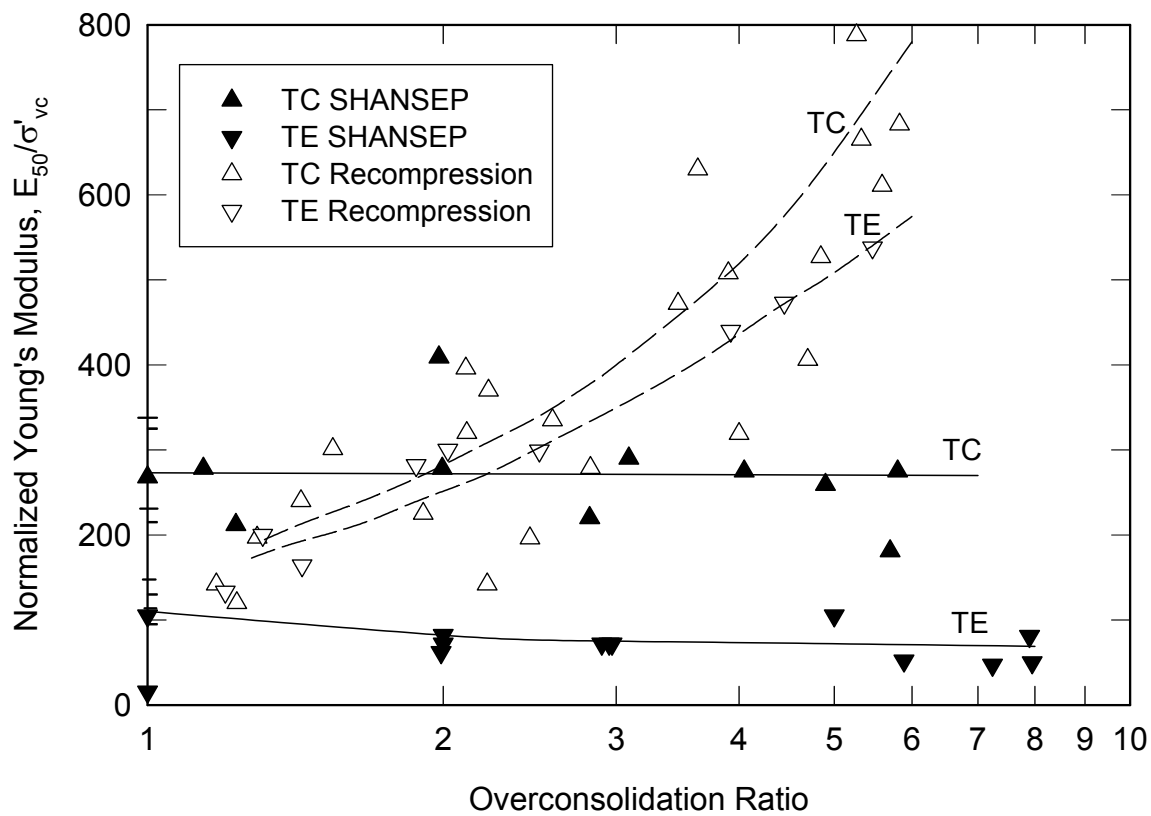


Figure 8.4 Comparison of SHANSEP and Recompression CK_0U Triaxial Modulus Data on Natural BBC (after Ladd et al. 1999)

IL consolidation tests and the consolidation phase of SHANSEP DSS tests on specimens that all had SQD ratings of A or B (i.e., ε_v at $\sigma'_v 0 < 2\%$). At low to moderate OCRs, the s_u/σ'_{v0} ratios in Fig. 8.5 are similar, but for high OCRs (i.e., within the highly weathered crust) there are significant differences. Figure 8.6b plots the SHANSEP calculated s_u profile (using a best fit σ'_p line from Fig. 8.6a) and the measured "point" values of s_u from Recompression tests. The differences in s_u for the high OCR crust material are evident (although these should be reduced for stability analysis due to strain incompatibility with the lower clay). However, the strengths become equal within the deeper lower OCR clay for which the average Liquidity Index of the bulk soil equals 1.5 and the sensitivity based on Nilcon vane tests averages 9 (DeGroot and Lutenegger 2003).

In summary, the Recompression technique is strongly recommended for highly structured clays (e.g., Champlain clays) and is preferred for more reliable undrained stress-strain behavior in general if high quality samples are available. However, Recompression tests cannot, by definition, measure values of σ'_p and give only depth specific values of s_u . Thus a separate program of consolidation tests is needed to check the reasonableness of the measured s_u/σ'_{v0} ratios and

for settlement and CU stability analyses. SHANSEP CK_0U tests have the advantage of producing stress history data and must be used for truly normally consolidated deposits.

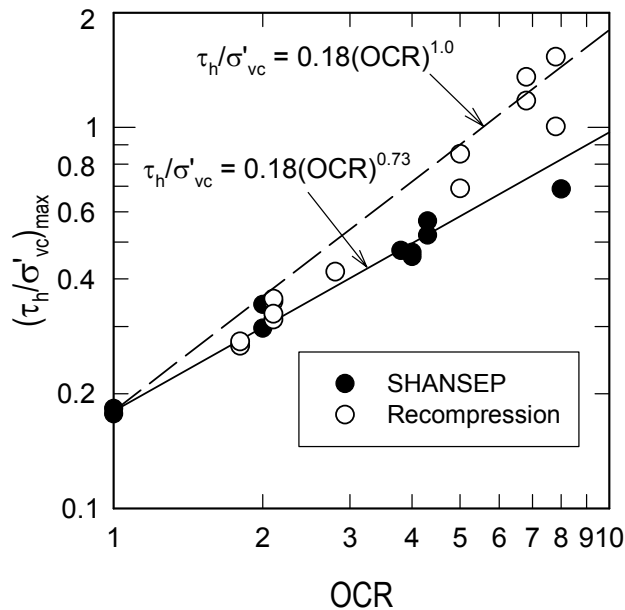


Figure 8.5 Comparison of SHANSEP and Recompression CK_0UDSS Strength Data on CVVC (after DeGroot 2003)

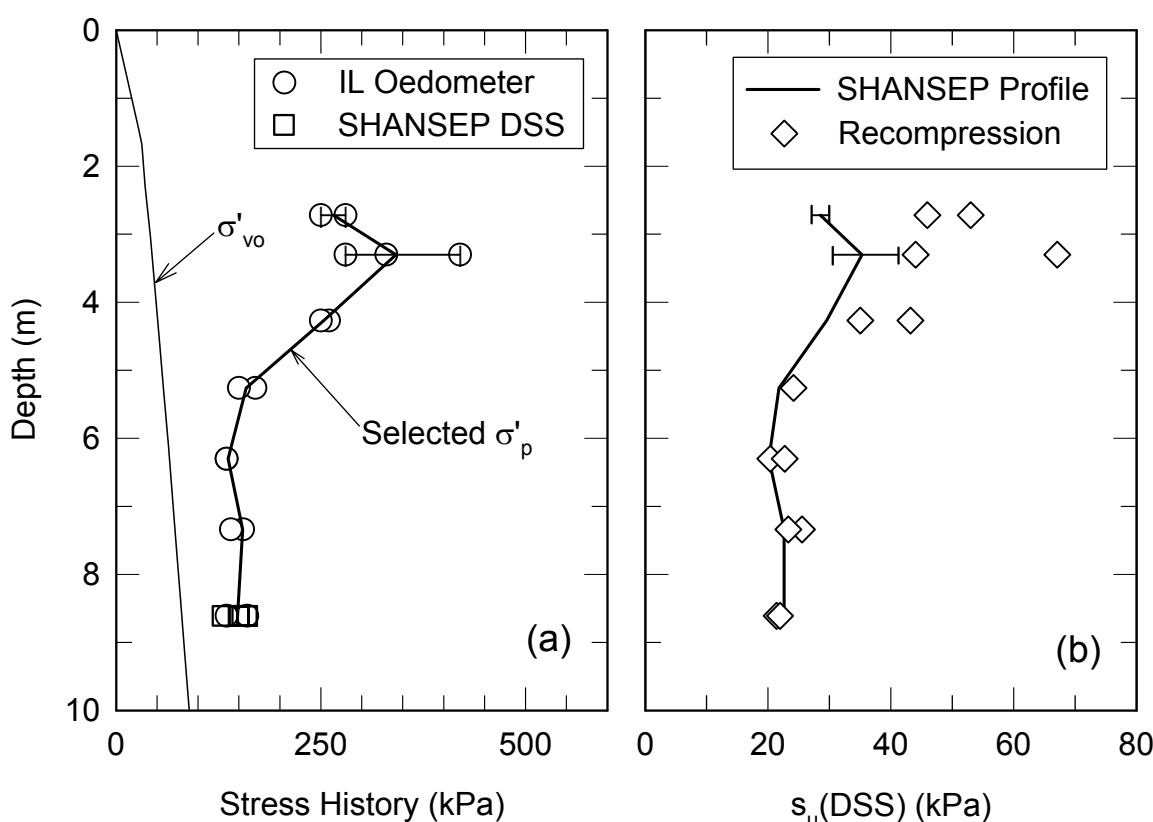


Figure 8.6 CVVC UMass Site: (a) Stress History Profile; (b) SHANSEP and Recompression DSS Strength Profiles (after DeGroot 2003)

8.3 Interpretation of Strength Data

After conducting a laboratory undrained shear strength test program (i.e., with triaxial and/or DSS tests), the measured laboratory peak strengths (q_f for TX and τ_{hmax} for DSS) may require adjustment depending on the particular design problem. The following text discusses potential corrections due to five factors:

1. Definition of s_u appropriate for stability analyses
2. The effects of strain compatibility
3. The difference between triaxial and plane strain shear (σ_2 effect)
4. Three-dimensional end effects
5. $s_u(\text{ave})$ for isotropic stability analyses versus strength parameters for anisotropic analyses.

It will become evident that each of the first four factors can affect the outcome by a nominal 10 to 15%, but that they generally tend to cancel out. This partly explains why simplified interpretations of CK₀U strength data usually do not result in unexpected failures (i.e., they predict the same FS as a rigorous evaluation due to compensating errors). However, one should be aware of these factors since the net result of the various corrections vary with soil type, failure geometry and the quality and type of strength data being evaluated.

Definition of s_u for USA. An Undrained Strength Analysis (USA) for loads on *saturated* soft clays is by definition a " $\phi = 0$ " analysis. For bearing capacity analyses using N_c for $\phi = 0$, the theoretically correct definition of s_u corresponds to the peak point on the Mohr circle (q) since the theoretical failure surfaces are oriented at $\pm 45^\circ$ for the active and passive zones. However, when performing undrained stability analyses with a method of slices, the definition of s_u becomes controversial.

Chapter 31 of Lambe and Whitman (1969) suggests that $s_u = q_f = 0.5(\sigma_1 - \sigma_3)_f$ since $\phi = 0$, and many leading experts agree with that assumption. But the authors disagree because:

- If the location and geometry of the critical failure surface is reasonable (e.g., location of the critical circle or wedge shaped surface with the active and passive zones approximating $45 \pm \phi'/2$, even though $\phi = 0$ in the analysis),
- Then s_u should be defined as the available shear strength on the failure plane at failure, i.e., $\tau_f = q \cos \phi'$ (the point of tangency of the Mohr Circle to the effective stress failure envelope).

The difference between these assumptions is not

trivial. When selecting design strengths from CK₀U triaxial tests, the $\cos \phi'$ term lowers s_u by 10 to 15% for typical values of ϕ' equal to $29 \pm 3^\circ$. Henceforth, s_u is defined as τ_f for USA with a method of slices. If incorrect, the error is at least on the safe side, whereas the other definition might overestimate the FS by 10 to 15%.

Adjustments for Strain Compatibility, Intermediate Principal Stress and 3-D End Effects. The following conclusions come from the material presented in Sections 7.1 and 7.4.

- *Strain Compatibility:* The peak shear strength occurs at different shear strains (γ) for different modes of failure, followed by strain softening (especially in compression). Hence the average strength that can be mobilized along a potential failure surface is less than the average of the peak strengths. The reduction is roughly 10 to 15% in brittle, sensitive soils with a design $\gamma \approx 1 - 2\%$ (strain at maximum mobilized strength) and is about 5 to 10% in plastic, insensitive soils with a design $\gamma \approx 10 - 15\%$.
- *Intermediate Principal Stress (b effect):* Undrained shear in plane strain leads to higher strengths than measured in triaxial tests. The increase is $9 \pm 6\%$ in compression ($\delta = 0^\circ$) and $22 \pm 3\%$ in extension ($\delta = 90^\circ$), for an average increase of 15%.
- *3-D End Effects:* For typical embankment failures, the actual factor of safety, FS(3D), is about $10 \pm 5\%$ higher than the FS(2D) computed from conventional analyses which assume an infinitely long plane strain failure. The magnitude of the increase can be refined based on the estimated dimensions of the potential failure using Eq. 7.3.

Estimation of $s_u(\text{ave})$ for Isotropic Stability Analyses. Assume that one has stress-strain (q vs. ϵ_a) data from triaxial CK₀UC/E tests performed at a slow rate (0.5 – 1.0%/hr) on high quality specimens of a soft clay having an approximately linear variation in strength with the δ angle. Adjustments to the average of the peak strengths, $q_{fp} = 0.5[q_f(C) + q_f(E)]$, based on the foregoing discussion become:

- Times 0.875 to define s_u as $\tau_f = q \cos \phi'$ (for $\phi' = 29^\circ$)
- Times 0.90 to account for strain compatibility (average of $10 \pm 5\%$) reduction

- Times 1.15 to correct for triaxial to plane strain conditions (average of 9% and 22%)
- $0.875 \times 0.90 \times 1.15$ leads to $s_u(\text{ave}) = 0.90 q_{fp}$.

Thus for a plane strain failure, a simple averaging of the measured triaxial peak strengths leads to a computed FS(2D) that would be 10% too high. However, 3-D end effects typically increase the FS(2D) by 10% and hence using q_{fp} with a conventional 2-D stability analyses would yield a reasonable estimate of the actual FS(3D).

Based on the above example and set of assumptions, selecting q_{fp} for the design $s_u(\text{ave})$ would be reasonable for non-varved deposits. However, the net result of the various corrections vary with soil type, the quality of the test specimens and procedures, and the likely failure geometry. Therefore it is recommended that selection of $s_u(\text{ave})$ as q_{fp} from triaxial data should always be checked with Level C estimates of undrained strength ratios based on the empirical correlations presented in Table 7.2. If the results do not agree, evaluate each of the correction factors. Also note that the example did not consider rate effects, which may warrant a nominal 10% reduction in q_{fp} for highly plastic and organic soils. Finally, remember that the use of $s_u(\text{ave}) = q_{fp}$ already includes 3-D end effects.

If the CK_0U test program is restricted to DSS tests, using $s_u(\text{ave}) = \tau_{h\max}$ will usually provide design strengths that lie between those for plane strain shearing and those which already include some 3-D effects (Ladd 1991, DeGroot et al. 1992). Thus explicit consideration of 3-D effects using Eq. 7.3 may yield factors of safety that are somewhat too high.

Estimation of s_u for Anisotropic Stability

Analyses. This subsection now focuses on selection of anisotropic undrained strength parameters for non-circular stability analyses for the CU Case (Example 3 in Table 7.1, although the methodology also applies to circular arc analyses). The recommended minimum testing program consists of CK_0U TC, TE and DSS tests. The test data for OC clay could come from either Recompression tests or SHANSEP tests (with $t_c = 1$ day), whereas SHANSEP tests (with $t_c = t_p$) should be used for NC clay. It is assumed that the stability analyses will develop profiles of σ'_{vc} within the foundation clay and then compute the vertical and lateral variations in s_u using the SHANSEP equation with design values of S and m to obtain values of s_u/σ'_{vc} .

The suggested procedure for developing plane strain values of $s_u(\alpha)$, where α is the inclination of the failure surface from the horizontal, involves

the following steps. The objective is to first obtain values of S and m for shear in plane strain compression (τ_c) and extension (τ_e) and direct simple shear (τ_d) and then decide how $s_u(\alpha)$ varies between these three modes of failure. Note: values of $s_u(\alpha)/\sigma'_{vc}$ and τ/σ'_{vc} will be shown as $s_u(\alpha)$ and τ for simplicity unless otherwise noted.

Step 1). Plot representative curves of $\tau = q \cos \phi'$ versus $\gamma = 1.5 \varepsilon_a$ from the TC/TE tests and τ_h vs. γ from the DSS tests for NC soil and at one $OCR > 1$. These shear stresses are denoted by τ_{tc} , τ_{te} and τ_d , respectively.

Step 2). Select a design γ that approximately maximizes $\tau_{ave} = 1/3(\tau_c + \tau_d + \tau_e)$, where $\tau_c = 1.1\tau_{tc}$, $\tau_e = 1.2\tau_{te}$ (to convert triaxial to plane strain) and $\tau_d = \tau_h$. The selected strain should emphasize the stress strain data for NC soil since this zone will usually provide most of the resistance in stability analyses for the CU Case.

Step 3). For in situ NC soil, the anisotropic shear parameters selected for design at the design γ are mean values of

- $S_c = \tau_c/\sigma'_{vc}$, $\tau_c = 1.1\tau_{tc}$ for PSC ($\delta = 0^\circ$) with the failure surface oriented at $\alpha = 45 + \phi'/2$
- $S_e = \tau_e/\sigma'_{vc}$, $\tau_e = 1.2\tau_{te}$ for PSE ($\delta = 90^\circ$) with the failure surface oriented at $\alpha = -(45 - \phi'/2)$
- $S_d = \tau_h/\sigma'_{vc}$, for DSS with an unknown orientation of the failure surface since $\delta = 45 \pm 15^\circ$

(Note: $\alpha = \theta - \delta$, where $\theta = 45 + \phi'/2$ is the angle between the σ_{1f} plane and the failure plane).

Step 4). For in situ OC soil, use the same basic procedure as in Step 3, but now applied to tests with $OCR \geq 1$ to obtain τ/σ'_{vc} vs. OCR for the three modes of failure. These data then provide values of S and m for OC clay.

The above methodology assumes a complete set of tests for both OC and NC clay, which will seldom be true (the James Bay case history presented in Ladd 1991 being an exception). For example, a SHANSEP CK_0U program might be restricted to triaxial and DSS tests at $OCR = 1$ with $t_c = t_p$. The resulting S values from Step 3 might then simply be increased by 10% and m assumed equal to 0.8 for OC clay. Or if the program lacks reliable TE data (since these tests can be seriously affected by piston friction, filter strips, etc.), one might select a value of S_e based on trends measured for other soils.

Figure 8.7 plots values of S treated for strain compatibility versus PI for shear in compression, DSS and extension for non-layered clays which can be used for guidance. The data mostly come from Table 4 of Ladd (1991), but with adjustments for triaxial vs. plane strain and consolidation time (plus judgment) to correspond

to plane strain shearing of truly normally consolidated clays. These values of S could be increased by some 10% to estimate anisotropic parameters for overconsolidated clays.

Case History. This example is a continuation of the TPS offshore breakwater project discussed at the end of Section 5.2. It describes the development of anisotropic strength profiles for evaluating the stability of the Stage 3 construction of the Redesign cross-section shown in Fig. 5.10. The index properties and measured σ'_p data for the 7.2 m thick Sergipe clay were plotted in Fig. 5.12 and Fig. 5.13 showed the stress history selected for consolidation and stability analyses.

Figure 8.8 summarizes the results of UTEXAS3 (Wright 1991) non-circular stability analyses with Spencer's (1967) method of slices and anisotropic strengths. The foundation clay was divided into five zones for 1-D consolidation analyses to obtain profiles of σ'_{vc} used to compute s_u . Zone 1 represents virgin soil (no increase in strength during construction) and Zones 2, 3 and 4 represent consolidation under increasing applied stresses ($\Delta\sigma_v = 50$ kPa under the Stage 1 stability berm; $\Delta\sigma_v = 85$ kPa under the lower portion of the

Stage 2 slope; and $\Delta\sigma_v = 120$ kPa under the upper portion of the Stage 2 construction to El. + 3.0). Zone 5 represents conditions under the centerline of the breakwater in order to calibrate the consolidation model by comparing measured versus predicted settlements during Stage 2 construction and the halt and then during final Stage 3 filling from El. + 2.75 m to 5.25 m. The latter occurred between early April, 1992 (shortly after MIT became involved) and the end of October, 1992. Although analyses were made for different times, only those for $t_c = 5/15/92$ are presented, which corresponds to 21 months consolidation under Stage 1 and 14 months under Stage 2.

The automated CK_0U strength testing program using the SHANSEP reconsolidation technique included the following tests:

- For virgin (OC) clay ($t_c = 1$ day): 3 TC, 2 TE and 3 DSS all at $OCR = 1$ and 1 TC at $OCR = 2.2$
- For NC clay ($t_c = 2$ hr): 2 DSS and 3 CAUDSS with $\tau_{hc}/\sigma'_{vc} = 0.09$ to 0.13 (used to assess the benefit of in situ consolidation with a horizontal shear stress as per Section 4.11 and Fig. 19 of Ladd 1991).

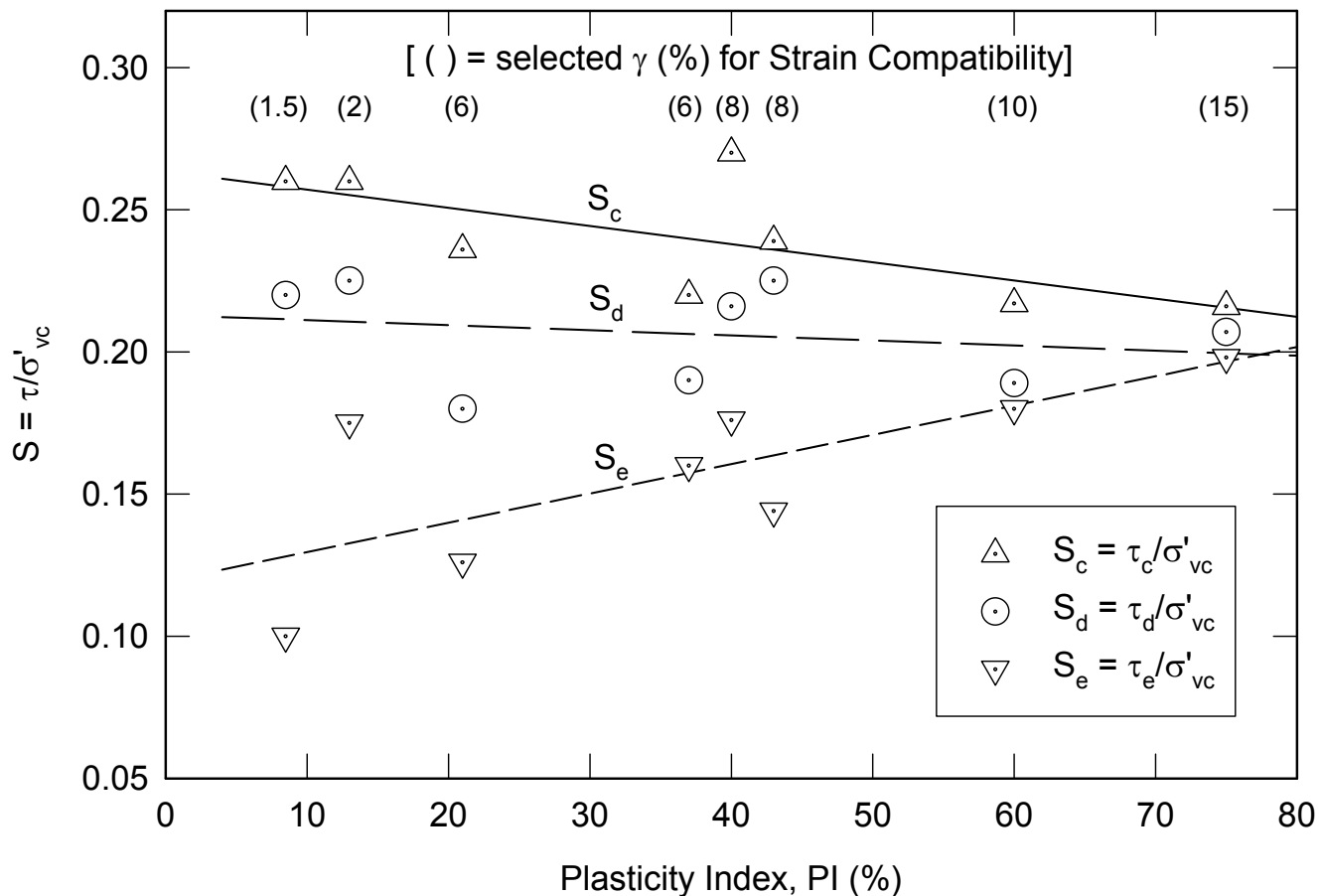


Figure 8.7 Plane Strain Anisotropic Undrained Strength Ratios vs. Plasticity Index for Truly Normally Consolidated Non-Layered CL and CH Clays (mostly adjusted data from Ladd 1991)

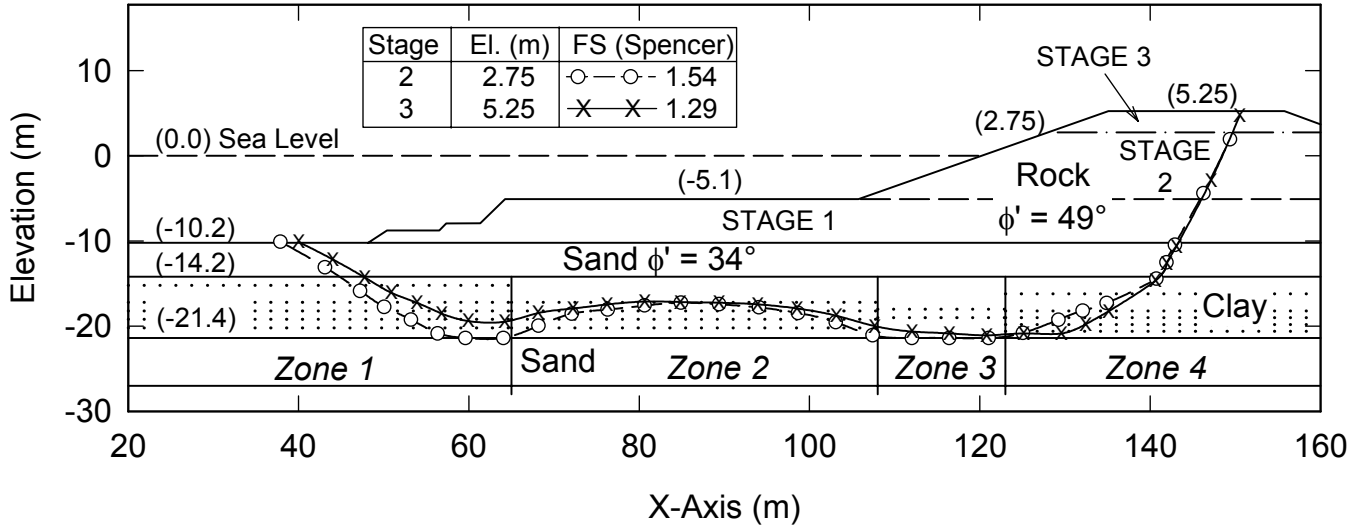


Figure 8.8 TPS Stability Analyses for Redesign Stages 2 and 3 Using SHANSEP $s_u(\alpha)$ at $t_c = 5/15/92$ (Lee 1995)

The triaxial tests were sheared at $\dot{\epsilon}_a = 0.5\%/\text{hr}$, whereas the strain rate for all of the DSS tests was varied between $\dot{\gamma} = 5.0\%/\text{hr}$ (standard rate) and $0.5\%/\text{hr}$ due to concerns about the strain rate sensitivity of the clay.

A design shear strain of $\gamma = 6\%$ was selected to account for strain compatibility. Further corrections to the triaxial data were: $\tau = q\cos 30^\circ$ for the definition of s_u ; q increased 9% and 22% to convert TC and TE to plane strain; and q reduced by about 10% to model EOP consolidation for NC clay. For OC clay, $m = 0.80$ was selected based on the one OC TC test (0.77) and $m = 0.88(1-C_s/C_c) = 0.81$. Strengths from the DSS tests were selected at $\dot{\gamma} = 0.5\%/\text{hr}$. This process lead to the SHANSEP design parameters shown in Table 8.2.

The failure of the initial design (Fig. 5.10) was back analyzed to check that the SHANSEP parameters were consistent with the friction angles selected for the rockfill and upper silty sand. 1-D consolidation analyses [ABAQUS program for large strains with the Modified Cam Clay model and bi-linear e-log k relationships to make $c_v(\text{OC}) = 10c_v(\text{NC})$] computed profiles of σ'_{vc} within Zones 2, 3 and 4 (Fig. 8.8), which were then used to calculate DSS strength profiles. Figure 8.9 plots elevation vs. $s_u(D)$ for both virgin (OC) clay and for $t_c = 5/15/92$ (about two months after the start of Stage 3 filling) within Zones 2 and 4. This plot shows little strength gain under the stability berm, but significant strengthening within the upper and lower portions of the clay beneath the crest of the breakwater.

Table 8.2 SHANSEP Design Parameters for Sergipe Clay (Ladd and Lee 1993)

Clay	S_c	S_d	$S_e^{(1)}$	Comment
Virgin	0.24	0.22	0.18	$m = 0.8$
NC	0.22	0.19	0.16	CK_0U
NC	-	0.22	-	CAU ⁽²⁾

⁽¹⁾ Selected values 0.02 higher than computed based on judgment

⁽²⁾ For $\tau_{hc}/s_u = 0.67 = \text{nominal } 1/\text{FS} = 1/1.5$. However, not used since consolidation analyses predicted very little virgin consolidation within the central portion of the clay.

The UTEXAS3 stability program handles anisotropy by linear interpolation between specified points of $s_u(\alpha)$ and α within each Soil Number (a soil layer having a constant strength over its thickness). Figure 8.10 shows how anisotropy was modeled for both overconsolidated (virgin) clay and normally consolidated clay (i.e., where σ'_{vc} exceeded the design σ'_p profile plotted in Fig. 5.13). The figure normalizes $s_u(\alpha)$ by $s_u(D)$ for each layer. Point C represents failure in compression ($\delta = 0^\circ$) for $\alpha \geq 60^\circ$ ($\alpha = \theta - \delta$, with $\theta = 45 + \phi'/2 = 60^\circ$) and point E represents failure in extension ($\delta = 90^\circ$) for $\alpha \leq -30^\circ$. Because of uncertainty in the δ angle for failure in DSS, point D is horizontal between $\alpha = 0^\circ$ to $\alpha = 30^\circ$ (i.e., corresponding to $\delta = 45 \pm 15^\circ$). Finally, the dashed horizontal lines in Fig. 8.8 within the clay show the different Soil Numbers (layers) for Zones 1 through 4. The average $s_u(D)$ for each

layer was determined from Fig. 8.9, and then Fig. 8.10 was used to specify the variation in $s_u(\alpha)$.

Figure 8.8 shows the computed FS(2D) for Stage 2 at the end of the halt in construction and for the final Stage 3 filling to El. + 5.25 m, which was completed in October, 1992, along with the location of the non-circular failure surfaces. The hump in the failure surfaces is caused by the low $s_u(D)$ near El. - 17 m (Fig. 8.9). Lee (1995) made detailed reliability analyses that considered uncertainties in the strengths of the rockfill, sand and clay, clay thickness, 3-D end effects, method of stability analysis, etc. These showed a nominal probability of failure for final construction of only 0.01% (i.e., less than the $P_f = 0.1\%$ desired by the contractor). They also indicated that the halt in construction was not necessary, but this would have been hard to substantiate without the

additional site characterization and refined back analyses of the failure.

8.4 Principal Recommendations

Computer automated stress path triaxial cells enable better quality CK_0U test data in less time and cost than manually operated equipment, especially for tests that are reconsolidated into the normally consolidated region. Since relatively few laboratories have this specialized capability, the establishment of more facilities would help to enhance geotechnical education and practice. Unfortunately, most practitioners do not realize that the cost of running automated CK_0U tests can be largely offset by deleting UUC and CIUC tests. Nor do they appreciate the fact that the extra effort to obtain more reliable strength parameters can result in significant overall cost savings via more economical designs and the reduced likelihood of delays and claims due to unexpected performance.

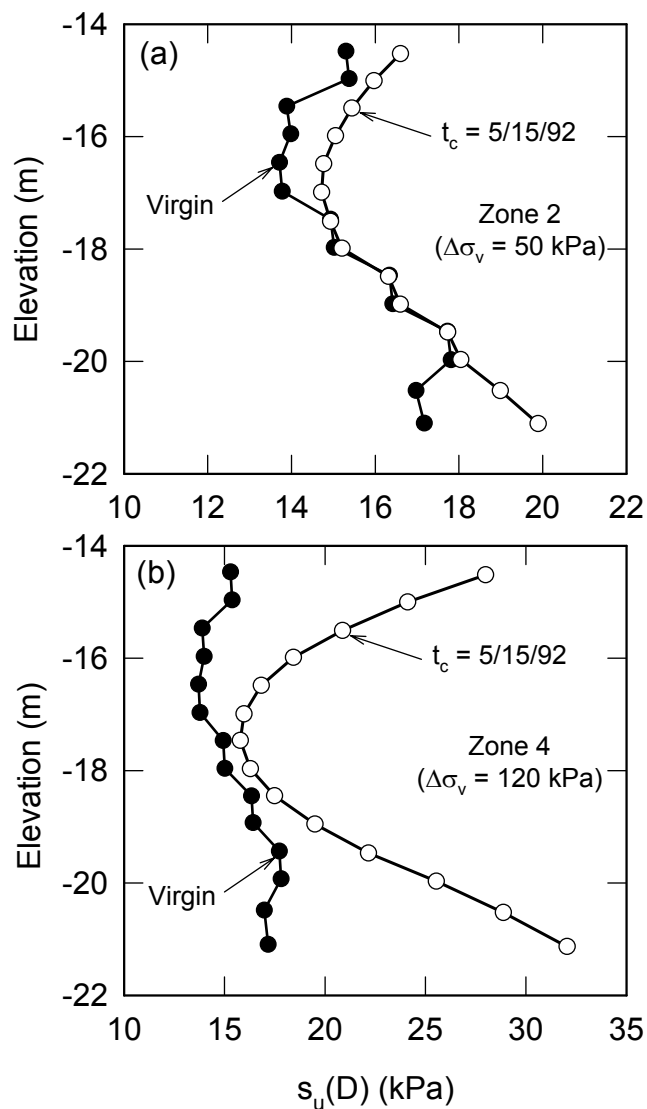


Figure 8.9 SHANSEP DSS Strength Profiles for TPS Stability Analysis for Virgin and Normally Consolidated Sergipe Clay: (a) Zone 2; (b) Zone 4 (Lee 1995)

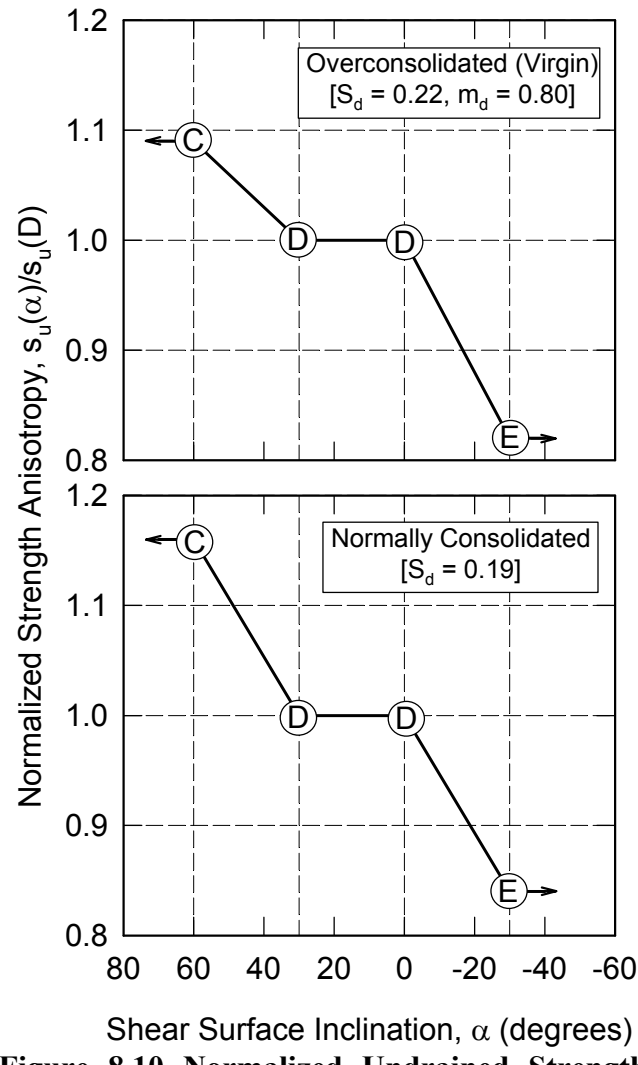


Figure 8.10 Normalized Undrained Strength Anisotropy vs. Shear Surface Inclination for OC and NC Sergipe Clay (Ladd and Lee 1993)

The Recompression and SHANSEP reconsolidation techniques used for CK_0U testing each have advantages and limitations. Recompression to the in situ stresses generally provides more realistic stress-strain-strength data, particularly for structured soils, but is largely restricted to evaluating the stability of overconsolidated clay for the UU Case (initial loading). It also requires an estimate of the in situ K_0 . SHANSEP has the advantage of providing 1-D compression curves for estimating σ'_p and CR (especially true with automated equipment) and gives strengths for both the UU and CU Cases, but assumes that the normalized parameters measured on destructured soil also apply to virgin OC clay. The SHANSEP values of S and m tend to be too low, especially for highly structured clays; the undrained stiffness also is too low. However, SHANSEP must be used for in situ soils that are (or will become) truly normally consolidated, along with a preshear consolidation time that does not allow secondary compression (i.e., $t_c \approx t_p$).

The selection of design strengths from CK_0U triaxial data should consider potential corrections for the definition of s_u [shear stress on potential failure surface rather than $q = 0.5(\sigma_1 - \sigma_3)$] and the effects of σ_2 , strain compatibility and 3-D slope stability end effects. Although each of these corrections equals about ± 10 to 15% , they tend to cancel out. For isotropic analyses, with soils having a near linear reduction in s_u from compression to extension ($\delta = 0$ to 90°), $s_u(\text{ave})$ usually can be taken either as the average of the peak triaxial strengths [$q_f(C)$ and $q_f(E)$] or the peak τ_h from direct simple shear (DSS) tests. Selection of anisotropic strengths, $s_u(\alpha)$, is more complex, as illustrated by the case history on the TPS offshore breakwater.

9 SUMMARY AND CONCLUSIONS

The paper recommends testing programs, testing methods and data interpretation techniques for developing design parameters for settlement and stability analyses for soft ground construction projects, i.e., for conditions where construction will load the cohesive foundation soil beyond its preconsolidation stress. Table 1.1 summarizes the relevant soil properties (design parameters) for settlement and stability analyses and also defines most of the common symbols used in the text.

The paper starts with a general methodology for site characterization, which includes a combination of in situ and laboratory tests, and then suggests specific recommendations regarding:

- Soil stratigraphy and soil classification (Section 3)
- Undisturbed sampling, radiography and assessing sample disturbance (Section 4)
- In situ testing for soil profiling and some soil properties, principally with the field vane test (FVT) and the piezocone (CPTU) (Section 5)
- Laboratory consolidation testing (Section 6)
- Laboratory consolidated-undrained (CU) shear testing (Section 8), which is preceded by a section summarizing key aspects of undrained shear behavior (Section 7).

The paper hopes to move the state-of-practice closer to the state-of-the-art and thus is intended for geotechnical practitioners and teachers, not researchers.

The section on sampling and sample disturbance lists specific recommendations at the end of each major topic, wherein Sections 5 through 8 each conclude with a summary of the principal recommendations. Many of the recommendations for improving practice are relatively easy to implement and entail little or no extra cost. Examples within this category include:

Undisturbed Sampling (Section 4.1)

- Use sufficient drilling mud weight and depth to prevent bottom heave prior to sampling (Fig. 4.2 presents guidance).
- Use fixed piston samplers ($D \geq 76$ mm, thin walls and near zero clearance ratio) to improve sample quality and recovery.
- Keep samples in tubes for shipping to the laboratory and use the debonding technique described in Fig. 4.3 to minimize disturbance during extrusion.

Assessing Sample Quality (Section 4.3)

- Run strength index tests (Torvane, lab vane, etc.) above and below all specimens used for consolidation and CU strength testing and evaluate s_u/σ'_{v0} .
- Evaluate vertical strain at the effective overburden stress (SQD, Fig. 4.6) from all 1-D consolidation tests.
- Compare values of the maximum slope of the virgin compression ratio, CR_{\max} (see example in Fig. 4.7).

In Situ Testing (Section 5)

- The FVT is the most reliable in situ test for estimating $s_u(\text{ave})$ and OCR for *homogeneous* clays (minimal shells and sand zones) using the correlations presented in Figs. 5.1 and 5.2.
- The CPTU is the best in situ test for soil profiling, but is generally less reliable for estimating $s_u(\text{ave})$ and OCR due to problems with the accuracy of q_t and u_2 data and the large uncertainty in empirical correlations.

Consolidation Testing (Section 6)

- Perform Atterberg Limits on trimmings of known w_n for all tests (at least for the first series of tests).
- For IL oedometer tests, use a reduced load increment ratio (say 0.5 vs. the standard doubling) when testing soils with an S-shaped virgin compression curve. Use plots of strain (not void ratio) vs. $\log \sigma'_v$ obtained at a constant t_c that approximates the maximum t_p for NC soil (not at 24 hr, which includes added secondary compression strains).
- Consider switching to CRS consolidation testing in order to obtain continuous compression curves with direct measurements of k_v and c_v in much less time than required for conventional one-day IL load tests (e.g., Figs 6.2 and 6.5).
- Use the Becker et al. (1987) strain energy method for estimating σ'_p from rounded compression curves (Fig. 6.4)
- Compare values of c_v (NC) with the empirical correlation between c_v and Liquid Limit presented on page 7.1-144 of Navfac DM 7.1 (1982).

Conventional Triaxial Compression Tests (Section 7.2)

- Delete UUC tests. They often exhibit excessive scatter and reliance on such tests to estimate $s_u(\text{ave})$ always depends on a fortuitous cancellation of uncontrollable errors, i.e., the strength increase due to fast shearing in compression must be offset by a strength decrease due to sample disturbance. Values of $s_u(\text{UUC})$ can easily be either 25 to 50% too high or too low depending upon the soil type and sample quality.
- Delete CIUC tests as they produce values of s_u/σ'_c that are unsafe for design.
- The cost savings are better spent on consolidation and CK_0U tests.

Level C Estimates of $s_u(\text{ave})$ for UU Case (Section 7.3)

- For very low OCR cohesive soils, the in situ strength should equal or exceed $s_u(\text{ave}) = S\sigma'_{v0}$, where $S = 0.22 \pm 0.03$. Table 7.2 presents refined estimates of S as a function of soil type.
- For higher OCR soils, $s_u(\text{ave})/\sigma'_{v0} = S(\text{OCR})^m$, where $m = 0.8 \pm 0.1$.

Recommendations for two aspects of site characterization do involve a significant change in practice. The first relates to the use of radiography. As discussed in Section 4.2, radiography is highly cost effective since it

enables one to logically plan a laboratory test program (i.e., where to cut the tubes for each engineering test) based on prior knowledge of the locations of the best quality material of each representative soil obtained from the site. Access to regional radiography facilities would advance geotechnical practice by reducing the likelihood of running costly tests on poor quality or non-representative soil that produce misleading data. The second recommendation concerns the ability to conduct CK_0U triaxial compression (TC) and extension (TE) and direct simple shear (DSS) tests. As described in Table 7.1, these tests should be run in order to obtain design strengths for stability analyses for the CU Case, i.e., where staged construction is used to increase the strength of the foundation clay. The development of computer automated stress path triaxial equipment enables better quality CK_0U test data in less time and cost than manually operated equipment, especially for tests that are reconsolidated into the normally consolidated region. Practitioners need to realize that the extra effort to conduct CK_0U tests can result in significant overall cost savings for projects with marginal stability. Hence, like radiography, establishment of regional facilities having this capability is recommended to advance geotechnical education and practice.

Section 8.2 discusses the pros and cons of using the Recompression and SHANSEP reconsolidation techniques for CK_0U triaxial and DSS test programs and Section 8.3 presents recommended procedures for developing design strength parameters from these tests. The latter includes the appropriate definition of s_u and corrections for the effects of σ_2 , strain compatibility and 3-D slope stability end effects.

10 ACKNOWLEDGMENTS

The authors thank Kiewit Engineering Co. for permission to publish data from the Northern Ontario highway project and likewise ERTC of ChevronTexaco for data from the preloading project in Nigeria. They also thank Dr. John T. Germaine, head of MIT's geotechnical laboratory, for sharing his experiences with undisturbed sampling and lab testing and Tom Lunne, Discipline Manager, of NGI for providing information on CPTU testing and NGI's testing practice.

This paper is a slightly revised version of that published in the Proceedings of the *Soil and Rock American 2003* conference held June 22 – 26 at MIT. The authors appreciate comments on the

original paper by Les Bromwell, Chris Hunt, Steve Saye, and, most especially, Allen Marr.

REFERENCES

Aas, G., Lacasse, S., Lunne, T. and Hoeg, K. (1986). "Use of in situ tests for foundation design on clays." *Proc. ASCE Spec. Conf. In Situ '86*, ASCE GSP 6, 1-30.

Andresen, A., and Kolstad, P. (1979). "The NGI 54-mm sampler for undisturbed sampling of clays and representative sampling of coarser materials." *Proc. of the Int. Conf. on Soil Sampling*, Singapore, 1-9.

ASTM (2002). *Annual Book of Standards, Vol. 4.08, Soil and Rock (I): D420 - D5779*. West Conshohocken, PA, USA.

Azzouz, A.S., Baligh, M.M. and Ladd, C.C. (1982). "Cone penetration and engineering properties of the soft Orinoco Clay." *Proc. of 3rd Inter. Conf. on Behavior of Offshore Structures*, MIT, 1, 161-180.

Azzouz, A.S., Baligh, M.M., and Ladd, C.C. (1983). "Corrected field vane strength for embankment design." *J. Geotech. Eng.*, ASCE, 109(5), 730-734.

Baldi, G., Hight, D.W., and Thomas, G.E. (1988). "State-of-the-Art: A re-evaluation of conventional triaxial test methods." *Advanced Triaxial Testing of Soil and Rock*, ASTM STP 977, 219-263.

Baligh, M.M. (1985). "The strain path method." *J. Geotech. Eng.*, 111(9), 1108-1136.

Baligh, M.M., Azzouz, A.S., and Chin, C.T. (1987). "Disturbances due to ideal tube sampling." *J. of Geotech. Eng.*, 113(7), 739-757.

Becker, D.E., Crooks, J.H., Been, K., and Jefferies, M.G. (1987). "Work as a criterion for determining in situ and yield stresses in clays." *Can. Geotech. J.*, 24(4), 549-564.

Berman, D.R., Germaine, J.T., and Ladd, C.C. (1993). "Characterization of engineering properties of Boston Blue Clay for the MIT campus." Research Rept. 93-16, Dept. of Civil & Environ. Eng., MIT, 146p.

Berre, T., and Bjerrum, L. (1973). "Shear strength of normally consolidated clays." *Proc., 8th Int. Conf. on Soil Mech. and Found. Eng.*, Moscow, 1, 39-49.

Bjerrum, L. (1972). "Embankments on soft ground: SOA Report." *Proc. Specialty Conference on Performance of Earth and Earth-Supported Structures*, ASCE, Purdue, 2, 1-54.

Bjerrum, L. (1973). "Problems of soil mechanics and construction on soft clays." *Proc., 8th Int. Conf. Soil Mech. and Found. Eng.*, Moscow, 3, 111-159.

Bjerrum, L., and Landva, A. (1966). "Direct simple shear tests on Norwegian quick clay." *Geotechnique*, 16(1), 1-20.

Chandler, R.J. (1988). "The in-situ measurement of the undrained shear strength of clays using the field vane: SOA paper." *Vane Shear Strength Testing in Soils Field and Laboratory Studies*, ASTM STP 1014, 13-44.

Christian, J.T., Ladd, C.C., and Baecher, G.B. (1994). "Reliability applied to slope stability analysis." *J. of Geotech. Eng.*, 120(12), 2180-2207.

Clayton, C.R.I., Siddique, A., and Hopper, R.J. (1998). "Effects of sampler design on tube sampling disturbance - numerical and analytical investigations." *Geotechnique*, 48(6), 847-867.

DeGroot, D.J. (2003). "Laboratory measurement and interpretation of soft clay mechanical behavior." *Soil Behavior and Soft Ground Construction*. ASCE GSP 119, MIT, 167-200.

DeGroot, D.J., Germaine, J.T., and Ladd, C.C. (1994). "Influence of nonuniform stresses on measured DSS stress-strain behavior." *J. Geotech. Eng.*, ASCE, 120(5), 892-912.

DeGroot, D.J., Ladd, C.C., and Germaine, J.T. (1992). "Direct simple shear testing of cohesive soils." Research Report R92-18, Center for Scientific Excellence in Offshore Engineering, MIT, 153pp.

DeGroot, D.J., and Lutenegger, A.J. (2003). "Geology and Engineering properties of Connecticut Valley varved clay." *Characterisation and Engineering Properties of Natural Soils*, Tan et al. (eds.), Balkema, 1, 695-724.

Dyvik, R., Lacasse, S., and Martin, R. (1985). "Coefficient of lateral stress from oedometer cell." *Proc. 11th Int. Conf. on Soil Mech. and Foundation Eng.*, San Francisco, 2, 1003-1006.

Foott, R., and Ladd, C.C. (1981). "Undrained settlement of plastic and organic clays." *J. Geotech. Eng. Div.*, 107(8), 1079-1094.

Gauer, P., and Lunne, T. (2003). "Quality of CPTU: Statistical analyses of CPTU data from Onsøy." Research Report 20001099-2, NGI.

Germaine, J.T. (2003). Personal Communication.

Germaine, J.T., and Ladd, C.C. (1988). "Triaxial testing of saturated cohesive soils: SOA paper." *Advanced Triaxial Testing of Soil and Rock*, ASTM STP 977, 421-459.

Haley & Aldrich, Inc. (1993). "Final report on special laboratory and in situ testing program, Central Artery (I-93)/Tunnel (I-90) Project, Boston, Massachusetts." Prepared for the Massachusetts Highway Department.

Hight, D.W. (2003). "Sampling effects in soft clay: An update on Ladd and Lambe (1963)." *Soil Behavior and Soft Ground Construction*. ASCE GSP 119, MIT, 86-122.

Hight, D.W., Böese, R., Butcher, A.P., Clayton, C.R.I., and Smith, P.R. (1992). "Disturbance of the Bothkennar Clay prior to laboratory testing." *Geotechnique*, 42(2), 199-217.

Hight, D.W., and Leroueil, S. (2003). "Characterisation of soils for engineering purposes." *Characterisation and Engineering Properties of Natural Soils*, Tan et al. (eds.), Balkema, 1, 255-360.

Jamiolkowski, M., Ladd, C.C., Germaine, J.T., and Lancellotta, R. (1985). "New developments in field and laboratory testing of soils." *Proc., 11th Int. Conf. on Soil Mechanics and Foundation Eng.*, San Francisco, 1, 57-154.

Kenney, T. C. (1964). "Sea-level movements and the geologic histories of the post-glacial marine soils at Boston, Nicolet, Ottawa and Oslo." *Geotechnique*, 14(3), 203-230.

Koutsoftas, D.C., and Ladd, C.C. (1985). "Design strengths for an offshore clay." *J. Geotech. Eng.*, 111(3), 337-355.

Lacasse, S., and Berre, T. (1988). "State-of-the-Art: Triaxial testing methods for soils." *Advanced Triaxial Testing of Soil and Rock*, ASTM STP 977, 264-289.

Lacasse, S., Ladd, C.C., and Baligh, M.M. (1978). "Evaluation of field vane, Dutch cone penetrometer and piezometer probe testing devices." Res. Report R78-26, Dept. of Civil Eng., MIT, 375p.

Ladd, C.C. (1991). "Stability evaluation during staged construction (22nd Terzaghi Lecture)." *J. of Geotech. Eng.*, 117(4), 540-615.

Ladd, C.C., Azzouz, A.S., Martin, R.T., Day, R.W., and Malek, A.M. (1980). "Evaluation of the compositional and engineering properties of offshore Venezuelan soils, Vol. 1: Orinoco Clay." Res. Report R80-14, Dept. of Civil Engr., MIT, 286p.

Ladd, C.C., and Edgers, L. (1972). "Consolidated-undrained direct simple shear tests on saturated clays." Res. Report R72-82, Dept. of Civil Engr., MIT.

Ladd, C.C., and Foott, R. (1974). "New design procedure for stability of soft clays." *J. of the Geotech. Eng. Div.*, 100(GT7), 763-786.

Ladd, C.C., Foott, R., Ishihara, K., Schlosser, F., and Poulos, H.G. (1977). "Stress-deformation and strength characteristics: SOA report." *Proc., 9th Int. Conf. on Soil Mechanics and Foundation Eng.*, Tokyo, 2, 421-494.

Ladd, C.C., and Lambe, T.W. (1963). "The strength of 'undisturbed' clay determined from undrained tests." *Symposium on Laboratory Shear Testing of Soils*, ASTM, STP 361, 342-371.

Ladd, C.C., and Lee, S-M. (1993). "Engineering properties of Sergipe Clay: TPS Progress Rept. No. 4." Research Rept R93-07, Dept. of Civil and Environmental Eng., MIT, 200p.

Ladd, C.C., Moh, Z-C., and Gifford, D.G. (1971). "Undrained shear strength of soft Bangkok clay." *Proc. 4th Asian Regional Conf. on Soil Mech. and Foundation Eng.*, Bangkok, Vol. 1, 135-140.

Ladd, C.C., Whittle, A.J., and Legaspi, D.E., Jr. (1994). "Stress-deformation behavior of an embankment on Boston Blue Clay." *Proc., Vertical and Horizontal Deformations of Foundations and Embankments*. ASCE GSP 40, College Station, 2, 1730-1759.

Ladd, C.C., Young, G.A., Kraemer, S.R. and Burke, D.M. (1999). "Engineering properties of Boston Blue Clay from special testing program." *Special Geotechnical Testing: Central Artery/Tunnel Project in Boston, Massachusetts*. ASCE GSP 91, 1-24.

Lambe, T.W., and Whitman, R.V. (1969). *Soil Mechanics*. 1st Ed., John Wiley and Sons, Inc., New York, NY.

La Rochelle, P., Leroueil, S., and Tavenas, F. (1986). "Technique for long-term storage of clay samples." *Can. Geotech. J.*, 23(4), 602-605.

Lee, S-M. (1995). "Stability and deformation during stage construction of an offshore breakwater in soft clay." PhD Thesis, Dept. of Civil and Environmental Eng., MIT, 551p.

Lefebvre, G., Ladd, C.C., Mesri, G., and Tavenas, F. (1983). "Report of the testing committee." *Committee of Specialists on Sensitive Clays on the NBR Complex*, SEBJ, Montreal, Annexe I.

Leroueil, S. (1994). "Compressibility of clays: Fundamental and practical aspects." *Proc., Vertical and Horizontal Deformations of Foundations and Embankments*. ASCE GSP 40, College Station, 1, 57-76.

Lunne, T. (2003). Personal Communication.

Lunne, T., Berre, T., and Strandvik, S. (1997a). "Sample disturbance effects in soft low plasticity Norwegian clay." *Proc. of Conference on Recent Developments in Soil and Pavement Mechanics*, Rio de Janeiro, 81-102.

Lunne, T., Robertson, P.K., and Powell, J.J.M. (1997b). *Cone Penetration Testing in Geotechnical Practice*. Chapman & Hall, London.

Marchetti, S. (1980). "In situ tests by flat dilatometer." *J. Geotech. Eng. Div.*, 106(3), 299-321.

Marr, W.A. (2002). "State of the Practice: Geotechnical laboratory testing." *XVII Seminario Venezolano de Geotecnia*, Venezuela.

Mayne, P.W. (1980). "Cam-clay predictions of undrained strength." *J. Geotech. Eng. Div.*, 106(11), 1219-1242.

Mesri, G. (1975). Discussion of "New design procedure for stability of soft clays." by C.C. Ladd and R. Foott, *J. Geotech. Eng. Div.*, 101(4), 409-412.

Mesri, G., and Castro, A. (1987). "C_a/C_c concept and K₀ during secondary compression." *J. Geotech. Eng.*, 113(3), 230-247.

Mesri, G., and Feng, T.W. (1992). "Constant rate of strain consolidation testing of soft clays." *Marsal Volume*, Mexico City, 49-59.

Mesri, G., and Hayat, T.M. (1993). "The coefficient of earth pressure at rest." *Can. Geotech. J.*, 30(4), 647-666.

Mesri, G., Kwan Lo, D.O., and Feng, T.W. (1994). "Settlement of embankments on soft clays." *Proc., Vertical and Horizontal Deformations of Foundations and Embankments*. ASCE GSP 40, College Station, 1, 8-56.

Mitchell, T.J., DeGroot, D.J., Lutenegger, A.J., Ernst, H., and McGrath, V. (1999). "Comparison of CPTU and laboratory soil parameters for bridge foundation design on fine grained soils: a case study in Massachusetts." *Transportation Research Record* No. 1675, 24-31.

Navfac DM-7.1 (1982). *Soil Mechanics*. Facilities Engineering Command, U.S. Dept. of the Navy, Alexandria, VA, 364p.

Robertson, P.K. (1990). "Soil classification using the cone penetration test." *Can. Geotech. J.*, 27(1), 151-158.

Saada, A.S., and Townsend, F.C. (1981). "State-of-the-art: Laboratory strength testing of soils." *Symp. on Laboratory Shear Strength of Soil*, ASTM STP 740, 7-77.

Sandbækken, G., Berre, T., and Lacasse, S. (1986). "Oedometer testing at the Norwegian Geotechnical Institute." *Consolidation of Soils: Testing and Evaluation*, ASTM STP 892, 329-353.

Santagata, M.C., and Germaine, J.T. (2002). "Sampling disturbance effects in normally consolidated clays." *J. of Geotech. and Geoenvirons. Eng.*, 128(12), 997-1006.

Saye, S.R. (2003). "Assessment of soil disturbance by the installation of displacement sand drains and prefabricated vertical drains." *Soil Behavior and Soft Ground Construction*. ASCE GSP 119, MIT, 325-362.

Saye, S.R., Ladd, C.C., Gerhart, P.C., Pilz, J., and Volk, J.C. (2001). "Embankment construction in an urban environment: the Interstate 15 experience." *Foundations and Ground Improvement*, ASCE GSP 113, Virginia Tech., 842-857.

Sheahan, T.C., DeGroot, D.J., and Germaine, J.T. (1994). "Using device-specific data acquisition for automated laboratory testing." *Innovations in Instrumentation and Data Acquisition Systems*. Transportation Research Record 1432, 9-17.

Sheahan, T.C., and Germaine, J.T. (1992). "Computer automation of conventional triaxial equipment." *Geotech. Test. J.*, ASTM, 15(4), 311-322.

Sheahan, T.C., Ladd, C.C., and Germaine, J.T. (1996). "Rate-dependent undrained shear behavior of saturated clay." *J. of Geotech. Eng.*, 122(2), 99-108.

Spencer, E. (1967). "A method of analysis of the stability of embankments assuming parallel inter-slice forces." *Géotechnique*, 17(1), 11-26.

Tanaka, H. (2000). "Sample quality of cohesive soils: lessons from three sites, Ariake, Bothkennar and Drammen." *Soils and Foundations*, 40(4), 57-74.

Tanaka, H. (2003). Personal Communication.

Tanaka, H., Rito, R., and Omukai, N. (2002). "Quality of samples retrieved from great depth and its influence on consolidation properties." *Can. Geotech. J.*, 39(6), 1288-1301.

Tanaka, H., Sharma, P., Tsuchida, T., and Tanaka, M. (1996). "Comparative study of sample quality using several types of samplers." *Soils and Foundations*, 36(2), 57-58.

Tavenas, R., Jean, P., Leblond, P., and Leroueil, S. (1983). "The permeability of natural soft clays, Part II: Permeability characteristics." *Can. Geotech. J.*, 20(4), 645-660.

Terzaghi, K., Peck, R.B., and Mesri, G. (1996). *Soil Mechanics in Engineering Practice – 3rd Edition*. John Wiley and Sons, NY.

Vaid, Y.P., and Campanella, R.G. (1974). "Triaxial and plane strain behavior of natural clay." *J. Geotech. Eng. Div.*, 100(3), 207-224.

Wissa, A.E.Z., Christian, J.T., Davis, E.H., and Heiberg, S. (1971). "Consolidation at constant rate of strain." *J. of the Soil Mech. and Found. Div.*, 97(SM10), 1393-1413.

Wright, S.G. (1991). "UTEXAS3, a computer program for slope stability calculations." Shinoak Software, Austin, TX, Revised Sept. 1991.